Impact Characterisation on the Low-Voltage Electrical Networks Resilience Level Facing the Integration of Photovoltaic Generation and Hydrogen-Based Energy Storage

Rusber Octavio Rodríguez Velásquez

Doctoral thesis to qualify for the degree of doctor of engineering
Double diploma thesis between the Universidad Industrial de Santander and the Université de Franche-Comté

UIS Director
German Alfonso Osma Pinto
PhD in Electrical Engineering
UIS Co-directors
Gabriel Ordóñez Plata
PhD in Electrical Engineering
Javier Enrique Solano Martínez
PhD in Electrical Engineering

UBFC Director
David Bouquain
PhD in Electrical Engineering
UBFC Co-directors
Damien Paire
PhD in Electrical Engineering
Daniel Hissel
PhD in Electrical Engineering

Universidad Industrial de Santander
Faculty of physical-mechanical engineering
School of Electrical, Electronic and Telecommunications Engineering
Ph.D. in Engineering, Area, Electrical Engineering
Bucaramanga
2024

Dedication

Dear readers,

It is with deep gratitude and emotion that I dedicate this work to all of you who have been a fundamental part of my journey towards completing this thesis. Each of you has left an indelible mark on my life and has contributed significantly to this achievement.

First and foremost, I wish to dedicate this work to my Lord Jesus Christ, who has been my constant guide and has enlightened my path at every step. I owe Him everything and thank Him for giving me the strength and determination to overcome any obstacle.

To you, my beloved wife Johanna Niño, my unwavering companion on this arduous journey. Since the first day of my thesis, you have been by my side, sharing moments of happiness and the toughest challenges. Your unconditional love and support have motivated me to move forward. I promise to strive daily to contribute to your happiness as you do for me. I love you infinitely.

To my mother, Gladiz Velásquez, you have always been present with your love and pride for me. Your encouragement and motivation have driven me to strive and achieve my goals. Thank you for believing in me and for being my greatest inspiration. I also dedicate this work to the memory of my father, Octavio Rodríguez. Although he is no longer physically with us, his unconditional support and willingness to listen to my ideas and provide objective feedback continue to inspire me. His legacy lives on in every achievement I make.

And I cannot forget my lovely siblings, a source of learning and growth. I love you dearly and wish you, too, can learn from me as I have learned from you. To all of you, I dedicate this achievement with the deepest affection. Without your love, support and encouragement, this journey would have been much more difficult. Every page of this book is imprinted with my gratitude for having you close to me.

With love and gratitude;

Rusber Rodríguez

Acknowledgements

I want to express my deep gratitude to all the people and institutions that have been fundamental in developing my doctoral thesis. This achievement is possible thanks to their support and contribution.

First and foremost, I thank God for giving me the strength to overcome all the setbacks and challenges I faced throughout this academic journey. To my beloved wife, my tireless companion, thank you for being my emotional support at every step and accompanying me from beginning to end. To my family, an inexhaustible source of inspiration, thank you for the constant encouragement to keep going.

My gratitude also goes to my thesis directors, who guided and facilitated the development of my research. I am grateful to the *Universidad Industrial de Santander* and the *Université Bourgogne Franche-Comté* for their support in terms of workspace, computer equipment and academic resources, allowing me to explore and present the results of my research. To my friends in Colombia, Canada and France, I sincerely thank you for making this academic journey an enriching and enjoyable experience. Your technical support and shared knowledge were pillars that contributed to the success of my thesis.

Special thanks to the institutions that provided me with financial support: *i)* The *Universidad Industrial de Santander*, my deepest gratitude for granting me a forgivable credit that made my studies possible. *ii)* The Emerging Leaders in the Americas Program (ELAP) grant, which financed my internship at the *Université de Sherbrooke* in Canada, extending my academic perspective. *iii)* The French Embassy in Colombia, whose financial support facilitated my travel from Colombia to France, thus broadening my research horizons. *iv)* The *Université Bourgogne Franche-Comté*, for the opportunity to be part of its team as a salaried researcher for a year, contributing significantly to my training. *v) France Travail*, whose contribution was vital in the last year of the thesis when other resources were scarce.

To all of you, my sincere thanks. The trust placed in me will be honoured with continued dedication and tireless effort. This achievement is not only mine but also that of those who believed in my potential - thank you for being part of this pivotal chapter in my academic life!

Table of Contents

List of Tables

Pag.

List of Figures

Pag.

Acronyms

AC alternating current

CDF cumulative distribution function

Ch report's chapters

CI critical infrastructure

CUF current unbalance factor

DC direct current

DER distributed energy resources

DG distributed generation

DSM demand-side management

E^{3}T Department of Electrical, Electronic and Telecommunications Engineering

EEB Electrical Engineering Building

EL electrolyser

ELVB emergency low voltage bus

EMR energy macroscopic representation

EMS energy management strategy

ESS energy storage system

FC fuel cell

GLVB general low voltage bus

H_2 hydrogen

H_2-ESS hydrogen-based energy storage system

HILP high-impact low-probability

LIHP low-impact high-probability

LPSP lost of power supply probability

LV low-voltage

LVSB low voltage supply bus

MAPE mean absolute percentage error

MCEER Multidisciplinary Centre for Earthquake Engineering Research

MPPT maximum power point tracking

MV medium-voltage

PCC point of common coupling

PDF probability density function

PE permanent-effect

PEMFC proton exchange membrane fuel cell

PV photovoltaic

R_{comp} comprehensive resilience

R_{III} type III resilience

R_{II} type II resilience

R_{I} type I resilience

RES renewable energy sources

RMS root mean square

RQ research question

Sa spectral acceleration

SC self-consumption

SG self-generation

SO specific objective

TB transfer bus

THDi total harmonic distortion of current

THDv total harmonic distortion of voltage

TSP total supply probability

UIS *Universidad Industrial de Santander*

UKERC U.K. Energy Research Centre

VUF voltage unbalance factor

List of Parameters and Variables

The following list describes the symbols of the variables and parameters used within the document's body.

AC electrical network

$\vec{\mathbf{u}}_{fd}$	Feeder voltage vector
$\vec{\mathbf{i}}_{net}$	Feeder current vector
$\mathbf{S}_{\phi}$	Complex power of the ϕ-phase
P_{ϕ}	Active power of the ϕ-phase
Q_{ϕ}	Reactive power of the ϕ-phase
$\mathbf{i}_{load\phi}$	Load current of the ϕ-phase
$\vec{\mathbf{i}}_{load}$	Load current vector
$\mathbf{Z}_{l}$	Complex impedance of a wire conductor at nominal frequency
R_{l}	Resistance of a wire conductor
X_{l}	Inductive reactance of a wire conductor at nominal frequency

Electrolyser (EL) system

U_{el}	Voltage of a single EL cell
I_{el}	Current of a single EL cell
η_{e}	Energy effiency of an EL cell
N_{S_el}	Series cells in the EL stack
N_{S_el}	Parallel branches in the EL stack
N_{c}	Total number of cells in the EL stack

T_a	Room temperature
T_{EL}	Temperature of the EL stack
U_{EL}	Voltage of the EL stack
I_{EL}	Current of the EL stack
$\dot{m}_{H_2\_gen}$	H_2 production ratio of the EL stack
η_F	Faraday efficiency for the EL stack
$\mathbf{i}_{ELs_{\phi}\_ref}$	Reference current for the ϕ-phase of the EL system
$\vec{\mathbf{i}}_{ELs\_ref}$	Reference current vector for the EL system
$\vec{\mathbf{u}}_{ELs}$	Voltage vector of the EL system rectifier
$\mathbf{u}_{PCC_{\phi}\_EL}$	Voltage of the ϕ-phase at the coupling point of the EL system
$\vec{\mathbf{u}}_{PCC\_EL}$	Voltage vector at the coupling point of the EL system
$\mathbf{S}_{ELs\_ref}$	Reference complex power for the EL system
$\vec{\mathbf{S}}_{ELs\_ref}$	Reference complex power vector for the EL system
$\vec{\mathbf{s}}_{EL_{\phi}}$	Power ratio vector reference for the EL system phases
fp_{ELs_ref}	Reference power factor for the EL system
P_{EL_ref}	Reference power for the EL stack
η_{INV}	Efficiency of the EL system inverter
P_{ELs}	Active power of the EL system
Q_{ELs}	Reactive power of the EL system
$\mathbf{S}_{ELs}$	Complex power of the EL system
$\vec{\mathbf{S}}_{ELs}$	Complex power vector of the EL system
$\vec{\mathbf{i}}_{ELs}$	Current vector of the EL system

Fuel cell-battery backup system

U_{fc}	Voltage of a single fuel cell
I_{fc}	Current of a single fuel cell
$\dot{m}_{H_2\_fc}$	H_2 consumption ratio of a single fuel cell
N_{S_fc}	Series cells of the fuel cell (FC) stack
N_{P_fc}	Parallel cell of the FC stack
U_{FC}	Voltage of the FC stack
I_{FC}	Current of the FC stack
$\dot{m}_{H_2\_con}$	H_2 consumption ratio of the FC stack
I_{FCs_ref}	Reference current for the FC system
P_{FC_ref}	Reference power for the FC stack
P_{FC}	Power of the FC stack
η_{conv}	Efficiency of the FC system converter
U_{FCs}	Voltage of the FC system
I_{FCs}	Current of the FC system
U_b	Voltage of a single battery
I_b	Current of a single battery
Cap_b	Storage capacity of a single battery
E_m	Open-circuit voltage of a single battery
SOC_b	State of charge of the batteries
N_{b_s}	Number of batteries in series
N_{b_p}	Number of branches in the battery pack
U_{Bat}	Voltage of the battery pack
I_{Bat}	Current of the battery pack
U_{bk}	Voltage of the backup system on the DC side

I_{BK}	Current of the backup system on the DC side
$\vec{\mathbf{i}}_{bk\_ref}$	Reference current vector for the backup system
$\vec{\mathbf{i}}_{bk}$	Current vector of the backup system
$\vec{\mathbf{u}}_{inv}$	Voltage vector of the backup system inverter
$\mathbf{S}_{bk}$	Complex power of the backup system
η_{inv}	Efficiency of the backup system inverter

Photovoltaic (PV) system

U_c	Voltage of a single PV cell
I_c	Current of a single PV cell
I_{sc}	Short circuit current of a single PV cell
U_{oc}	Open circuit voltage of a single PV cell
n_s	Series cells of a PV module
n_p	Parallel cells of a PV module
N_{st}	Series modules of a PV array
N_{ar}	Parallel arrays of a PV system
U_{oc_mod}	Open circuit voltage of a PV module
I_{sc_mod}	Short circuit current of a PV module
U_{mod}	Voltage of a PV module
I_{mod}	Current of a PV module
U_{PV}	Voltage of the PV array
U_{PV_ref}	Reference voltage for the PV array
I_{PV}	Current of the PV array
η_{inv_PV}	Efficiency of the PV system inverter
fp_{PV}	Power factor of the PV system

P_{PVs}	Active power of the PV system
$P_{\phi PVs}$	Active power of the PV system per phase
$Q_{\phi PVs}$	Reactive power of the PV system per phase
$\mathbf{S}_{\phi PVs}$	Complex power of the PV system per phase
$\mathbf{i}_{\phi PVs}$	ϕ-phase current of the PV system
$\mathbf{u}_{\phi PVs}$	ϕ-phase voltage of the PV system
$\vec{\mathbf{i}}_{PVs}$	Current vector of the PV system
$\vec{\mathbf{u}}_{PVs}$	Voltage vector of the PV system
$\vec{\mathbf{u}}_{PCC}$	Voltage vector of the PV system coupling point
R_{l_PV}	Wire resistance interconnecting the PV system to the grid
X_{l_PV}	Wire inductive reactance interconnecting the PV system to the grid

Comprehensive resilience

Type I resilience

$\rho[F_p\|d]$	Failure probability of the poles due to the d-event
$\rho[F_ln\|d]$	Failure probability of the line sections due to the d-event
$fr_{[p\|d]}.$	Fragility function of the poles facing the d-event
$fr_{[ln\|d]}$	Fragility function of the line sections facing the d-event
$\rho[F_p\|d]$	Failure probability of the poles due to the d-event
d	Index for a disruptive event risk
N_D	Number of disruptive risk events
PDF_d	Probability distribution function of the intensity of the d-event
$\rho[F_{CI}]$	Probability of critical infrastructure collapse
$\rho[F_{CI}\|d]$	Probability of critical infrastructure collapse due to the d-event
ρ_d	Probability of occurrence of the d-event

$SSP_{\|d}$	Stress state probability index with respect to the d-event
$SSP_{\|HILP}$	Total stress state probability
R_I	Type I resilience

Type II resilience

η_{bk}	Backup factor
T_{bk}	Backup time
$CDF(lh_{out})$	Cumulative distribution function of outage length
i	Index of outage
T_{out_i}	Length of the i-outage
$Load_{bk}$	Load supported in emergency
lh_{out}	Length of outages
N_{out}	Number of outage during the observation time
ρ_{out}	Power outage state factor
$PDF(lh_{out})$	Probability density function of outage length
ρ_{off}	Probability of no supply
T_{tot}	Total observation time
TSP	Total supply probability index
$Load_{tot}$	Total load of the LV network
R_{II}	Type II resilience

Type III resilience

u	Voltage
f	Electrical frequency
VUF	Voltage unbalance factor

$THDv$	Total harmonic distortion of voltage
I	Current
p_{loss}	Energy losses
p_{ls}	Percentage energy losses in line section
CUF	Current unbalance factor
$THDi$	Total harmonic distortion of current
I_{pu}	Per unit current
f_{pu}	Per unit frequency
u_{pu}	Per unit voltage
QP_k	Quality parameter k
$\Gamma(QP_k)$	Normalisation operator for the k-quality parameter
ϕ_k	Normalised function of the k-quality parameter
$\phi_u(u_{pu})$	Normalised function of the voltage
$\phi_f(f_{pu})$	Normalised function of the electrical frequency
$\phi_{VU}(VUF)$	Normalised function of the voltage unbalance factor
$\phi_{HDv}(THDv)$	Normalised function of the total harmonic distortion of voltage
$\phi_I(I_{pu})$	Normalised function of the line current
$\phi_l(ls)$	Normalised function of the energy losses
$\phi_{CU}(CUF)$	Normalised function of the current unbalance factor
$\phi_{HDi}(THDi)$	Normalised function of the total harmonic distortion of current
Φ_k	Resilience index corresponding to the k-quality parameter
Φ_u	Resilience Index of voltage
Φ_f	Resilience Index of electrical frequency
Φ_{VU}	Resilience Index of voltage unbalance factor
Φ_{HDv}	Resilience Index of harmonic distortion of voltage

Φ_I	Resilience Index of line current
Φ_l	Resilience Index of energy losses
Φ_{CU}	Resilience Index of current unbalance factor
Φ_{HDi}	Resilience Index of harmonic distortion of current
T_{meas}	Data logging time
OR_V	Operation resilience of voltage
OR_I	Operation resilience of line current
$\overline{OR}_I$	Current operation resilience for a node
$P_{Rat\_}N_i$	Rated power of i-node
N	Number of nodes in the LV network
N_i	Index of the i-node
j	Index of the j-line section
$load_k$	Index of the k-load
L_{S-k}	Line from S-node to k-node
$R_{III\_}Net$	Type III resilience of the whole LV network
$R_{III\_}N_i$	Type III resilience of the i-node
$R_{III\_}load_k$	Type III resilience of the line supplying the k-load
R_{III}	Type III resilience

EEB-UIS case study

$fr_{[CI\|d]}$	Infrastructure fragility due to the d-event
$\Phi(x\|\mu_\alpha,\sigma_\alpha)$	logo-normal CDF for a disruptive event
x	Intensity variable for the disruptive event
μ_α	x-log values' mean for the disruptive event
σ_α	x-log values' standard deviation for the disruptive event

Sa	Spectral acceleration of an earthquake
$\rho[E \geq Sa\|Sa]$	Exceeding probability for each Sa-value of the earthquakes
$SSP_{\|quake}$	Stress state probability related to earthquakes
$SSP_{\|wind}$	Stress state probability related to strong winds
$SSP_{\|HILP}$	Total stress state probability related to disruptive events
ρ_{out}	Probability of power outage for the EEB-UIS feeder
ρ_{off}	Probability of non-supply for the EEB-UIS loads
N_1	Node 1 corresponding to low voltage supply bus (LVSB)
N_2	Node 2 corresponding to emergency low voltage bus (ELVB)
N_3	Node 3 corresponding to the load circuit of the 5^{th} floor (TP5)
N_4	Node 4 corresponding to general low voltage bus (GLVB)
N_5	Node 5 corresponding to the load circuit of the 1^{st} floor (TP1)
N_6	Node 6 corresponding to the load circuit of the 2^{nd} floor (TP2)
N_7	Node 7 corresponding to the load circuit of the 3^{rd} floor (TP3)
N_8	Node 8 corresponding to the point of common coupling (PCC/TP4)
N_8	Node 9 corresponding to the PV system
L_{1-2}	Line section interconnecting the LVSB and the ELVB
L_{2-3}	Line section interconnecting the ELVB and the TP5
L_{1-4}	Line section interconnecting the LVSB and the GLVB
L_{4-5}	Line section interconnecting the GLVB and the TP1
L_{4-6}	Line section interconnecting the GLVB and the TP2
L_{4-7}	Line section interconnecting the GLVB and the TP3
L_{4-8}	Line section interconnecting the GLVB and the TP4/PCC
L_{8-9}	Line section interconnecting the PCC and the PV system
$R_{III} - N_2$	Operation resilience (R_{III}) at the ELVB/n_2

$R_{III} - N_4$	Operation resilience (R_{III}) at the GLVB/n_4
$R_{III} - N_8$	Operation resilience (R_{III}) at the PCC/n_4
$R_{III} - EEB$	Operation resilience (R_{III}) of the EEB-UIS electrical network

Resumen

Título: Caracterización de la afectación del nivel de resiliencia de redes eléctricas de baja tensión ante la integración de generación fotovoltaica y almacenamiento de energía a base de hidrógeno [*]

Autor: Rusber Octavio Rodríguez Velásquez [**]

Palabras Clave: Resiliencia eléctrica, Redes de baja tensión, Almacenamiento de energía, Gestión de la energía, Sistemas fotovoltaicos, Pilas de combustible, Almacenamiento de energía basado en hidrógeno.

Descripcion: Esta tesis analiza la resiliencia eléctrica de las redes de baja tensión (LV). También aborda la creciente instalación de sistemas solares fotovoltaicos (PV) en las redes de LV, acompañado de la integración de sistemas de almacenamiento de energía (ESS) para mejorar el rendimiento de las energías renovables. La interconexión no planificada de sistemas PV y ESS puede afectar a las redes eléctricas e influir en su respuesta a las perturbaciones. Esta investigación requiere un concepto adecuado de *"resiliencia eléctrica de la red"*, que evalúe la capacidad de una red LV que integre PV y ESS para soportar, absorber y superar eventos adversos. Mientras que las evaluaciones de resiliencia existentes se centran en eventos de alto impacto y baja probabilidad, esta tesis propone un enfoque integral para evaluar la resiliencia en redes LV, considerando tanto las interrupciones importantes como los incidentes menores. La metodología integra la fragilidad, la continuidad del suministro y la calidad del servicio, abordando el vacío existente entre estudios independientes. La tesis también explora los beneficios potenciales de la incorporación de ESS basadas en hidrógeno (H_2-ESS) en las redes LV para mejorar la confiabilidad.

El enfoque propuesto se aplica a la instalación eléctrica del Edificio de Ingeniería Eléctrica (EEB-UIS) de la Universidad Industrial de Santander (UIS), Colombia. El análisis del caso revela que el EEB-UIS tiene un riesgo bajo en cuanto a eventos de alto impacto, con oportunidades para fortalecer la confiabilidad y la resiliencia de la operación. El estudio identifica problemas de sobretensión y desequilibrio de carga, sugiriendo estrategias como un sistema de respaldo H_2-ESS e implementar gestión de la energía. La red eléctrica EEB-UIS se modela utilizando Matlab & Simulink, esto permite simulaciones para evaluar la influencia de la ubicación, capacidad y operación de los sistemas PV y H_2-ESS en el rendimiento de la red LV. Los resultados indican que una gestión eficaz de las fuentes distribuidas mejora la resiliencia eléctrica, especialmente en fiabilidad y calidad de funcionamiento. La tesis proporciona un análisis exhaustivo de la resiliencia aplicable a microrredes y redes LV, destacando el potencial para extender la metodología a redes de distribución de media tensión.

[*] Tesis de doctorado

[**] Facultad de Ingenierías Físico-Mecánicas. Escuela de Ingenierías Eléctrica, Electrónica y de Telecomunicaciones.
Director: German Alfonso Osma Pinto, Doctor en Ingeniería Eléctrica.

Abstract

Title: Impact characterisation on the low-voltage electrical networks resilience level facing the integration of photovoltaic generation and hydrogen-based energy storage [*]

Author: Rusber Octavio Rodríguez Velásquez [**]

Keywords: Electrical resilience, Low voltage networks, Energy storage, Energy management, Photovoltaic systems, Fuel cells, Hydrogen-based energy storage.

Description: This thesis analyses the electrical resilience of low-voltage (LV) networks. It also addresses the escalating installation of on-grid photovoltaic (PV) solar systems in LV networks, accompanied by integrating energy storage systems (ESS) to enhance renewable energy performance. The unplanned interconnection of PV and ESS can impact electrical networks, influencing their response to disturbance events. This research requires an appropriate concept of *"network electrical resilience"*, evaluating the ability of an LV electrical grid that integrates PV and ESS to withstand, absorb and overcome adverse events. While existing resilience assessments primarily focus on high-impact, low-probability events, this thesis proposes a comprehensive approach to evaluate resilience in LV networks, considering both major disruptions and minor incidents. The methodology integrates fragility, supply continuity, and service quality, addressing the gap between independent studies. The thesis also explores the potential benefits of incorporating hydrogen-based ESS (H_2-ESS) in LV networks to enhance reliability.

The proposed approach is applied to the electrical installation of the Electrical Engineering Building (EEB-UIS) at the *Universidad Industrial de Santander* (UIS), Colombia. Case study analysis reveals that the EEB-UIS has low risk regarding high-impact events, with opportunities to strengthen reliability and operation resilience. The study identifies overvoltage issues and load unbalance, suggesting strategies such as an H_2-ESS backup system and implementing energy management. The EEB-UIS power grid is modelled using Matlab & Simulink, allowing simulations to assess the influence of the PV and H_2-ESS location, capacity, and operation on LV network performance. Results indicate that effective distributed source management enhances electrical resilience, particularly in reliability and operation quality. The thesis provides a comprehensive resilience analysis applicable to microgrids and LV networks, emphasizing the potential for extending the methodology to medium voltage distribution networks.

[*] Doctoral thesis

[**] Faculty of Physical and Mechanical Engineering. Department of Electrical, Electronic and Telecommunications Engineering.
Director: German Alfonso Osma Pinto, PhD in electrical engineering.

General Introduction

Solar photovoltaic (PV) systems installed in low-voltage (LV) networks are increasing. The high PV penetration could affect the network's operation in terms of service quality and equipment loadability. The performance of LV networks could be analysed with an "*electrical resilience*" assessment. Electrical resilience represents the network's ability to face and overcome disturbances with a low deviation from the regular operation. It seeks to identify the weaknesses of the system and define strengthening strategies. PV integration could be analysed as a disturbance affecting the operation quality. This thesis aims to evaluate the resilience of the LV networks, integrating the influence of PV systems' connection, size, and operation. It attempts to assess the contribution of energy storage systems (ESS) as hydrogen-based ESS (H_2-ESS) and energy management strategies (EMS). Nevertheless, there is a lack in the consulted literature about a procedure to evaluate electrical resilience in LV networks. There is also uncertainty on the benefit of assessing the electrical resilience of LV networks.

This thesis searches for a resilience definition tailored for LV through the approaches and scenarios used in various domains. Then, it proposes a comprehensive electrical resilience assessment methodology, allowing the analysis of the interconnection of PV and H_2-ESS. Then, it applies the comprehensive resilience assessment to a case study with a warm tropical climate and variable cloudiness. This chapter describes the research remarks, the problem statement, the research questions, and the objectives. Then, it presents the scope, the contributions of the thesis, and the scientific dissemination achieved. Finally, it exposes the structure of this report.

Preliminary remarks about the research

The design of an electrical distribution network must guarantee quality conditions for network operators and users. These conditions are supply continuity, voltage regulation, energy

losses, loadability, and power balance, among others (Deboever *et al.*, 2018). A correct design must ensure the regulatory operating conditions during regular operation and contingencies. Contingencies could be line disconnections, lightning, short-circuit or power variations. These could be due to severe weather conditions, malicious damage by humans, non-linear loads, manoeuvres on the networks, and equipment in poor condition (Dehghanian *et al.*, 2018).

The integration of distributed generation (DG) systems based on renewable energies could also alter the operation of the electrical systems, introducing uncertainty regarding the power generated. Such is the case of PV systems, in which sporadic variations in solar irradiance cause intermittent power generation. Also, the excess PV power not self-consumed in the installation is directed to the supply network, causing inverse power flows. These issues could lead to adverse effects on service quality. Small-scale PV has increased into LV networks among residential and commercial users (Shabbir *et al.*, 2022). LV networks are mainly designed with a radial topology with unidirectional power flows.

Although electric power systems have reached a good level of reliability, the modifications introduced by the connection of small power producers require a specific assessment of the reliability of these new systems.Distribution networks present various functional characteristics, such as loads dispersed in several locations, variable topology and electrotechnical phenomena that must be considered in order to model the events that may occur (Megdiche, 2020). Incorporating distributed energy resources (DER) could modify the operation of the electrical system. It could relieve the loadability of the feeder and power lines and reduce or increase energy losses. However, it could alter regular operations and increase vulnerability to disruptive events (Sadeghian & Wang, 2020).

Researchers such as Brinkel *et al.* (2020) and Aleem *et al.* (2020) have proposed strategies to mitigate the adverse effects of renewable energy sources and encourage their implementation. Also, Hellman *et al.* (2017) and Sun *et al.* (2020) have investigated ESS to mitigate the intermittency of the power generated by PV and wind farms. Murayama *et al.* (2018) implemented ESS to correct voltage regulation and low power factor problems in distribution net-

works. Among the ESS, hydrogen (H_2) energy storage has gained ground due to its capacity for storing large amounts of energy and diverse applications. H_2-ESS finds utility in hybrid generation systems and microgrids for isolated loads or on-grid support, incorporating an electrolyser (EL) and a H_2 reservoir tank, and a fuel cell (FC) for power generation (S. Ma *et al.*, 2021).

On the other hand, electrical resilience is defined as the power network's ability to withstand disturbances without losing the primary operating conditions, reduce the impact on the service quality, recover after the event and adapt to new operating conditions (Rahman *et al.*, 2021). A resilience assessment could characterise the performance of an electrical network. It could be helpful to analyse the effects of the PV integration and the contribution of H_2-ESS to increase network resilience. It could also allow for comparing the performance of strategies to mitigate an adverse event impact. In electrical engineering, the definition proposed by the UK Cabinet Office (2011) for electrical systems infrastructure stands out. They define it as the ability to anticipate, absorb and adapt to a disruptive event and quickly recover.

The U.K. Energy Research Centre (UKERC) describes resilience as the ability of an energy system to tolerate disturbances and continue to deliver energy to users successfully. It indicates that a resilient system can rapidly recover from shocks and provide alternative means of meeting energy demands in external changes circumstances (Chaudry *et al.*, 2011). The researchers consulted have mainly studied the resilience of electrical power systems to extreme and high-impact events. The main events analysed are earthquakes (Ferrario *et al.*, 2022; Nazemi *et al.*, 2020), strong winds (L. Ma *et al.*, 2022; Sabouhi *et al.*, 2020), intentional attacks (Wu *et al.*, 2022; Han *et al.*, 2021), floods (Dvorak *et al.*, 2021), and ice storms (Hou *et al.*, 2023). They evaluate the ability of the electrical systems to withstand several disruptions and contain the emergency.

Studies on the resilience of electrical systems facing medium and low-impact events are addressed to a lesser extent (Mishra *et al.*, 2021; Poulin & Kane, 2021). These assessments include power outages of common origin (Lagrange *et al.*, 2020) and alterations in electrical operating parameters (Mehrjerdi & Hemmati, 2020). They are mainly oriented to distribution networks and microgrids. Their approaches focus on the continuity of power supply in case of

contingency. In this field, energy storage has a notable role to play. For example, Li *et al.* (2017) analyse the use of distributed energy sources such as DG and the integration of natural gas and hydrogen networks to improve the electrical resilience of distribution networks in the face of natural disasters. Galvan *et al.* (2020) evaluate the contribution of PV systems and battery energy storage to the distribution networks' resilience.

Some researchers have studied resilience by the capacity of the electrical system to operate in the isolated mode during power outages. For instance, Hussain & Musilek (2022) study using electric vehicles (EV) to support the electrical networks in outages. It also discusses reusing discarded EV batteries as backup systems for homes and buildings. Tian & Talebizadehsardari (2021) propose using EVs as a backup system for commercial and residential facilities. Other authors like Gupta *et al.* (2019) consider the resilience of an electrical installation as an energy independence level. Integrating an ESS allows energy source diversification and energy management strategies (EMS) implementation. Then, an electrical system could be disconnected from the local supply network in the event of a malfunction and self-supply in power outages. Likewise, Lagrange *et al.* (2020) and Rosales-Asensio *et al.* (2019) analyse the use of ESS for enhancing resilience during outages and integrating EMS to reduce operating costs and strengthen the electrical system performance.

All approaches consulted on the electrical resilience of LV systems point to the ability of the networks to overcome adverse events and recover normal operating conditions after disruptions, guaranteeing the continuity and quality of the supply. However, the literature review appreciates that it has yet to find a unified definition of electrical resilience for LV networks. Some definitions of resilience are qualitative, and the relationship between the approaches needs to be clarified. There needs to be a clear electrical resilience orientation for LV networks. Thus, this thesis proposes a methodology for evaluating the comprehensive electrical resilience of LV networks with PV integration. It also analyses the performance of H_2-ESS integration and EMS to mitigate the adverse effects of PVs. The goal of this thesis is to contribute to the planning of resilient LV networks.

Problem statement

Integrating the PV systems in the LV networks could cause sporadic and intermittent variations in power flows. These effects could be due to short-term weather variations in solar irradiance and temperature (Home-Ortiz *et al.*, 2022). Variations could violate the quality of electrical parameters and sometimes lead to a service collapse (IEEE, 2018). The behaviour of electrical networks in the face of adverse events could be evaluated based on electrical resilience. However, electrical resilience studies mainly aim at power systems facing high-impact disruptive events. They analyse the electrical system infrastructure robustness and the service continuity reliability. More research is still needed in the field of low-impact, high-frequency disturbances.

Researchers have studied two approaches related to the LV networks resilience: *i)* The maximum value of a disturbance that an electrical system can withstand before losing normal operating conditions. And, *ii)* the electrical system capacity to maintain the power supply to critical loads when the operation of the primary power source has been affected or suspended. The first focuses on determining the maximum PV capacity that an LV network can support in a PCC without losing the operational continuity (Chathurangi *et al.*, 2022). This analysis is known as "hosting capacity." However, it evaluates the PV's peak power and the acceptable penetration level, and it does not assess the network's performance in the face of disturbances. The second prioritises the time that an electrical system can guarantee the continuity of the service in the isolated mode in a power outage (Younesi *et al.*, 2022). It also does not consider the effects on the network's performance.

Since PV and ESS integration in LV networks has become widespread in recent years, evaluating their effects on the networks' operation would be convenient. There is also a need to establish complementary operating conditions for the existing LV networks and plan resilient networks in the medium and long-term. Moreover, the growing interest in H_2-based systems draws attention to H_2-ESS for integration into LV networks and take advantage of their features.

ESS could absorb sudden power variations and store energy for backup. H_2 could also link to applications such as heating, cooling and recharging H_2-vehicles. Therefore, there is a need to establish a methodology to assess the electrical resilience of LV networks. The assessment should identify the network's weaknesses and propose strengthening strategies. It would be possible to evaluate the benefit of the H_2-ESS and apply EMS to enhance resilience against adverse events. This way determines the appropriate favourable conditions for integrating PV systems.

Rationale for the research

The analysis of the electrical resilience of LV grids is a crucial topic, given the importance of maintaining a reliable power supply in adverse situations. However, the literature review has highlighted a gap in assessing the electrical resilience of LV networks. The concepts and approaches applied at present have been diverse and have often focused on power infrastructure performance or system reliability without providing a comprehensive approach. The main objective of this research is to propose a comprehensive methodology that addresses this gap and allows for a complete assessment of the LV power systems resilience. The proposed methodology should consider different approaches, allowing a complete analysis of the resilience of the LV power grid according to the types of disturbances it faces. It includes:

- High-impact disturbances, where the ability of the LV grid to withstand natural catastrophes is assessed.
- Low-impact disturbances, where the ability of the power grid to recover from frequent power outages due to common causes is analysed.
- Grid modifications and distributed generation interconnection to assess the ability of the grid to adapt to permanent changes that alter its operation.

Furthermore, in a current context where PV and hydrogen-based systems are gaining relevance, the opportunity to analyse the influence of these systems on the electrical resilience

of LV networks has been identified. The integration of H_2-ESS and PV systems could improve the reliability and quality of service of the electrical grids, so it is proposed to analyse their contribution through the assessment of electrical resilience. To test the effectiveness of this methodology, a specific case study has been selected: the power grid of the Electrical Engineering Building (EEB-UIS) at the *Universidad Industrial de Santander* in Colombia. This network has an on-grid PV system and several energy meters that allow a detailed characterisation of its operation. Although the focus is on a long and medium-term analysis, it is essential to note that the configuration of the energy meter dataloggers limits the possibility of analysing transient effects caused by the integration of distributed generation. Whereas the processor of the EEB-UIS meters can provide information on transient events, it is recognised that simulations are necessary to fully assess the effects of the H_2-ESS and PV systems. Then, these simulations are limited to quasi-static power flows due to the constraints of the data recorded by the meters.

It is important to note that this research focuses on a warm tropical climate area according to the case study location. Then, it is intended to analyse electrical grids under these specific climatic conditions. It is considered that climatic conditions could have a significant impact on the effects of PV systems on LV grids and the load demand of the installation. Although this research is carried out in a particular case study with specific climatic conditions and metering resources, the proposed methodology has an expandable scope and can be applied to LV grids in general. The specific focus on the case study has been adopted to limit the scope of the PhD thesis, but the methodology could be adapted and applied in broader contexts in future work. The following sections develop the objectives and scope of this thesis.

1. Research questions and objectives

LV systems must deal with disruptive events that could affect service quality and cause power outages. They must guarantee their reliable operation in the medium and long-term. Adverse events are high-impact, such as natural disasters and low-impact, such as weather variations. Integrating PV systems could modify the network operating, causing benefits and damages. The electrical grid operators could establish strategies to take advantage of the PVs to face disturbances. Then, plan resilient networks considering PV systems' current or future integration. The thesis's objectives align with the research questions' definition and approach for analysing and improving the resilience of LV electrical networks. It raises a general research question and six specific questions covering the thesis's matters:

General research question
Could a methodology be specifically defined to assess the resilience of LV electrical networks in a warm tropical climate, integrating the electrical performance?

This thesis intends to answer the following research questions (RQ):

- **RQ1.** What kind of information about an LV electrical network that integrates or could integrate PV systems does it require to carry out a comprehensive resilience assessment between the capability to supply users and the operation performance?
- **RQ2.** How could an LV network that integrates PV systems improve the performance of the operation and the capacity to respond to disruptive events?
- **RQ3.** Does the resilience assessment allow comparing the performance of energy management strategies for mitigating disturbances in the LV networks operation?

- **RQ4.** Is incorporating H_2-ESS a viable strategy to increase the resilience of the LV electrical networks?
- **RQ5.** How could it determine if an LV power grid is more resilient on a daily basis?
- **RQ6.** Is it possible to periodically analyse an LV network's resilience level? Would the resilience assessment tool present up-to-date information about future threats and actions to address those threats?

This thesis proposes the following general objective to address the RQs:

General objective
Characterising the influence of specific factors as the location, the installed capacity and operation mode of photovoltaic (PV) generation and hydrogen-based energy storage systems (H_2-ESS) on the resilience level of low-voltage (LV) electrical networks.

Compliance with the general objective involves the following specific objectives (SO):

- **SO1.** Determining the resilience evaluation indices for an LV electrical network that allows analysing the performance of the integration of PV generation and H_2-ESS.
- **SO2.** Establish a procedure to assess the resilience of LV electrical networks with the injection of power from PV systems and H_2-ESS.
- **SO3.** Evaluate the effects of the integration of PV generation systems and H_2-ESS on the resilience of a LV electrical network.
- **SO4.** Analyse the sensitivity of the resilience of an LV electrical network to variations in the level of penetration and location of the PV systems and the H_2-ESS and the application of energy management strategies.

The global relationship between questions, objectives and research needs arises after the literature review and the state-of-the-art development on the impacts and benefits of PV

and H_2-ESS. Moreover, the approach of assessing the electrical resilience of the LV networks for analysis of vulnerabilities and improvement opportunities. Figure 1 shows the relationship between the research questions (RQ) and the thesis objectives (SO). It also presents the contribution of the report's chapters (Ch) for achieving the objectives.

Figure 1

Relationship outline between the thesis' research questions and objectives.

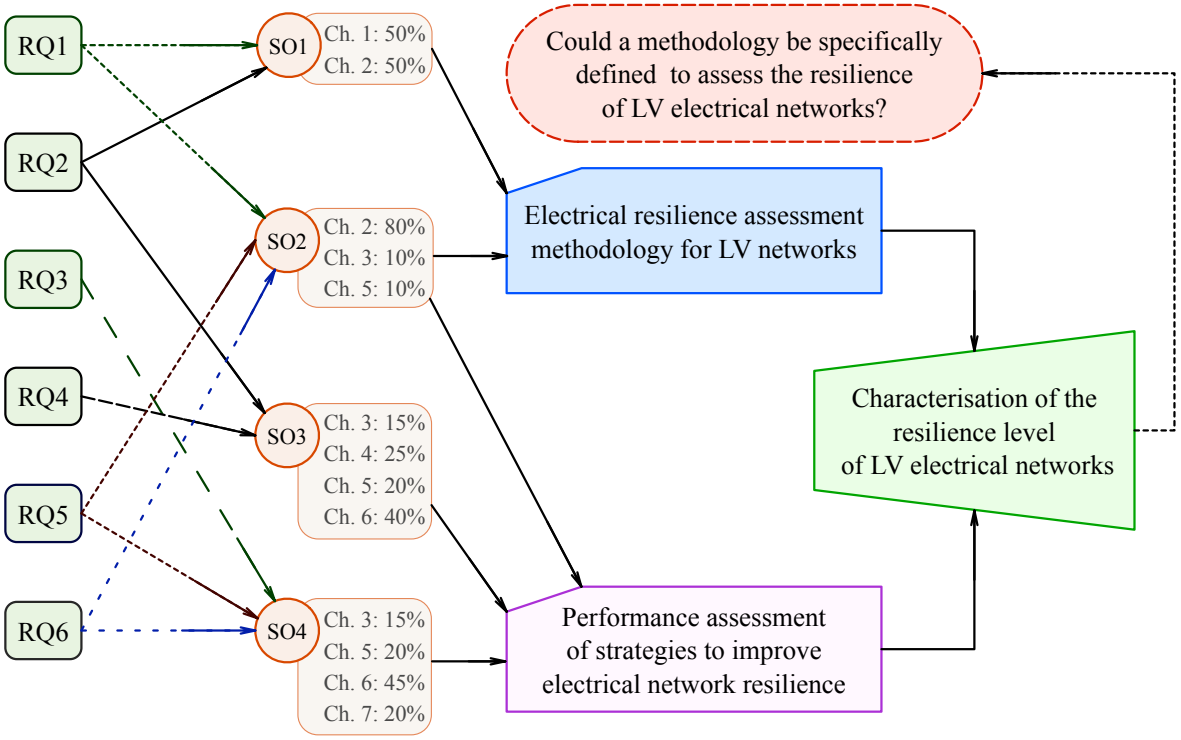

Research scope

This thesis covers the electrical resilience assessment of the LV networks that integrate or could integrate PV generation and are located in warm tropical climates. It proposes studying the H_2-ESS integration applying EMS to strengthen network resilience. It determines the resilience indicator parameters for an LV electrical network based on robustness, operation continuity and quality. It fits resilience indices and proposes a methodology to analyse electrical resilience. It includes high-impact catastrophic events, power outages and quality issues that could cause unfavourable conditions related to the PV systems.

The methodology proposal considers a feedback phase that allows weak network points to be identified and improvement strategies to be defined. It focuses on strengthening the supply's capacity and quality. The feedback integrates quasi-static power flow simulations with 10 minutes of sampling time, allowing the electrical network performance to be analysed. Resilience-strengthening strategies use H_2-ESS and EMS. The resilience assessment proposal has a long-term focus on the robustness of the electrical infrastructure, a medium-term focus on supply continuity capacity, and a short-term focus on service quality.

The proposed methodology is applied to a university building that meets the scope of the thesis. The building has a dedicated feeder and smart meters on the distribution busbars and integrates a PV system. It is also located in a warm tropical climate and variable cloudiness region. Then, this thesis analyses the implementation of a EMS to improve the network's performance in the face of variations in the PV power generated and the load demanded.

Thesis development

This doctoral thesis has been developed within the framework of a double degree co-tutelle agreement between the universities *Universidad Industrial de Santander*–UIS, Colombia, *Université Bourgogne Franche-Comté*–UBFC and *Université de Franche-Comté*–UFC, France. Its preparation covers three stages from September 2019 to December 2023, as outlined in Figure 2. Each stage has had a strategic contribution to the development of the thesis. The stages are described below.

Stage 1: Training at the UIS. This phase has been developed in the facilities of the Department of Electrical, Electronic and Telecommunications Engineering (E^3T), at UIS in Bucaramanga, Colombia. It was from September 2019 to December 2021. It encompassed training in the modelling and analysis of power systems and the development of research in the electrical resilience of power systems. Furthermore, it covers the preparation of the PhD thesis proposal, the arrangement of the case study and the procedure for establishing the co-tutelle agreement.

Figure 2

Timeline of doctoral thesis development.

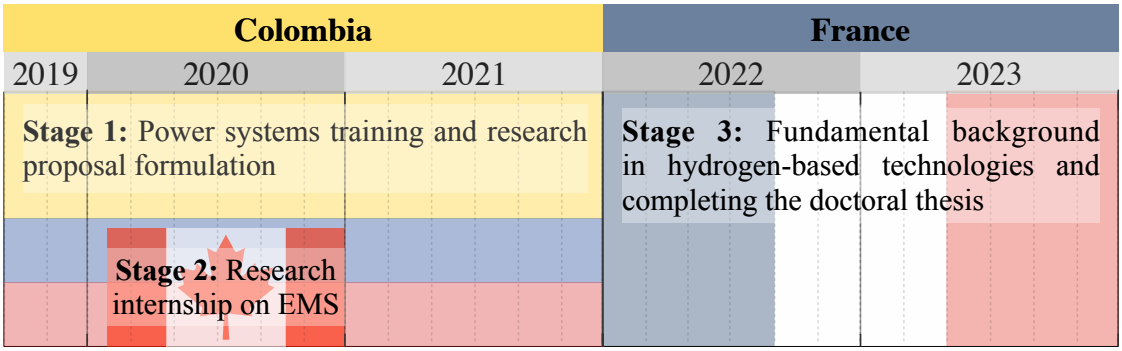

Stage 2: Research internship. The internship took place within the period of Stage 1; it was carried out at the e-TESC Lab of the *Université de Sherbrooke*–UdeS, in Sherbrooke, Canada. It comprised February to December 2020. The internship focused on the development of energy management strategies (EMS). Work was done on the energy management of electric vehicles with multiple sources. Also, an approach to the management of distributed generation sources in power systems was made.

Stage 3: Training at the UBFC. This phase has been developed between January 2022 and December 2023. It has taken place at the FC lab, FEMTO-ST institute of the UBFC in Belfort, France. It covers training in the modelling and analysing systems for hydrogen production, storage and use. The thesis approach has been fine-tuned, and the research proposal has been implemented.

Contributions

Assessing the resilience of LV networks provides information for planning. It would allow improvement strategies for the performance of the operation in the face of short-term climatic disturbances, such as sudden and intermittent variations in solar irradiance and medium-term climatic disturbances, such as temperature variations at different times of the year. Evaluating the resilience of an electrical network against disturbances in operation allows comparing the performance of conventional strategies for mitigating adverse effects by PV integration.

Likewise, it is possible to evaluate the contribution of EMS when ESS are involved. The specific contributions of this PhD thesis are the following:

- This research analyses the existing concepts of electrical resilience in the literature to develop a suitable definition for the resilience of low-voltage (LV) electrical networks. This definition is fundamental to establishing a clear framework to advance the assessment and improvement of the electrical resilience of LV grids.

- Based on the proposed definition of electrical resilience, this thesis presents an original methodology for assessing the resilience of LV grids incorporating PV generation. This methodology is characterised by its comprehensiveness, addressing three distinctive categories of disturbances that power systems may face: *i)* High-impact, low-probability disturbances. *ii)* Low-impact, high-probability disturbances. And *iii)* permanent supply quality disturbances. The methodology provides an integral tool for decision-making in electricity resilience management.

- The definition and methodology of electrical resilience assessment are applied in a concrete case study, illustrating the characteristics and advantages of this approach. The case study focuses on the power grid network of a university building with critical loads, a PV system and a smart metering system. This practical application highlights the applicability and usefulness of the methodology in an actual situation.

- The work includes power flow simulations that integrate the assessment of electrical resilience. These simulations allow a detailed analysis of the influence of hydrogen storage systems (H_2-ESS) and energy management strategies (EMS) on the electrical resilience of the grid in the case studied. Furthermore, the sensitivity of these systems as a function of their connection point and rated capacity is investigated, providing crucial information for the optimisation and improvement of electrical resilience in similar scenarios.

These contributions represent significant advances in understanding and improving electrical resilience in LV grids with PV generation, with practical applications and results that

positively impact the efficiency and reliability of LV power grids. The following section describes the scientific publication contributions accomplished throughout the thesis.

Scientific dissemination

The thesis development has achieved the publication of four papers directly related to the thesis field and two complementary papers. One more paper has been written to submit for evaluation. The dissemination achieved with this thesis is detailed below.

Journal publication–peer-reviewed:

- **Rodriguez, R.**, Osma, G., Bouquain, D., Solano, J., Ordoñez, G., Paire, D., Roche, R., & Hissel, D. (2024). Electrical resilience assessment for low-voltage buildings. *Energy & Buildings*, 313, 114217. doi: 10.1016/j.enbuild.2024.114217 (ENB, Q1 SCImago 2023).

- **Rodriguez, R.**, Osma, G., Bouquain, D., Solano, J., Ordoñez, G., Paire, D., Roche, R., & Hissel, D. (2022). Sizing of a fuel cell–battery backup system for a university building based on the probability of the power outage length. *Energy Reports*, 8, 708-722. doi: 10.1016/j.egyr.2022.07.108 (EGYR, Q2 SCImago 2022).

- **Rodriguez, R.**, Osma, G., Solano, J., Roche, R. & Hissel, D. (2021). A framework for the resilience of LV electrical networks with photovoltaic power injection. *Tecnura*, 25, 71-89. doi: 10.14483/22487638.18629

- Pinzon, O., Gaviria, D., Parrado, A., **Rodriguez, R.**, & Osma-Pinto, G. (2022). Assessment of power quality parameters and indicators at the point of common coupling in a low voltage power grid with photovoltaic generation emulated. *Electric Power Systems Research*, 203. doi: 10.1016/j.epsr.2021.107679 (EPSR, Q1 SCImago 2022).

- Parrado, A., **Rodriguez, R.** & Osma, G. (2021). Resilience assessment in a low-voltage power grid with photovoltaic generation in a university building. *International Review*

of Electrical Engineering, 16(4), 344-359.
doi: 10.15866/iree.v16i4.2032 (IREE, Q3 SCImago 2021).

Complementary Journal publication–peer-reviewed:

- **Rodriguez, R.**, Trovão, J. P., & Solano, J. (2022). Fuzzy logic-model predictive control energy management strategy for a dual-mode locomotive. *Energy Conversion and Management*, 253, 1–13. doi : 10.1016/j.enconman.2021.115111 (ECM, Q1 SCImago 2022).

- **Rodriguez, R.**, Osma, G., & Ordoñez, G. (2022). Sizing of a scattered housing microgrid in a remote rural area. *Renewable Energy and Power Quality Journal*, 20, 43–48. doi: 10.24084/repqj20.214 (RE&PQJ, Q4 SCImago 2022).

Structure of the thesis

This thesis comprises seven chapters addressing the research questions and developing the set objectives:

- **Chapter 2. Theoretical and conceptual framework:** It exposes an overview of the development of PV and H_2-ESS and presents the thesis' state-of-the-art. It deepens in the negative effects of integrating PV generation in LV electrical networks. Finally, it focuses on the existing approaches to evaluating electrical systems' resilience.

- **Chapter 3. Electrical resilience assessment proposal:** It presents the remarks on the electrical resilience in LV networks. It establishes a categorisation for the resilience analysis. Then, it proposes a methodology for assessing electrical resilience in LV networks.

- **Chapter 4. Description of the case study electrical network:** The case study is the Electrical Engineering Building (EEB-UIS) at the *Universidad Industrial de Santander* in Colombia. This chapter describes the electrical network of the EEB-UIS and the arrangement of the smart meters. This information allows the analysis of its electrical resilience and the development of the feedback phase.

- **Chapter 5. Assessing the electrical resilience of the EEB-UIS:** It exposes the application of the electrical resilience assessment methodology in the EEB-UIS. This chapter analyses the comprehensive electrical resilience of the EEB-UIS under the current network conditions.

- **Chapter 6. EEB-UIS LV network model for the resilience feedback phase:** This chapter shows the EEB-UIS network model for the feedback stages to carry out simulations, define ways of improvement, propose sensitivity analysis and test energy management strategies.

- **Chapter 7. Resilience feedback analysis:** This chapter develops feedback based on the electrical resilience analysis of the EEB-UIS to identify the factors to improve the network. It studies improvement strategies considering the integration of H_2-ESS and EMS. It compares through simulations and performs sensitivity analysis for the H_2-ESS and PV systems.

- **Chapter 8. Contribution and general conclusions:** This chapter summarises the thesis' contribution and the objectives' compliance. Then, it stands out the thesis conclusions.

2. Theoretical and Conceptual Framework

Electrical networks are constantly changing to meet the growing power demand, expand coverage, incorporate new technologies, and future project requirements. Electrical systems planning tends to become more environmentally friendly, integrating renewable energy sources (RES), such as photovoltaic (PV) solar systems on large and small-scale. PV systems generate intermittent power. Therefore, the integration of energy storage system (ESS) could be suitable for greater use of PV power production, even in interconnected systems. Hydrogen-based ESS (H_2-ESS) stand out in this field. H_2-ESS have shown advantages at medium and

large-scale. Also, some studies report their feasibility in low-power systems. H_2-ESS could represent an excellent opportunity for integrating hydrogen applications at LV level.

Under this approach, this chapter describes the growth of PV and H_2-ESS and their integration into LV networks. It focuses on the effects that PV might cause in the LV networks operation. It also presents the concept of electrical resilience. This chapter is organised as follows: Section 2.1 describes PV systems evolution and participation in LV networks. Section 2.2 delves into The impacts of PV systems integration. Section 2.3 focuses on hydrogen-based energy storage system. Section 2.4 presents the concept of electrical resilience. Finally, Section 2.5 summarises the results of the bibliographic review.

2.1 Evolution of photovoltaic solar systems in low-voltage networks

PV systems have been in development since the discovery of the PV effect in 1839 by Edmond Becquerel and the design of the first functional solar cell in 1954 with an initial efficiency of 4%. Since then, the PV evolution focused on low-power applications such as rural telephony, and from 1958 the PVs were mainly used for space applications. Around 1973, the private sector and some governments invested in PV systems to supply remote housing and water pumps. By 1983, more than 5000 households were supplied by PV systems worldwide (Ramakumar & Bigger, 1993). The installation of PV systems continued to be developed mainly in industrial applications and power for isolated areas. There was also a steady decline in the price of PV module manufacturing and commercial design improvements, reaching more than 15% efficiency (Hagemann, 1996).

The integration of PV systems in residential and commercial buildings began in the early 1990s when PVs were installed to self-consumption (SC) (Singh *et al.*, 2021). This trend continued until 2009, when the first centralised solar plant DeSoto Solar Energy Center, was installed at a 230 kV transmission line level in Florida, USA (Shah *et al.*, 2015). Since then, PV systems have been involved in low and medium-voltage distribution networks and high-voltage power systems. In the last decade, PV systems have stood out for the progressive reduction of the

acquisition cost and their growth in the participation of the world energy matrix. The cost of electricity generated by PV systems has decreased by approximately 89% since 2010. As of 2021, the average cost of PV systems is 330 USD/kW. It is one of the renewable energy sources with the most significant increase in installed electrical power and also generates approximately 4 million jobs. Figure 3 presents PV installed capacity and power addition worldwide (REN21, 2023).

Figure 3

Installed capacity of PV power worldwide in the last decade.

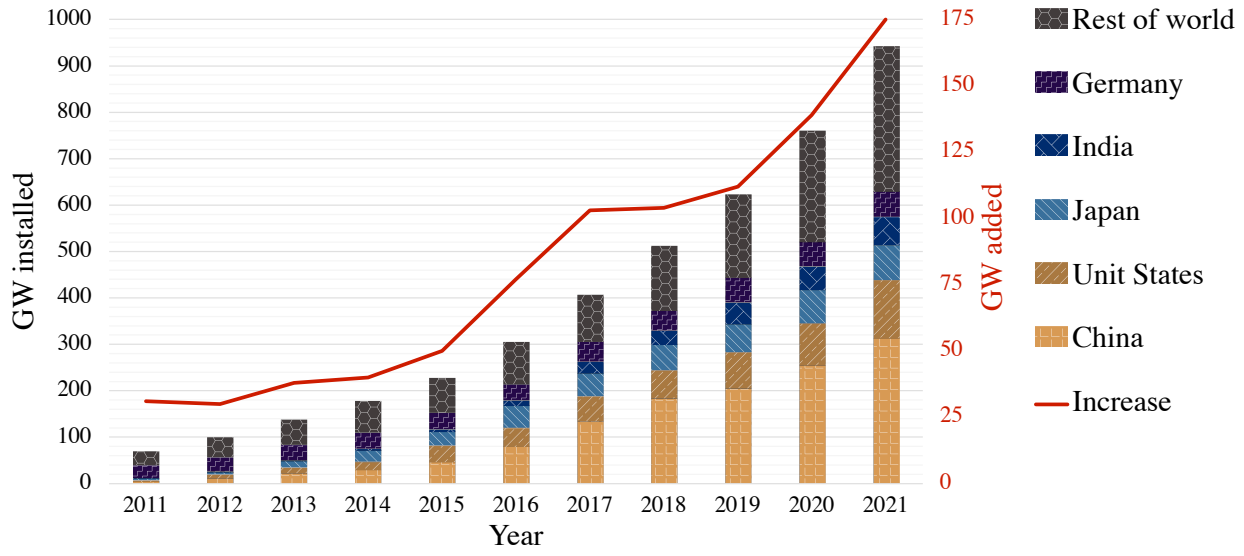

PV power generation corresponds to 5% of global demand. On the 175 GW of PV power added in 2021, 42.8% belonged to the residential and commercial sectors destined for SC, mostly installed on rooftops. 40% of the installed global PV electrical power corresponds to low-power sectors. Nevertheless, the number of projects is high since these installations are designed for less than 100 kW and fit to distributed generation systems installed on distribution networks (REN21, 2023). Many countries are currently directing political efforts to increase the participation of PV systems in LV networks to tend locally to the growing demand for power and benefit from renewable energy and the loss reduction provided by distributed generation.

In the residential and commercial sectors, PV modules are installed on the rooftops and facades of buildings. Some projects have also taken advantage of surfaces such as parking lots, garden roofs, and terraces to double use the PV systems (Agathokleous & Kalogirou, 2020). PV systems installations in buildings face challenges such as the availability of area, the interference of shadows from civil constructions or nearby vegetation and variations in solar irradiance. These factors affect the PV systems operation causing intermittence in the generated power and preventing the PV system from generating the maximum power (Shukla *et al.*, 2016).

Because of the intermittence of PVs and their strict dependence on solar irradiance, it is usual for interconnected PV systems to be configured to operate at the point of maximum power. They inject the generated energy into the primary supply network (Kurdi *et al.*, 2022). The PV power could meet part of the demand of the building, and the power network would supply the missing power or absorb the surplus. Figure 4 shows the typical demand profile of a residential building and the standard generation profile of a PV system in a tropical region. Here, the hours of the greatest generation do not reach the hours of most significant demand. Around noon, the generated PV power supplies the demand, and the surpluses could be injected into the grid.

Figure 4

Typical demand profile of a residential user and standard generation profile of a PV system.

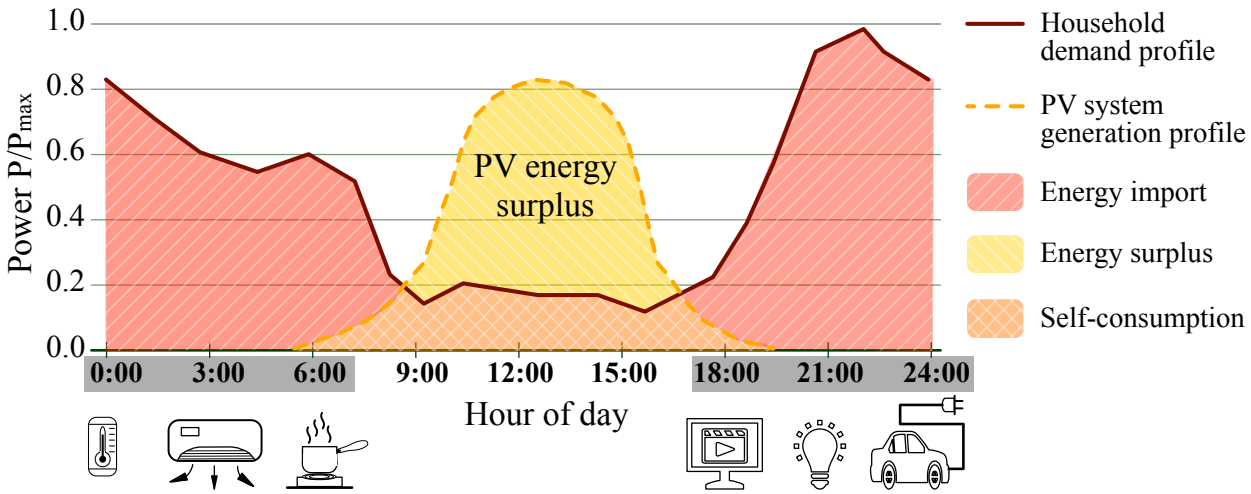

Some researchers have studied the integration of ESS to store and dispatch the generated PV energy. For example, Sharma *et al.* (2020) found it possible to lower the annual electricity cost by installing an ESS for a typical house in southern Norway. In the same way, Zou *et al.* (2022) present a techno-economic analysis of an interconnected PV-battery system performance in an office building. The study uses EMS to maximise SC. Other approaches consider demand-side management (DSM) strategies to shift the hours of most significant demand towards the hours of greatest PV generation. They use differential energy tariffs, financial incentives or penalties for injecting PV power to the local network (Clauß *et al.*, 2017).

This trend has led governments to step up efforts and investments to increase the penetration of RES where PV systems play an essential role in integration into LV networks (REN21, 2023). This way, planning resilient LV networks in the face of the massive integration of PV systems is advisable to ensure their proper functioning and obtain the most significant benefit (Panigrahi *et al.*, 2020).

2.2 Effects of the photovoltaic systems on low-voltage networks

Installing PV on LV networks alters the electrical operation, which could be beneficial in some instances and detrimental in others. PV integration impacts depend on the network architecture, the weather conditions, and the PV's size and setting (Bajaj *et al.*, 2020). Some points in favour could be greater reliability, energy loss reduction, and user economic benefits. Some disadvantages at the LV networks level could be intermittent generation, reverse power flows and overvoltage at the PCC (S. Ma, Chen, & Wang, 2018). In the consulted literature, three groups of effects were identified: *i)* Effects on supply reliability. *ii)* Effects on electrical protections. And, *iii)* Effects on the supply quality. They are described below.

2.2.1 Effects on supply reliability

The PV systems integration could modify the energy reliability of users. It promotes SC and alleviates dependency on the local power grid. Some researchers have analysed the con-

tribution of PV systems to increase network reliability when combined with ESS. For example, Galvan *et al.* (2020) evaluate the potential of the PVs to support the power supply against natural disasters. They integrate a battery-ESS backup system. The performance metrics are the total customer-hours of the outage and customer energy not supplied. Also, Su *et al.* (2019) propose an accurate methodology to evaluate the electrical distribution networks' reliability when PV systems are involved. The assessment proposal analyses the PV's positive and negative impacts on network reliability. It considers three indices of PV generation: The rated power, the power interruption probability, and the power fluctuation. It also integrates two indices for supply in island mode: The average supply time and the average energy for island mode.

2.2.2 Effects on electrical protections

The protection devices of a conventional distribution network are fuses, reclosers, and circuit breakers. Fuses are intended to act against permanent fault currents by generating a permanent current cut-off that requires the attention of a grid operator. Reclosers are orientated to temporary faults that cause high currents of short duration to cut off the current flow during the fault. In prolonged faults, the reclosers remain open until operator intervention. The protection farthest from the supply bus must act first before a fault to isolate the section affected by the failure. The other protections act in sequence if the primary protection does not work. The tripping time of the protections is longer as they get closer to the feeder (Javadian & Massaeli, 2011). Based on exposure by Ates *et al.* (2016) and Paliwal *et al.* (2014), the conventional LV protection schemes have potential vulnerability to the PV integrationdue to three technical issues: *i)* The PV could cause bidirectional power flows in the network. Hence, the coordination of protections based in a unidirectional way could be ineffective. *ii)* The network could present high variations in the current magnitude before switching or abrupt PV generation variations. *iii)* The short-circuit current could increase when PVs are involved.

2.2.3 Effects on the supply quality

The PV power injection could affect the supply quality of LV networks. The variation in solar irradiance and the shading of the PV modules cause sudden variations in the power generated. It could trigger intermittent power injection that affects the performance of the PV system and the electrical network. Some effects could be waveform deformation, power unbalances, reverse power flows, and harmonic distortion (S. Ma, Su, *et al.*, 2018). PVs could cause overvoltage, especially if they are located in the tail of the distribution circuits (Deboever *et al.*, 2018). Figure 5 shows an example of a PV installed at the tail end of a distribution circuit. Here, the PCC is a low-demand node. Furthermore, the PV system generates more power than the load demand, and surplus power is injected into the network. It leads to a reverse power flow causing overvoltage at the PCC (Walling *et al.*, 2008).

Figure 5

Voltage regulation profile of an LV network with PV power injection at the tail point.

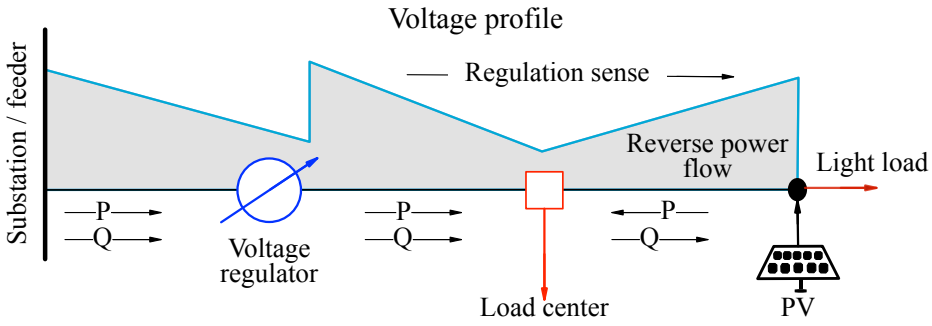

.

PV systems could also help to keep the service voltage parameter within acceptable limits (Aleem *et al.*, 2020). The strategic location of the PV systems reduces current levels in certain sections of the network, which improves voltage regulation and could reduce energy losses within specific scenarios (Montoya *et al.*, 2020). The location of the PV system is critical to achieving greater penetration. For example, Tedoldi *et al.* (2017) proposed a strategic PV system location allowing penetration of up to 50% of the feeder without violating the voltage regulation limits.

On the other hand, PV systems use power inverters to inject the power generated into the alternating current (AC) supply network. Non-linear power inverters could inject distorted and unbalanced current into the electrical system (Borghei & Ghassemi, 2021). An unbalanced power injection of the PV systems could lead to an unbalance in the service voltage; for example, in the case of a single-phase inverter (Emmanuel & Rayudu, 2017).

2.3 Hydrogen-based energy storage systems

Integrating DG and RES in electrical distribution networks has led to the need for monitoring, control and communication systems. It also occasionally requires ESS integration to ensure a proper operation (Celli *et al.*, 2017; Shi *et al.*, 2017). Storing energy could mitigate the negative impact of DG and provide flexibility and energy security for operators and users (Gupta *et al.*, 2019). The ESS incorporation has been studied in various electricity sectors, including residential users (*e.g.* (Murayama *et al.*, 2018; Shi *et al.*, 2017)) and in small-scale generation (*e.g.* (Abdeltawab & Mohamed, 2016; Choi *et al.*, 2016). In these studies, the use of renewable energies is a common factor.

The H_2-ESS could be a workable alternative to support the PV systems installation in LV networks. It can store much energy that could be used to supply critical loads in case of a long-term power outage. It could integrate EMS to support the network operation. PV energy could be used to produce green H_2 for multiple applications (Yue *et al.*, 2021). An H_2-ESS has three essential components: an electrolyser (EL), an H_2 storage tank and a fuel cell (FC). In the energy storage stage, the EL uses electrical energy to separate water molecules ($2H_2O$) into hydrogen ($2H_2$) and oxygen (O_2). A compression system injects the H_2 into a reservoir tank at high pressure. In the energy extraction stage, the FC uses the H_2, through a chemical reaction, supplies electricity, heat and water vapour (Ganeshan & Holmes, 2017). Figure 6 presents the diagram of an H_2-ESS and its relationship with some applications.

The H_2-ESS has a long useful life, and low pollution in operation, in its components' manufacture and final destination. The H_2-ESS allows the possibility of independently sizing

Figure 6

H_2-based storage system integration with other forms of energy.

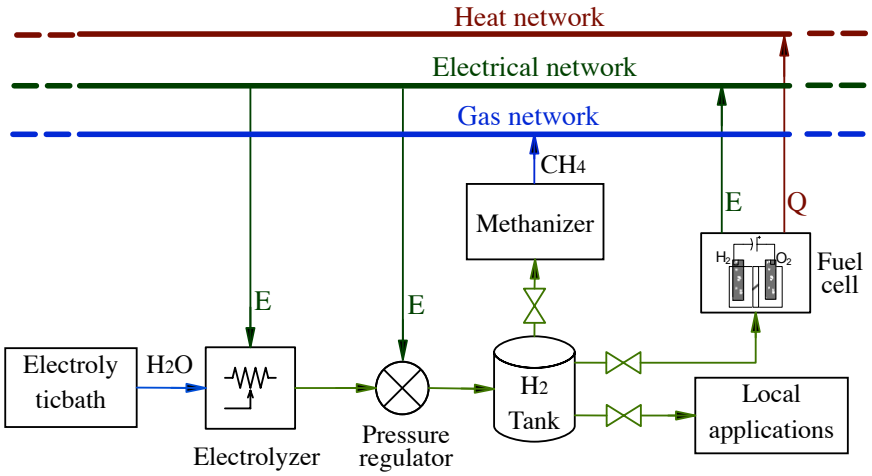

the EL as the capacity of the charging power; the storage tank as energy storage capacity; and the FC as discharge power capacity (Ganeshan & Holmes, 2017). In this sense, it could independently address the adverse effects of PV generation on LV distribution networks and program the operation of H_2-ESS through an EMS (Dong *et al.*, 2016). In this way, the EL could be used as an adjustable load to mitigate sudden variations in the power generated by the PV system. The H_2 tank would be an energy storage and backup medium for power outages. The FC could regulate the service voltage and mitigate the effects of sudden variations in demand (Mizutani *et al.*, 2016).

2.4 Resilience analysis in electrical networks

The concept of resilience has gained strength in the electrical engineering domain. The UK Cabinet Office (2011) define resilience as the ability to anticipate, absorb and adapt to a disruptive event and quickly recover. Also, the UKERC defines resilience as the ability of an energy system to tolerate disturbances and continue to deliver energy service to users successfully. It indicates that a resilient system can rapidly recover from shocks and provide alternative means of meeting energy service demands in external circumstances (Chaudry *et al.*, 2011). The reviewed literature mainly exposes two approaches for the analysis of resilience in LV networks: *i)*

Supply continuity against high-impact events. And *ii)* service quality in the face of low-impact disturbances. They are addressed below.

2.4.1 Supply continuity resilience in the face of high-impact events

The researchers consulted have mainly studied the resilience of electrical systems to extreme and high-impact events. The main events analysed are earthquakes, strong winds, and intentional attacks. They are called high-impact low-probability (HILP) events (Ferrario *et al.*, 2022; L. Ma *et al.*, 2022; Wu *et al.*, 2022). This approach evaluates the ability of the electrical systems' critical infrastructure (CI) to withstand HILP disruptions and contain the emergency. The CI are the towers, poles, substations and power lines. Resilience is measured by a factor of critical loads supplied during the emergency and the restoration time to supply the entire load. Table 1 summarises the analysis scenarios and the resilience indicators for electrical systems facing HILP events.

Resilience analyses involve three phases: *i)* The time the event occurs. *ii)* Disturbed operation state. And, *iii)* restoring system operation (Panteli & Mancarella, 2015). There are also three outstanding parameters: *i)* The probability distribution of HILP event occurrence. *ii)* The fragility of the system's CI before that HILP event. And, *iii)* the service restoration time (Sabouhi *et al.*, 2020). The HILP event frequency relates to the study region's reliability against catastrophes. The CI's fragility corresponds to its collapse probability in the face of a disruptive event. Service restoration time indicates recoverability through repairs or emergency actions. Strategies for strengthening CI involves system adaptations (Shakeri *et al.*, 2017). When a HILP event occurs, the priorities are the integrity of the electrical system, avoiding cascading outages and blackouts, and protecting the CI from catastrophic damage (Jasiūnas *et al.*, 2021). Figure 7 relates the characteristics of the electrical systems' CI and their response to a HILP disruption.

2.4.2 Service quality resilience in the face of a disturbance

The quality of the electrical service analysis focuses on network performance before low-

Table 1

Studies on resilience assessment in electrical networks.

Scenario	Indicator	Description
Several weather conditions	Generation cost (Shang, 2017)	It uses an isolated dynamic microgrid to supply during power outages
	Vulnerability, redundancy and adaptability (Espinoza *et al.*, 2016)	It evaluates the adaptation of power systems to frequent natural disasters
Hurricanes	Risk probability and robustness (Ouyang & Dueñas-Osorio, 2014)	It analyzes power systems with high probability of hurricanes
Natural disasters and human attacks	Supply capacity and restoration time (Bie *et al.*, 2017)	It analyses the infrastructure of power systems and the measures taken around the world
	Reliability, Island-mode (Rahimi & Davoudi, 2018; Haixiang *et al.*, 2017)	They analyse the capacity of DG sources such as electric vehicles and microgrids to improve the resilience of a residential electrical network
Natural disasters in cascade	Reliability and supply capacity (Cadini *et al.*, 2017)	It analyses the capacity of a transmission network to maintain the service in case of climatic disasters
Extreme weather events	Operation cost and power supply capacity (Chong *et al.*, 2017)	It proposes an operation strategy to improve the resilience of power systems

Figure 7

Resilience analysis of an electrical system facing a disruptive event (Shakeri et al., *2017).*

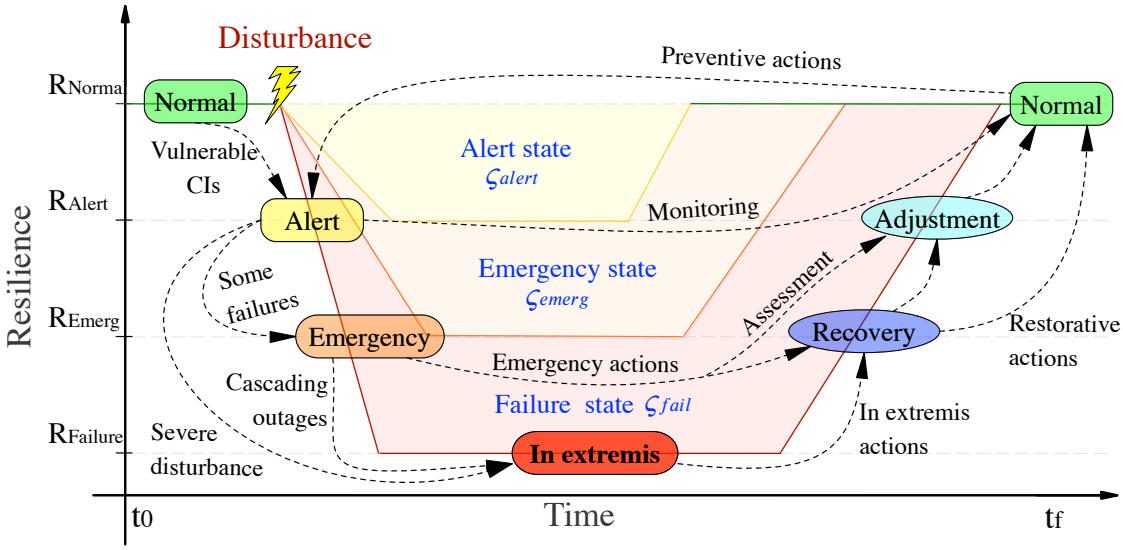

impact disturbances that affect electrical parameters and user comfort (Nowbandegani *et al.*, 2022). These disturbances can be classified into two groups: *i)* Low-impact high-probability (LIHP) events such as accidents of common origin, light failures and repairs causing power outages of short duration. Moreover, *ii)* permanent-effect (PE) events, such as the integration of energy sources or significant loads, could permanently affect the performance of the electrical network. These PE events mainly affect the voltage at the network nodes and fluctuations in power supply (Borghei & Ghassemi, 2021; Deboever *et al.*, 2018).

The electrical performance approaches have integrated a sustainability function $\phi(t)$ representing the electrical operation. For example, R. Rodriguez *et al.* (2021), and Baroud & Barker (2018) model the behaviour of the electrical system by $\phi(t)$ based on a normalised quality parameter. The $\phi(t)$ represents the probability that the network operates in normal conditions or that a disturbance does not occur. LIHP and PE events act as a disturbance function $e(t)$, beginning at time t_e. When the disturbance $e(t)$ is gone, the system experiences a transient state until it seeks stability. After time t_r, the restoring reaches a stable regular operation. Recoverability is the network capacity to reach normal operating conditions. Figure 8 represents the performance of a resilience evaluation index in the face of a disturbance.

Figure 8

Evolution of a resilience index in the face of a disturbance.

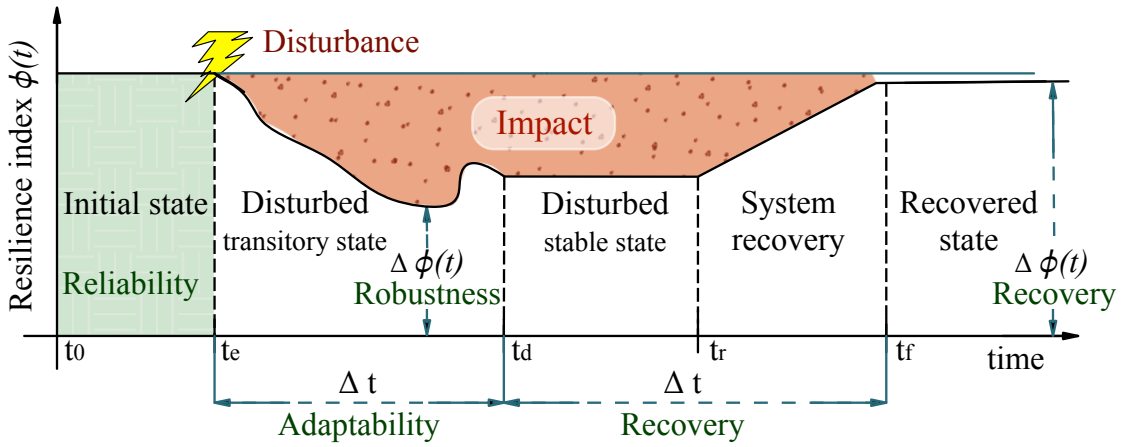

Besides, researchers such as Home-Ortiz *et al.* (2022) have used the concept of *Hosting*

Capacity to evaluate the DG penetration that a network node could support without losing operating conditions or violating regulatory values. Generally, they take the IEEE 1547 Standard (IEEE, 2018) as a reference for operating conditions. *Hosting Capacity* could be appropriated as a resilience metric. It seeks that the electrical networks will not lose the quality of operating conditions due to DG integration.

2.5 Summary of findings

This chapter deals with the integration of PV systems in LV networks. It finds that the trend toward massifying distributed PV systems in LV networks pose challenges regarding the operation of resilient electrical networks. It could make networks vulnerable to generated power fluctuations, and then it could affect the supply's continuity and quality. This chapter also addresses electrical resilience as a strategy for evaluating the performance of electrical networks. It has not found a unified concept to define resilience applied to LV networks. However, some studies are related to using DER to improve the response of LV networks to disturbances.

Existing approaches to electrical resilience could be applied to LV networks to define a comprehensive assessment. It should integrate resilience indices that address the following issues: *i)* The ability of critical infrastructure to withstand high-impact disruptions. *ii)* The capacity of the electrical network to guarantee power supply. And *iii)* the quality in operation.

This chapter provides progress towards the first specific objective (SO1): "Determining the resilience evaluation indices for a LV electrical network that allows analysing the performance of the integration of PV generation and H_2-ESS." It identifies vulnerable features of the supply's continuity and quality against PV integration. Likewise, it answers research questions RQ1 and RQ2, finding that a comprehensive resilience assessment requires information on the vulnerability of the electrical system's CI, on the reliability of serving users and on the quality of service. There are infrastructure, energy management, and hybrid measures to strengthen the resilience of the LV networks.

3. Electrical Resilience Assessment Proposal

This chapter presents a comprehensive electrical resilience (R_{comp}) assessment proposal for low-voltage (LV) networks. It focuses on existing resilience concepts in order to align a definition for LV networks. The critical infrastructure (CI) fragility, supply reliability and service quality approaches are addressed. It follows up on the first specific objective SO1: "Determining the resilience evaluation indices for an LV electrical network that allows analysing the performance of the integration of PV generation and hydrogen-based storage systems (H_2-ESS)." It also outlines the achievement of the SO2: "Establish a procedure to assess the resilience of LV networks with the injection of power from PV systems and H_2-ESS."

It answers research question one RQ1: "What kind of information about an LV electrical network that integrates or could integrate PV systems is required to carry out a comprehensive resilience assessment between the capability to supply users and the performance of the operation?" It further contributes to developing SO3 and SO4, and to answering RQ5 and RQ6. It is organised as follows: Section 3.1 highlights remarks on the resilience in LV networks. Section 3.2 sets out the R_{comp} proposal. Section 3.3 presents the resilience assessment facing HILP events. Section 3.4 describes the strategy to assess resilience regarding LIHP events. Section 3.5 proposes the methodology for evaluating resilience against PE events. Finally, Section 3.6 outlines the chapter conclusions.

3.1 Remarks on the assessment of the resilience in low-voltage networks

The critical infrastructure (CI) of an LV electrical network corresponds to the civil construction and physical elements exposed to possible disruptive threats. These components are feeders, poles, and electrical conductors. Distributed generation (DG) and self-generation (SG) systems are not considered CI for this research. The physical environment influences the relia-

bility of power transmission and distribution systems. Adverse weather conditions exert significantly higher stress on critical infrastructure (CI) than normal weather conditions. It is, therefore, necessary to consider the effects of adverse weather conditions in assessing electrical resilience (Billinton *et al.*, 2002). The supply continuity in the LV networks highly depends on the upstream supply. Issues in the feeders lead to an affectation on the LV side. Networks' CI could face HILP events such as extreme weather conditions and malicious attacks.

In addition, it is usual to schedule service interruptions for adequacy in the distribution networks. Users with critical loads have backup strategies such as supply by two independent distribution circuits, diesel generators or batteries. H_2-ESS and PV could contribute to power backup in case of outages. It is also essential to guarantee the quality of the service for the user. The quality is reflected in the supply continuity and parameters such as frequency and voltage regulation delivered to users. H_2-ESS and PV systems participate in the power flows and could benefit or detriment the quality of the service. In this way, the LV electrical networks cover aspects to apply a resilience analysis.

The concepts proposed by UK Cabinet Office (2011) and Multidisciplinary Centre for Earthquake Engineering Research (MCEER) (Bruneau *et al.*, 2003) are oriented to study CI's resilience against HILP events. Here, they assess possible damage with the CI fragility defined as the probability of collapse conditional on a catastrophic event (Sabouhi *et al.*, 2020). The concept by UKERC (Chaudry *et al.*, 2011) has an operational approach since it tries to analyse the electrical system's performance in the face of a disturbance that does not precisely cause the system's collapse but could affect the service's quality. Here, an operational sustainability index evaluates the electrical system performance facing a disturbance (R. Rodriguez *et al.*, 2021; Baroud & Barker, 2018). This thesis proposes to classify electrical resilience into three type-resiliences according to the disruption level and the effect-term as schematised in Figure 9. The proposed resilience classification for the LV network is described below.

- **Type I resilience (R_I):** It is the ability of the LV electrical network's critical infrastructure (CI) to withstand a high-impact low-probability (HILP) event without losing the supply continuity. The CI are feeders, poles and distribution lines. HILP events include natural disasters and high-impact disruptions. R_I depends on the CI's fragility, the HILP events' intensity and probability of occurrence. R_I could be improved by infrastructural strengthening measures.

- **Type II resilience (R_{II}):** It is the electrical system's capacity to maintain continuity of ser-

Figure 9

Resilience analysis classification proposal for LV electrical networks.

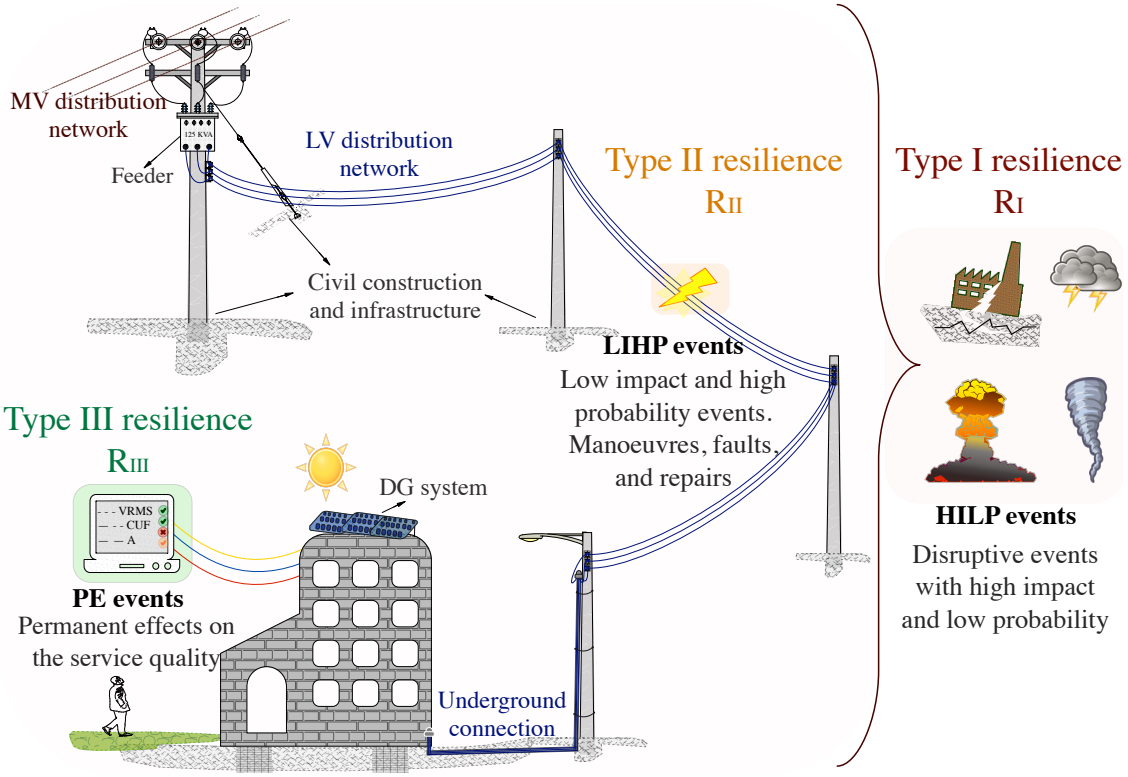

vice against low-impact high-probability (LIHP) disturbances under normal operating conditions. LIHP events involve outages of common origin that do not damage the electrical system's civil structure. They could be extended scheduled power outages, switching under load, and short-circuit failures. R_{II} depends on the feeder's reliability and corresponds to a mid-term analysis.

- **Type III resilience (R_{III}):** It is the electrical system's ability to guarantee service quality at the supply points considering the permanent-effect (PE) events. This thesis considers as PE events the integration of DG and SG since they could modify the operation of the LV network. A PE could become favourable or unbearable depending on the new performance of the electrical grid. R_{III} depends on the network's components and their settings. R_{III} could improve by installing equipment for quality correction or implementing energy management strategies (EMS).

Table 2 outlines the type-resilience classification, the focus of each and the disruptive events to which they relate. The following section outlines the electrical comprehensive resilience (R_{comp}) approach that this thesis proposes.

Table 2

Classification of electrical type-resilience for LV networks.

Type-resilience	Approach	Disturbance coverage
Type I (R_I)	Ability of the critical infrastructure of the electrical system to resist high-impact civil disturbances.	High-impact low-probability (HILP) events affecting the civil structure of the electrical grid. Such as natural disasters, hurricanes, earthquakes and floods. It also includes terrorist attacks, major power failures and similar disruptions.
Type II (R_{II})	Reliability of continuous supply to the critical loads of an electrical installation.	Low-impact high-probability (LIHP) events that produce short-term restoration power outages. Such as minor asset accidents, short circuit failures, scheduled power outages, power grid maintenance, etc.
Type III (R_{III})	Capacity of the electrical installation to guarantee the quality of the supply in the event of permanent changes in operation.	Events with permanent-effect (PE) in the operation of the electricity system, such as the incorporation of new energy sources, the reconfiguration of the grid, the inclusion of unbalanced loads and the occurrence of harmonic pollution, among others.

3.2 Comprehensive electrical resilience of LV networks

This research aims to assess the type-resiliences quantitatively. It analyses the specific contribution of each of them to determine a comprehensive electrical resilience (R_{comp}). The R_{comp} analysis comprises five parts, three concerning assessing the current resilience of the electrical installation. Two more parts focus on feeding back the results to develop strategies to strengthen the resilience of the electrical system. Figure 10 presents their sequential relationship, the parts comprising as described below.

Part 1 is the characterisation of the electrical network to be studied. It collects information about the HILP events in the study region representing threats. It determines the fragility

Figure 10

Methodology for the comprehensive electrical resilience assessment.

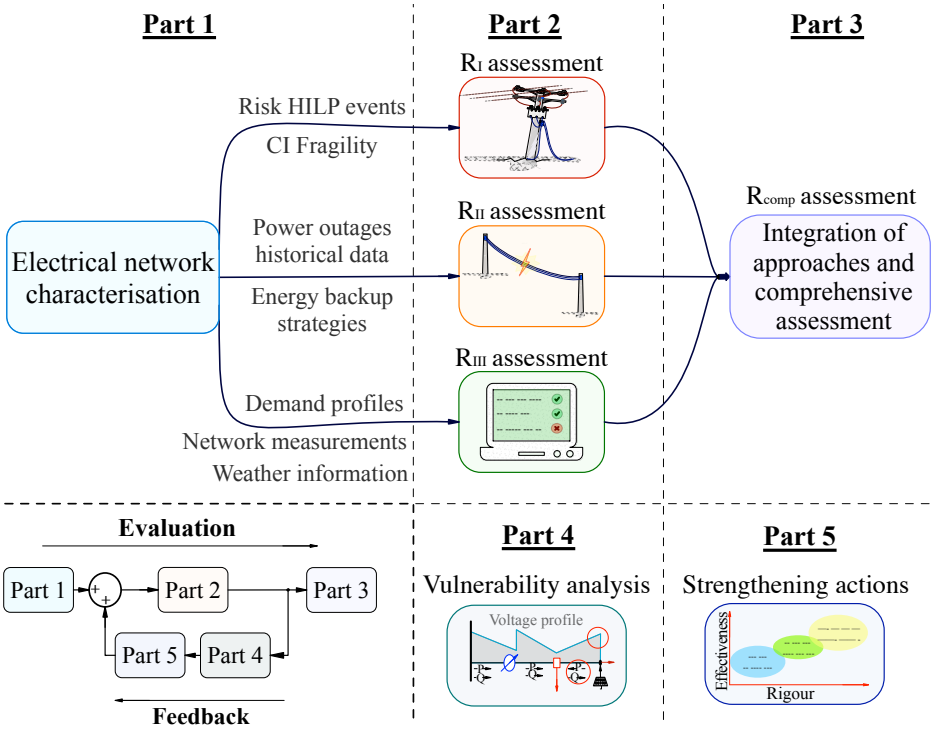

of the network's CI regarding HILP risk events. It also uses historical data on power outages, grid operation measurements, and weather information. Each type-resilience requires accurate information for its assessment. **Part 2** is the evaluation of the type-resiliences. It processes the information collected in Part 1 to determine R_I, R_{II}, and R_{III}. Their assessment methodology are exposed in sections 3.3, 3.4, and 3.5, respectively. **Part 3** is the analysis of the contribution of each type-resilience establishing R_{comp}.

Part 4 and **Part 5** are the feedback phases. They correspond to identifying weak aspects and proposing resilience-strengthening strategies, respectively. When possible, the feedback phase is optional for implementing measures to enhance resilience. These measures focus on implementing and managing H_2-ESS and PV systems. After a feedback measure, new assessments of the type-resiliences are necessary to establish the improvements.

In LV networks' type-resiliences, an implicit hierarchy governs their evaluation. This hierarchical structure demands specific prerequisites for assessing each level of resilience. At the

pinnacle of this hierarchy stands R_I, the most fundamental type-resilience, which must be a foundational requirement. Following in the ranking are R_{II} and R_{III}, each necessitating certain conditions for their assessment. In the case of R_{II}, an active infrastructure within the electrical system becomes imperative. This infrastructure enables the assessment of the system's resilience concerning its capability to handle disturbances and maintain functionality. Similarly, to evaluate R_{III}, an uninterrupted energy supply is essential. Without this crucial element, the assessment of R_{III} becomes infeasible, preventing the study of an electrical system's response when deprived of service.

Thus, R_I holds the highest rank in the implicit type-resilience hierarchy, acting as the foundational requirement. R_{II} and R_{III} follow suit, each building upon the previous level, forming a cohesive framework for comprehending the resilience of LV networks. Type-resiliences have the range $[0,1]$. Five characteristic resilience conditions are proposed: *i)* Ideal condition, here resilience is equal to 1. *ii)* Acceptable condition that has a range $[0.9\ ,\ 1)$. *iii)* Alert condition with a range $[0.7\ ,\ 0.9)$. *iv)* Emergency condition, range $(0\ ,\ 0.7)$. And, *V)* non-functional condition, here resilience is equal to 0. Then, the R_{comp} analysis indicates the overall likelihood that the electrical network operates correctly in an integral way. If any type-resilience is null, R_{comp} is also null since the electrical system cannot sustain the power supply. Figure 11 shows the split of R_{comp}. It presents a mathematical formulation sketch of the type-resilience approaches. The following sections outline the methodology for assessing the type-resiliences and the origin of their parameters.

3.3 Type I resilience before high-impact low-probability events

The R_I resilience assesses the capacity of an electrical network's CI to withstand HILP events. It is proposed to evaluate R_I as the probability that the network's CI will not collapse conditioned on HILP events. It allows an assessment between 0 and 1. The valuation $R_I = 1$ indicates there is no probability that the CI will collapse due to HILP events. The R_I assessment has three stages: *i)* The characterisation of HILP risk events. *ii)* The analysis of the CI network's

Figure 11

Comprehensive electrical resilience split.

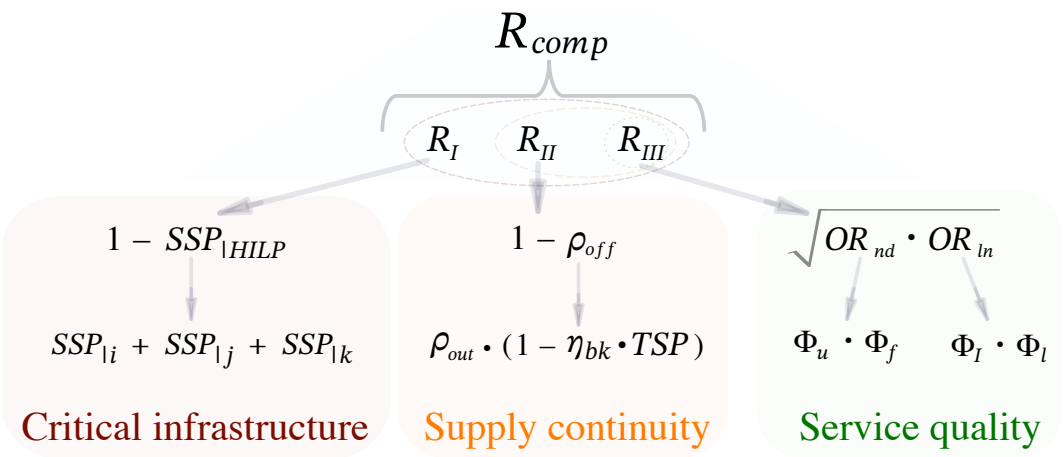

fragility regarding risk events. And *iii)* the integration of risks to determine R_I. Figure 12 shows the methodology for assessing R_I resilience. Then, the stages are described.

Figure 12

Methodology to assess type I resilience.

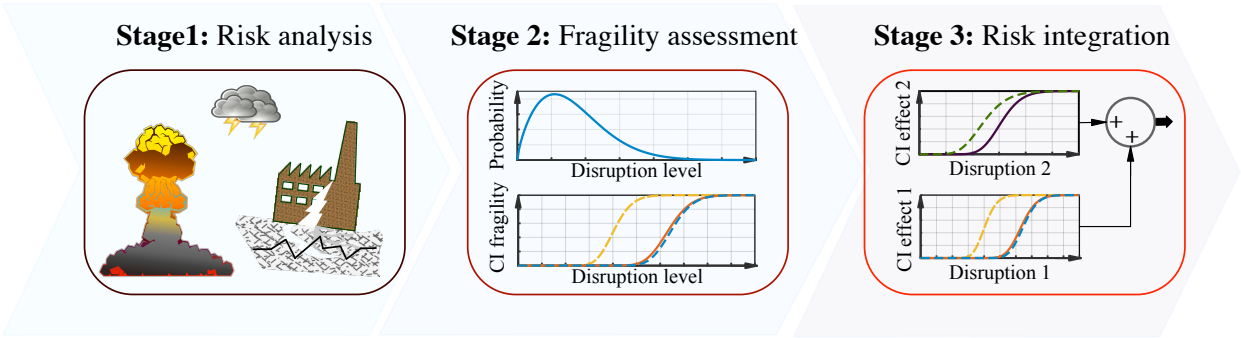

3.3.1 Stage 1: Analysis of HILP risk events

This stage analyses the meteorological risk conditions in the region of the electrical network under study. It identifies the HILP events in the study region according to historical information available. Then, it determines the recurrence and level of risk of the events. This stage selects the HILP events to analyse in the R_I assessment. A detailed analysis of each event is carried out to understand its possible impact on the network's CI and, in this way, to be able

to make informed decisions to strengthen and improve the R_I resilience of the system against future similar events.

The main risk events are earthquakes, strong winds, and intentional attacks. However, each region could have particular HILP risk events. The outputs of this stage are the number N_D of HILP events representing a collapse threat for the network's CI. The probability of occurrence ρ_d and the probability distribution function PDF_d of intensity for each d-event. ρ_d and PDF_d could be made from measurements in the study region, historical data, or standardised probability functions.

3.3.2 Stage 2: Assessment of CI fragility against risk HILP events

CI fragility is the probability of collapse as a function of disturbance intensity. It could be represented with a cumulative distribution function (CDF) since as the level of disruption increases, the likelihood of failure increases until it reaches 100% (Salman *et al.*, 2015). Determining the fragility functions requires an extensive study for each CI and event. The network's CI have a fragility performance concerning each HILP d-event. It is necessary to characterise the fragility for the poles $fr_{[p|d]}$ and the electrical lines $fr_{[ln|d]}$ concerning the d-event. This characterisation could be obtained through experimental, statistical methods, analytical techniques, expert judgment or the combination of methods (Tari *et al.*, 2021).

According to the research carried out by Salman *et al.* (2015) and Bjarnadottir *et al.* (2013), the fragility curve could be modelled with a log-normal CDF. This thesis proposes the stress state probability index $SSP_{|d}$ representing the probability that the network's CI collapses when the d-event occurs. Eq. (3.1) presents the $SSP_{|d}$ formulation. Here $\rho[d]$ is the probability ρ_d of the d-event, and $\rho[F_{CI}]$ is the probability that the CI will collapse. $\rho[F_{CI}|d]$ is the probability that the network's CI will collapse due to the d-event.

$$SSP_{|d} = \rho[d \cap F_{CI}] = \rho[d] \cdot \rho[F_{CI}|d] \tag{3.1}$$

Since the network's CI is the set of poles and lines, the probability $\rho[F_{CI}|d]$ is the union

of the failure probability of the poles $\rho[F_p|d]$ and the lines $\rho[F_{ln}|d]$ as Eq. (3.2) presents. Then, $\rho[F_p|d]$ and $\rho[F_{ln}|d]$ depend on the same d-event at the same time; they are overlapping probabilities. Thus, $\rho[F_{CI}|d]$ is the maximum value between $\rho[F_p|d]$ and $\rho[F_{ln}|d]$.

$$\rho\left[F_{CI}|d\right] = \rho\left[(F_p|d) \cup (F_{ln}|d)\right] = max\left\{\rho[F_p|d]\ ;\ \rho\left[F_{ln}|d\right]\right\} \tag{3.2}$$

According to the findings of Roy & Matsagar (2020), the probability $\rho[F_i|d]$ that the i-infrastructure fails given the d-event depends on the d-even's x-intensity. It is obtained from the infinite sum of the intercepts for each x_j intensity. Eq. (3.3) presents the mathematical development to calculate the probability of failure. Then, the sum represents the integral of the product between the probability $\rho[d_{|x}]$ that the d-event has x-intensity and the probability $\rho[F_{i|x}]$ that the i-infrastructure collapses at x-intensity.

$$\rho\left[F_i|d\right] = \sum_{j=1}^{\infty} \rho\left[d_{|x_j} \cap F_i\right] = \int_0^{\infty} \rho[d_{|x}] \cdot \rho[F_{i|x}] \cdot dx \tag{3.3}$$

$\rho[d_{|x}]$ and $\rho[F_{i|x}]$ correspond to the probability density function $PDF_d(x)$ and the fragility function $fr_{[i|d]}(x)$ respectively as a function of x-intensity. Integrating Eq. (3.2) and Eq. (3.3) into Eq. (3.1), and replacing the equivalent parameters, $SSP_{|d}$ could be rewritten as Eq. (3.4) shows. Here, x_d corresponds to the measurement unit for the d-event intensity in the range $[0,\infty)$. $SSP_{|d}$ should be evaluated for all N_D HILP risk events identified in Stage 1.

$$SSP_{|d} = max\left\{\int_0^{\infty} PDF_d(x_d) \cdot fr_{[p|d]}(x_d) \cdot dx_d\ ;\ \int_0^{\infty} PDF_d(x_d) \cdot fr_{[ln|d]}(x_d) \cdot dx_d\right\} \tag{3.4}$$

3.3.3 Stage 3: Integration of stress from HILP risk events

The R_I resilience considers the N_D risk events determined in Stage 1 and analysed in Stage 2. The total stress state probability ($SSP_{|HILP}$) is the union of the partial probabilities $SSP_{|d}$. $SSP_{|HILP}$ represents the probability that the network's CI will collapse due to HILP events. Considering that HILP events occur independently, the union of events equals their

sum as Eq. (3.5) presents. R_I resilience is the probability that the network's CI does not collapse facing HILP events. Then, R_I is the complement of $SSD_{|HILP}$ as Eq. (3.6) shows.

$$\begin{aligned} SSP_{|HILP} &= SSP_{|d_1} \cup SSP_{|d_2} \cup \cdots SSP_{|d_k} \cdots \cup SSP_{|d_N} \\ &\quad -(\, SSP_{|d_1} \cap SSP_{|d_2} + \cdots + SSP_{|d_1} \cap SSP_{|d_k} + \cdots) \\ &= \sum_{k=1}^{N_D} SSP_{|d_k} - \sum_{k=1}^{N_D} \left(\sum_{j=k+1}^{N_D} SSP_{|d_k} \cdot SSP_{|d_j} \right) \end{aligned} \tag{3.5}$$

$$R_I = SSP^C_{|HILP} = 1 - SSP_{|HILP} \tag{3.6}$$

3.4 Type II resilience against power outages

The R_{II} resilience is the ability of the electrical system to guarantee the supply facing LIHP events. This thesis evaluates R_{II} by the probability that the LV network supplies power in normal operating conditions. The R_{II} assessment has three stages: *i)* The characterisation of power outages due to LIHP events. *ii)* The reliability analysis of backup systems. And *iii)* the evaluation of the electrical system capacity to guarantee the supply. The stages are addressed below.

3.4.1 Stage 1: Power outages characterisation

LIHP events originate from various sources, such as short circuits caused by animals or tree branches, minor accidents involving assets, and scheduled power outages. These events do not result in significant damage to the electrical system's CI. However, a LIHP could lead to a power outage, typically resolved within minutes. Due to the diverse nature of LIHP events, they are categorised as power outages, and a power outage state factor ρ_{out} is defined in Eq. (3.7).

$$\rho_{out} = \frac{1}{T_{tot}} \cdot \sum_{i=1}^{N_{out}} \left(T_{out_i} \right) \tag{3.7}$$

ρ_{out} represents the probability of being in an outage state. Here T_{tot} is the observation time equal to or greater than one year. N_{out} is the total number of outages during T_{tot}, and i is the outage indicator. T_{out_i} corresponds to the i-outage length. The data could be measured or provided by the electrical network operator.

3.4.2 Stage 2: Backup systems reliability analysis

Electrical installations could integrate energy backup systems. These systems increase the supply continuity capacity providing power in an outage. The total supply probability (TSP) index is proposed to evaluate their contribution. TSP is the probability that the backup system will meet the demanded load during all outages in T_{tot}. The TSP index evaluates the power backup systems' contribution to the electrical installations' reliability. It highlights the effectiveness and reliability of a backup system to guarantee the continuity of power supply. Figure 13 presents the proposed methodology to determine TSP comprising four steps. The steps are detailed below.

- **Step 1: Information acquisition.** It collects historical data on the power outage lengths for at least one year. It characterises the backup system's power and energy size, operation modes, and the backup system's support load. The information collected must be rigorous and adequate, as Step 1 lays the groundwork for the reliability analysis.

- **Step 2: Power outages characterisation.** Here the history outage length data is organised into frequency intervals. This step fits the frequency intervals to a probability density function $PDF(lh_{out})$ based on the length of outages (lh_{out}). It characterises the PDF parameters to make a cumulative distribution function $CDF(lh_{out})$. The PDF and CDF functions represent the characterisation of the power grid concerning power outages of common origin.

- **Step 3: Backup time determination.** It models the electrical network supported by the backup system. It determines the backup time T_{bk} that it could supply through calcula-

Figure 13

Methodology to estimate the total supply probability (TSP).

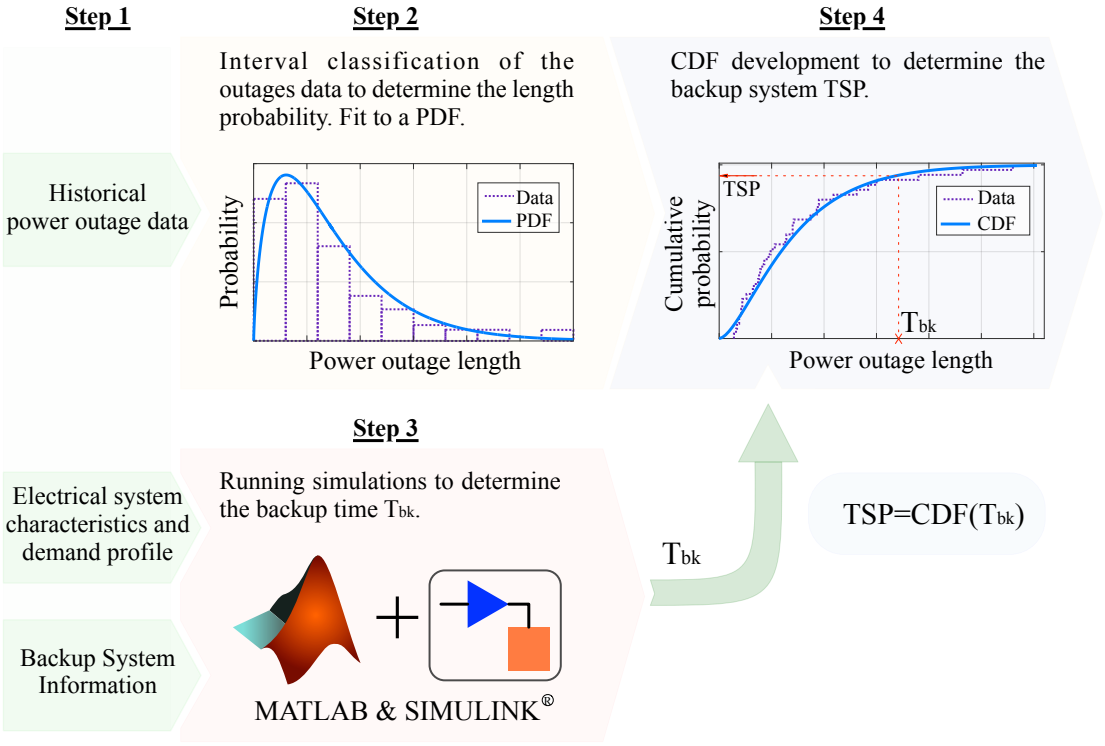

tions or simulations at maximum demand. In addition, the data analysis helps to size a backup system adapted to the electrical network under study to meet the needs in case of power outages.

- **Step 4: TSP definition.** It evaluates T_{bk} at $CDF(lh_{out})$ determined in the Step 2 to define TSP; $TSP = CDF(T_{bk})$. Considering that backup systems could be designed to support the critical load during a power outage, it is essential to consider a backup factor η_{bk}. The backup factor regards the scenario where the installation cannot support the entire load demand. The η_{bk} formulation is shown in Eq. (3.8). Here, $Load_{bk}$ is the load supported in emergency, and $Load_{tot}$ is the total LV network load.

$$\eta_{bk} = \frac{Load_{bk}}{Load_{tot}} \tag{3.8}$$

3.4.3 Stage 3: Evaluation of the supply continuity capacity

The two previous stages are used to determine the probability of no supply ρ_{off} as Eq. (3.9) presents. ρ_{off} is the probability that the electrical network will not supply the loads through the feeder or a backup system. On the other hand, R_{II} denotes the probability that the electrical network will successfully supply the demand before LIHP events. Then R_{II} could be expressed as the complement of ρ_{off} as Eq. (3.10) shows. This approach serves as an indicator to assess the overall reliability of the electrical system and its ability to maintain uninterrupted power supply during critical situations.

$$\rho_{off} = \rho_{out} \cdot \left(1 - \eta_{bk} \cdot TSP\right) \tag{3.9}$$

$$R_{II} = \rho_{off}^{C} = 1 - \rho_{off} \tag{3.10}$$

3.5 Type III resilience in the face of permanent effects

The R_{III} resilience is focused on analysing the quality of the power supply of an LV network. Thus, this research considers that PV systems permanently affect the operation quality due to intermittent power injection. It gets focused on essential parameters that guarantee a proper electrical service. The operation quality of LV networks is mainly reflected in voltage regulation, frequency stability, voltage unbalance and harmonic distortion (Parrado, 2020).

This thesis proposes to assess R_{III} by the probability that the network's quality parameters (QP) operate in acceptable values. This way, R_{III} has the range $[0,1]$. $R_{III} = 0$ implies that QPs are in unacceptable values that do not allow electrical operation. $R_{III} = 1$ indicates that the QPs always remain at ideal values. A four-stage methodology is proposed to evaluate R_{III}: *i)* The selection and measurement of electrical quality parameters (QP). *ii)* The normalisation of QPs in quality indices (ϕ_{QP}). *iii)* The evaluation of operation resilience indices (Φ_{QP}). *iv)* The integration of the operation resilience indices to find R_{III}. Figure 14 shows the R_{III} assessing

methodology; then, the stages are described.

Figure 14

Methodology to evaluate the operation electrical resilience.

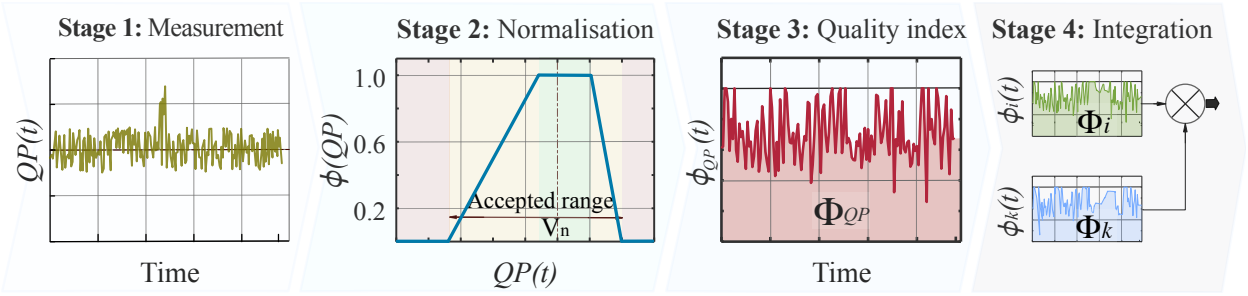

3.5.1 Stage 1: Selecting the electrical quality parameters

There are standards on quality of electrical service with an international scope, such as IEC 61000-3-6 (2008), EN 50160 (2010), ANSI C84.1 (2016), and IEEE Std 519 (2014). Also, the IEEE Std 1547 (2018) establishes criteria for the interconnection of DER in distribution networks. They set standards for the supply service and the interconnection of new components. This research proposes to classify the QPs into two groups: *i)* Voltage QPs related to the voltage supply quality. And *ii)* current QPs representing the quality of the current and power demanding the load.

According to the literature review, the QPs most affected by the PV systems integration are selected. Voltage QPs are voltage regulation (u), frequency (f), voltage unbalance factor (VUF), and total harmonic distortion of voltage ($THDv$). Current QPs are current level (I), energy losses (p_{loss}), current unbalance factor (CUF), and total harmonic distortion of current ($THDi$). By generalisation, u, f, and I are processed into per unit values u_{pu}, f_{pu}, and I_{pu}, respectively. p_{loss}, VUF, $THDv$, CUF, and $THDi$ are analysed in percentage values. These parameters must be measured and recorded during the operation of the electrical system. The measurement points should also be appropriately determined. The following stages describe the processing of the QPs data.

3.5.2 Stage 2: Normalisation of quality parameters

A normalisation operator $\Gamma(QP_k)$ based on international quality standards is proposed to analyse the QPs record. Here, QP_k is the k-quality parameter inspected. $\Gamma(QP_k)$ is a correspondence function that assigns a value ϕ_k between 0 and 1 depending on the measured value QP_k. The quality indices $\phi_u(u_{pu})$, $\phi_f(f_{pu})$, $\phi_{VU}(VUF)$, and $\phi_{HDv}(THDv)$ correspond to u, f, VUF, and $THDv$, respectively. Moreover, $\phi_I(I_{pu})$, $\phi_l(ls)$, $\phi_{CU}(CUF)$, and $\phi_{HDi}(THDi)$ correspond to I, p_{loss}, CUF, and $THDi$, respectively.

A normalised index $\phi_k(QP_k)$ has a range $[0,1]$ according to the following characteristic resilience conditions: *i)* Ideal condition, $\phi_k(QP_k) = 1$. *ii)* Acceptable condition, $\phi_k(QP_k) \in [0.9\ ,\ 1)$. *iii)* Alert condition, $\phi_k(QP_k) \in [0.7\ ,\ 0.9)$. *iv)* Emergency condition, $\phi_k(QP_k) \in (0\ ,\ 0.7)$. And, *V)* non-functional condition, $\phi_k(QP_k) = 0$. The operator $\Gamma(QP_k)$ is formulated as a piecewise linear function. A matching range of QP_k is identified for each operation resilience condition. The voltage and current QPs terms to determine correspondence ranges are described below.

For voltage quality parameters:

- *Voltage regulation index $\phi_u(u_{pu})$:* According to the EN 50160 (2010), and ANSI C84.1 (2016) standards, the voltage regulation in LV installations must not exceed ±5% under normal conditions. In the event of a contingency, a slightly wider voltage regulation tolerance of ±10% is deemed acceptable, as it allows for short-term deviations from the nominal voltage without causing significant disruptions to the system. However, it is crucial to promptly address and resolve the contingency to bring the voltage levels back within the normal range. Any significant deviation exceeding ±15% from the nominal voltage level is considered highly critical and potentially dangerous.

- *Frequency index $\phi_f(f_{pu})$:* In compliance with the EN 50160 (2010) and the ANSI C84.1 (2016) standards, frequency is a critical parameter that governs the stability of the electrical system. During normal operating conditions, the electrical supply frequency should

ideally remain within an admissible variation of ±1% from the nominal value. In the event of a contingency, a wider frequency variation is allowed. The standards recommend a deviation of up to −6% and +4% from the nominal frequency. Any frequency variation exceeding these permissible limits could have severe consequences. Such deviations would lead to instability within the electrical system, potentially causing cascading failures and, in the worst-case scenario, a complete blackout.

- *Voltage unbalance index $\phi_{VU}(VUF)$:* Following the EN 50160 (2010) and IEC61000-2-2 (2018), the VUF must be less than 2% in normal operating conditions. This level of VUF is essential to prevent excessive stress on the connected equipment and reduce losses. In ideal conditions, it is expected that the VUF should be even lower, aiming for less than 0.5%.

- *Voltage harmonic distortion $\phi_{HDv}(THDv)$:* Per the EN 50160 (2010) and IEEE Std 519 (2014), the voltage's $THDv$ should not exceed 8% in the LV supply. Individual harmonic distortions must be kept below 5% to ensure optimal system performance. Any values exceeding these limits indicate poor quality of electrical supply and demand immediate attention and corrective action.

The permissible limits values of the voltage QPs defined by the quality standards are used to define the correspondence with the set resilience conditions. Table 3 presents the proposed correspondence ranges for the voltage QPs and Figure 15 shows their normalisation operator $\Gamma_k(QP_k)$ graphs. In the following, the current QPs are addressed.

Table 3

Voltage QP ranges defining the normalised operation resilience indices.

Resilience range	Voltage QP range			
	u_{pu}	f_{pu}	$\%VUF$	$\%THDv$
Ideal– [1.0]	[0.98, 1.02]	$f_{pu} = 1.0$	[0.0, 0.5]	[0.0, 1.0]
Acceptable–[0.9, 1.0)	[0.95, 0.98); (1.02, 1.05]	[0.99, 1.01]	(0.5, 1.0]	(1.0, 3.0]
Alert–[0.7, 0.9)	[0.90, 0.95); (1.05, 1.10]	[0.97, 0.99); (1.01, 1.02]	(1.0, 1.5]	(3.0, 5.0]
Emergency–(0.0, 0.7)	(0.85, 0.90); (1.10, 1.15)	(0.94, 0.97); (1.02, 1.04)	(1.5, 2.0)	(5.0, 8.0)
Non-functional– [0]	$0.85 \geq u_{pu} \geq 1.15$	$0.94 \geq f_{pu} \geq 1.04$	$VUF \geq 2\%$	$THDv \geq 8\%$

Figure 15

Normalisation operators for voltage quality parameters.

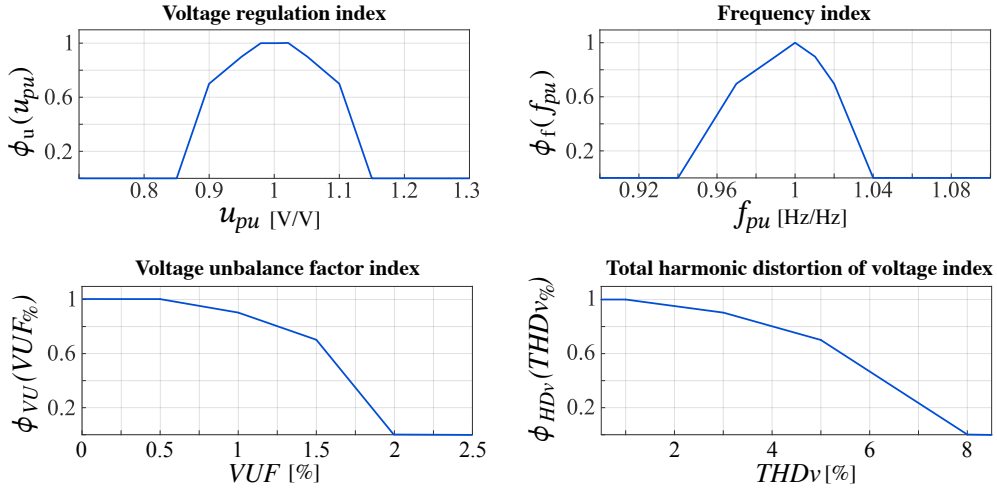

For current quality parameters:

- *Line current index $\phi_I(I_{pu})$:* Following the IEEE Std 1547 (2018) and the recommendations of IEEE Std 141 (1993). The electrical conductors of LV systems are designed to support a nominal current I_n. Operating them at no more than 80% of I_n is recommended to avoid overheating and possible accidents. I_n could be exceeded in contingency short periods. However, it must not exceed 110% of the conductor's rated current. A current greater than 120% of I_n is considered a failure.

- *Energy loss index $\phi_l(ls)$:* The acceptable percentage of losses in an LV line is generally set between 0% and 3%. Within this range, the losses are considered to be within standard tolerances and indicate a well-designed and efficient system. When power losses

fall within 3% to 5%, it serves as an alert, indicating a potential need for further analysis and improvements in the system's design or operation. Power losses exceeding 5% are considered indicative of a poor design and may result in issues affecting the electrical system's overall performance. In any case, power losses exceeding 10% are unacceptable and warrant urgent corrective measures.

- *Current unbalance index $\phi_{CU}(CUF)$:* The power quality standards do not provide limits for the current unbalance in LV networks. However, certain electrical network operators propose local regulations for its application. In LV networks with single-phase loads, achieving CUF values up to 100% is feasible without causing a system collapse. On the other hand, a three-phase network with an unbalanced voltage could lead to a current unbalance. A usual ratio indicates that a VUF of 2% corresponds to 40% of CUF, and a VUF of 0.5% corresponds to 10% of CUF (K. Ma *et al.*, 2020; Rafi *et al.*, 2020). In this way, a CUF less than 10% indicates a recommended operation, a CUF less than 40% is acceptable, and a CUF value between 40% and 100% indicates an alert condition. It is important to note that the current unbalance index does not consider non-operability conditions.

- *Current harmonic distortion $\phi_{HDi}(THDi)$:* Per IEC 61000-3-2 (2018) and IEC 61000-3-4 (1998), the allowable harmonic currents in LV networks depend on equipment class and load type. $THDi$ up to 30% may be permissible due to diverse load classes in LV. Additionally, IEEE Std 519 (2014) recommends constraining $THDi$ for LV networks based on the short-circuit current to nominal line current ratio. Accordingly, $THDi$ less than 3% signifies regular load operation. $THDi$ less than 5% is acceptable; values from 5% to 10% act as a warning. $THDi$ between 10% and 20% may indicate an emergency. In contrast, values exceeding 20% demand immediate attention.

According to the recommended QP values by the quality standards, the ranges of correspondence with the resilience conditions are proposed. Table 4 presents the proposed correspondence for the current QP, and Figure 16 shows their normalisation operators graphs.

Table 4

Current QP ranges defining the normalised operation resilience indices.

Condiction	Resilience range	Current QP range			
		I_{pu}	$\%ls$	$\%CUF$	$\%THDi$
Ideal	1.0	[0.0, 0.8]	(0, 1]	[0, 10]	[0, 3]
Acceptable	[0.9, 1.0)	(0.8, 1.0]	(1, 3]	(10, 40]	(3, 5]
Alert	[0.7, 0.9)	(1.0, 1.1]	(3, 5]	(40, 100]	(5, 10]
Emergency	(0.0, 0.7)	(1.1, 1.2)	(5, 10)	− − −	(10, 20)
Non-functional	0	$I_{pu} \geq 1.2$	$\%ls \geq 10\%$	− − −	$THDi \geq 20\%$

Figure 16

Normalisation operators for current quality parameters.

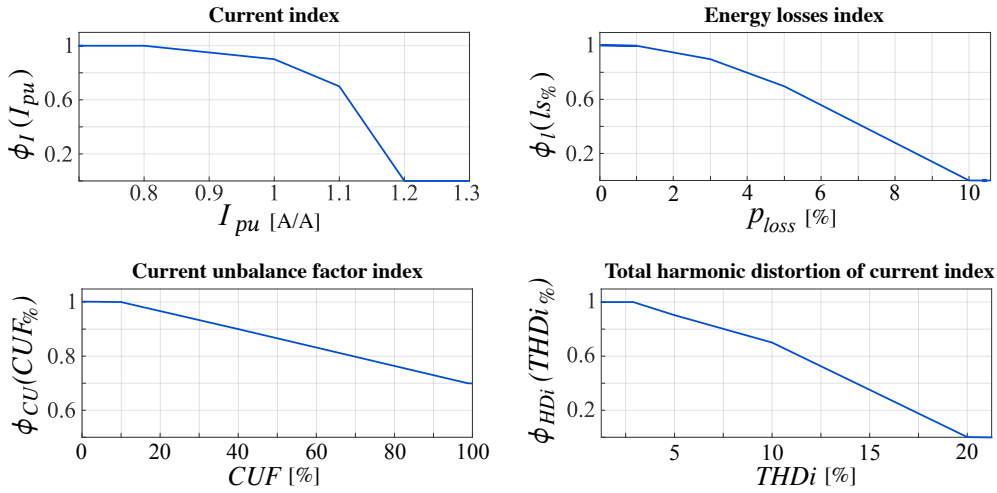

The quality index function $\phi_k(t)$ results from the correspondence of $\Gamma_k(QP_k)$ on $QP_k(t)$ as Eq. (3.11) expresses. $\phi_k(t)$ measures the electrical network's performance concerning the k-quality parameter.

$$\phi_k(t) = (\Gamma_k \circ QP_k)(t) \tag{3.11}$$

3.5.3 Stage 3: Operation resilience indices evaluation

The operation resilience index Φ_k indicates the probability that the associated QP_k parameter is in the accepted range during the measurement time T_{meas}. Φ_k is calculated by the average value of the normalised quality index function $\phi_k(t)$ as Eq. (3.12) presents. Φ_k has

the range [0, 1] representing the quality concerning the electrical network's k-parameter. T_{meas} could correspond to one day, week or month, depending on the assessment accuracy.

$$\Phi_k = \frac{1}{T_{meas}} \cdot \int_0^{T_{meas}} \phi_k(t) \cdot dt \tag{3.12}$$

This thesis analyses the voltage operation resilience OR_V and the current operation resilience OR_I. OR_V is the probability that a voltage node QPs are in the acceptable range. Then, OR_V is the compound probability $\rho[\Phi_u \cap \Phi_f \cap \Phi_{VU} \cap \Phi_{HDv}]$ that Eq. (3.13) shows. Similarly, OR_I is the probability that a line current QPs are in the acceptable range. It is the compound probability $\rho[\Phi_I \cap \Phi_l \cap \Phi_{CU} \cap \Phi_{HDi}]$ as Eq. (3.14) presents.

$$OR_V = \rho[\Phi_u \cap \Phi_f \cap \Phi_{VU} \cap \Phi_{HDv}] = \Phi_u \cdot \Phi_f \cdot \Phi_{VU} \cdot \Phi_{HDv} \tag{3.13}$$

$$OR_I = \rho[\Phi_I \cap \Phi_l \cap \Phi_{CU} \cap \Phi_{HDi}] = \Phi_I \cdot \Phi_l \cdot \Phi_{CU} \cdot \Phi_{HDi} \tag{3.14}$$

3.5.4 Stage 4: Operation resilience integration

A distribution network comprises multiple nodes and lines. Defining the point to evaluate R_{III} is crucial. This thesis considers the main supply and nodes interconnecting RES and special equipment essential for the R_{III} assessment. Figure 17 shows a 3-nodes and 4-line LV network circuit to exemplify the R_{III} evaluation cases. This network integrates a DG source, and the PCC is a critical node N_{PCC} associating a line L_{PCC}. The green dots indicate the voltage QPs measurement, and the orange loops the current QPs measurement. Three case for the R_{III} analysis are proposed: *i)* A punctual node assessment, *ii)* an overall assessment, and *iii)* a load quality assessment.

- **Punctual node assessment:** It refers to a particular node and its associated supply lines. A punctual assessment is recommended for the main supply node, a DG source's PCC node or a critical load node. It requires measuring the node voltage QPs and the current QPs of the lines directly injecting power into the node. For instance, a punctual R_{III} assessment

Figure 17

LV network circuit to assess R_{III} resilience.

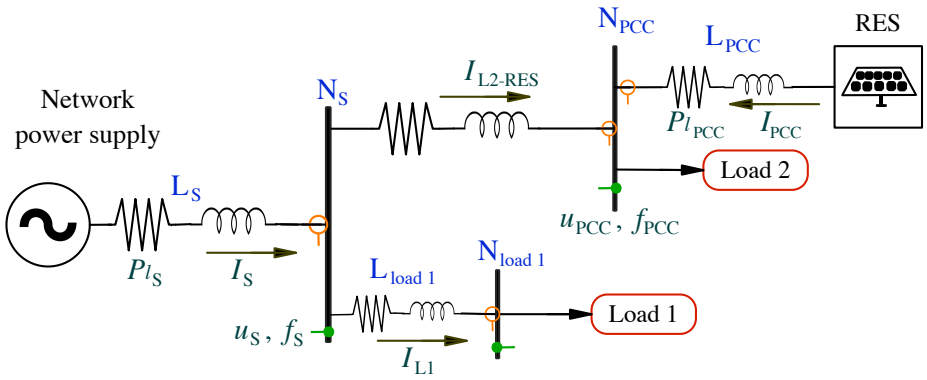

of the N_S and N_{PCC} nodes could be made from the network presented in Figure 17.

The current resilience for a node fed by more than one line is the weighted arithmetic average $\overline{OR}_I$ of the individual line OR_{I_j}. The weighting is the power contribution of each j-line. The R_{III} evaluation must consider that if OR_V or $\overline{OR}_I$ are null, R_{III} is also null. Likewise, R_{III} must consist of the contribution of benefit or harm of them. This way, this thesis proposes to quantify R_{III} by the geometric average between OR_V and $\overline{OR}_I$ as Eq. 3.15 presents.

$$R_{III}\_N_i = \sqrt{(OR_V\_N_i) \cdot \left(\overline{OR}_I\_N_i\right)} \tag{3.15}$$

- **Overall assessment:** This evaluation is proposed when possible to analyse R_{III} of several nodes of the LV network. It evaluates the operation resilience of the entire network R_{III}_Net. Then, R_{III}_Net is obtained by the weighted arithmetic average of the $R_{III}\_N_i$ available from the electrical network as Eq. (3.16) exposes. The weight of each node is proportional to its nominal power. Here, $P_{Rat}\_N_i$ is the rated power of the i-node. $R_{III}\_N_i$ is the computed R_{III} resilience for the i-node according to Eq. (3.15). N is the number of nodes in the network with an R_{III} punctual assessment. For the example in Figure 17, R_{III}_Net is the weighted arithmetic average between $R_{III}\_N_s$ and $R_{III}\_N_{PCC}$

$$R_{III}\_Net = \frac{\sum_{i=1}^{N} (P_{Rat}\_N_i) \cdot (R_{III}\_N_i)}{\sum_{i=1}^{N} P_{Rat}\_N_i} \tag{3.16}$$

- **Load quality assessment:** Identifying the loads that could harm the operation of the electrical network is essential. Therefore, this thesis proposes to evaluate the load performance $R_{III}\_load_k$. In the example of Figure 17, the node N_{load1} has not registered the voltage QPs. However, the current QPs of the line supplying N_{load1} are recorded.

  Then, it is proposed to calculate the demand performance of a load node by the OR_I of the line that supplies it as expressed by Eq. 3.17. Here, $OR_I\_L_{S-k}$ is the current operational resilience of the line supplying the node N_{load_k}. It is noted that the power requirements of the $load_k$ directly influence the $OR_I\_L_{S-k}$ performance.

$$R_{III}\_load_k = OR_I\_L_{S-k} \tag{3.17}$$

With the above, the proposed types of electrical resilience for LV networks and their assessment methodologies have been addressed in detail. The following section describes the contributions of this chapter.

3.6 Chapter conclusions

This chapter develops a proposal for assessing the electrical resilience of LV networks. The original proposal stands out for its comprehensiveness, involving three categories of disturbance levels faced by electrical systems. It assigns a type-resilience to each kind of disturbing event according to its impact and term. It identified three classifications: *i)* HILP events affect the electrical networks' infrastructure and could cause the rupture of distribution lines and the fall of poles and, therefore, a blackout of the system. *ii)* LIHP events such as overcurrent faults, short circuits, and manoeuvres could generate short power outages. *iii)* The distributed energy

resources integration has a permanent effect on electrical operation and could alter the service quality.

It proposes the assessment methodologies for type-resiliences. *i)* R_I to HILP events assessing the ability of the LV network's CI to withstand natural disasters. It detects HILP events representing threats to the LV network. It evaluates their probability of occurrence, intensity distribution and CI's fragility. *ii)* R_{II} to LIHP events assessing the capability of the LV network to recover from common origin outages. It also considers the contribution of energy backup systems to support common outages. *iii)* R_{III} analyses the service quality provided to users. It evaluates voltage and current quality parameters focusing on operational performance.

This chapter makes it possible to complete the first (SO1) and second (SO2) specific objective. It follows up on determining the resilience evaluation indices for LV networks that integrate H_2-ESS and PV systems. It proposes a methodology to evaluate the electrical resilience of LV networks. It delves into analysing the permanent effects of distributed generation (DG) sources on the supply service quality. It also contributes to SO3 and SO4 by identifying DG effects on the capacity for continuous supply and service quality. Likewise, it integrates a feedback phase allowing measures to strengthen electrical resilience.

It answers research question one (RQ1) and contributes to answering RQ5 and RQ6. It determines the information to assess electrical resilience according to the adverse event types. The feedback phase finds the strengthening of electrical resilience and compares its evaluation. It is possible to periodically analyse the resilience level of an electrical network by measuring the quality parameters and processing data referring to the proposed methodology. Then, determine the vulnerabilities of the network and establish preventive measures.

The following chapters present the application of the electrical resilience assessment proposed in this chapter in a case study. Chapter 4 describes the LV network case study. Chapter 5 covers the application of the resilience assessment parts 1, 2, and 3, referring to the actual conditions of the case study. Chapter 6 presents the case study model to develop the feedback phase. Then, Chapter 7 integrates the feedback phase and its contribution to the electrical re-

silience of the case study.

4. Description of the Case Study Electrical Network

This chapter describes the low-voltage (LV) electrical network of the case study. It corresponds to the Electrical Engineering Building (EEB-UIS) at the *Universidad Industrial de Santander* (UIS), Colombia. EEB-UIS is a university building with five floors and a basement. It supports academic and administrative activities for about 2500 students, professors and administrators. EEB-UIS has a dedicated transformer as a feeder and a diesel generator backup system for special loads. It also integrates a photovoltaic (PV) system installed on the roof of the building. In addition, the EEB-UIS has smart energy meters arranged to monitor the quality parameters of the main nodes and load circuits. These attributes make the EEB-UIS attractive to apply a comprehensive electrical resilience (R_{comp}) assessment. Thus, this chapter describes in detail the characteristics of the EEB-UIS network. It contributes to the development of the third (SO3) and fourth (SO4) specific objectives. It presents detailed case study information to develop the resilience analysis and apply feedback strategies. It is organised as follows: Section 4.1 presents remarks on the case study region. Section 4.2 describes the EEB-UIS electrical circuits. Section 4.3 exposes power backup system features. Section 4.4 covers the PV system interconnected to the EEB-UIS. Then, Section 4.5 shows the arrangement of smart meters for this research. Finally, Section 4.6 summarises the chapter's contributions.

4.1 Remarks about the case study region

EEB-UIS is situated in Bucaramanga, in the department of Santander, Colombia, at GMS N 7° 8' 29" W 73° 7' 17". Figure 18 presents the geographic location of the EEB-UIS. It is 960 meters above sea level, experiencing a warm tropical climate with average daily temperatures between 24 °C and 27 °C. Additionally, the area receives an average solar irradiance

of 4.8 $kWh/m^2/day$ (Hernández Contreras *et al.*, 2023). Bucaramanga's meteorological behaviour is subject to certain natural risks that must be considered. One significant concern is the potential for seismic activity, including earthquakes. Colombia is in a seismically active region, and Bucaramanga lies in an area prone to seismic events, making it essential for EEB-UIS to consider appropriate seismic safety measures and infrastructure resilience (Siravo *et al.*, 2019).

Figure 18

Geographical location of the EEB-UIS.

Another natural hazard to be considered is the risk of flooding. Bucaramanga, located in a tropical region, experiences rainy seasons, which can lead to flash floods and inundations.

The combination of heavy rainfall and hilly terrain can result in rapid water runoff, posing a threat to the surrounding areas, including UIS (Siravo *et al.*, 2019). Furthermore, strong winds occasionally affect Bucaramanga, especially during certain climatic events. Powerful gusts, such as those associated with tropical storms or hurricanes, could cause damage to structures, trees, and power lines. Therefore, the critical electrical infrastructure of the EEB-UIS could face intense wind events (A. Rodriguez *et al.*, 2021). This way, while Bucaramanga's warm tropical climate and favourable solar irradiance offer certain advantages, the EEB-UIS should consider the risks that earthquakes, floods, and high winds pose to its electrical critical infrastructure (CI).

4.2 Presentation of the EEB-UIS' electrical network

EEB-UIS is a five-story building intended for university classes and administrative work serving about 2500 people. It is powered by a step-down transformer 13.2 kV/127-230 V, 630 kVA Dyn5 arranged in an underground station. The transformer is fed by the local electricity company *Electrificadora de Santander S.A E.S.P.* (ESSA-ESP) through a 13.2 kV overhead circuit. EEB-UIS has a 250 kVA diesel generator to supply critical loads in case of power outages. It also integrates an 11.53 kW peak photovoltaic (PV) system. The PV surplus power could be exported to the UIS power grid through the EEB-UIS network. The building has smart energy meters set to measure the quality parameters (QP) required in this thesis. Figure 19 presents the single-line diagram of the EEB-UIS electrical network and the layout of the smart meters. Here the green and orange dots indicate the measurement of voltage and current QPs, respectively.

The EEB-UIS electrical network has been designed as a green building pilot and living laboratory integrating rational use of energy applications (Osma & Ordoñez, 2013). It has been used in research fields such as energy efficiency (Osma *et al.*, 2015), green-PV roofs (Osma & Ordoñez, 2019), and power quality analysis (Tellez, 2020; Parrado *et al.*, 2021). Taking advantage of the warm tropical climate, a heating system is unnecessary, and the air conditioning system is optional in most building areas. Part of the electrical wire ductwork is exposed and can be used

Figure 19

Electrical network diagram of the EEB-UIS.

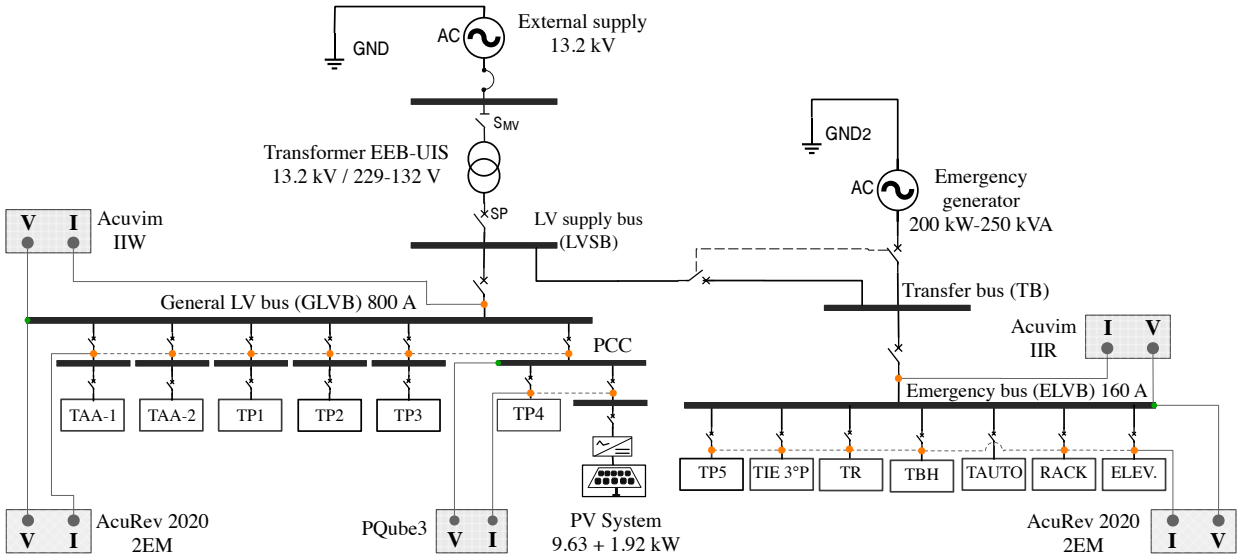

for academic and research practices. It has a dedicated feeder, and each floor and particular load has an individual distribution board. The attributes of EEB-UIS and the electrical grid allow it to be used as a case study. It meets the conditions to implement the resilience assessment proposed in Chapter 3. The following sections describe the EEB-UIS network's components, circuits and arrangement of smart meters.

4.2.1 Feeder

The EEB-UIS feeder is a Dyn5 630 kVA transformer manufactured by SIEMENS. It has an ONAN refrigeration system and a transformation ratio of 13.2/0.229 kV. Table 5 presents the main characteristics of the EEB-UIS feeder.

4.2.2 Load circuits and line sections

The EEB-UIS electrical network integrates 11 busbars, 11 line sections, 13 load circuits, one feeder and one distributed generation source. It has five busbars: *i)* the low voltage supply bus (LVSB), *ii)* the general low voltage bus (GLVB), *iii)* the transfer bus (TB), *iv)* the emergency low voltage bus (ELVB) and *v)* the fourth-floor board (TP4-PCC). LVSB is connected to the LV

Table 5

Characteristics of the transformer feeding the EEB-UIS.

Parameter	Value	Parameter	Value
Rated power	630 kVA	Breakdown voltage	40 kV
Nominal frecuency	60 Hz	Copper losses	1.285 kW
Low side voltage	229/132.2 V	Low side resistance	0.769 $m\Omega$
High side voltage	13.2 kV	High side resistance	1.706 Ω
Vector group	Dyn5		

side of the feeder and distributes the power to the GLVB and ELVB. GLVB supplies six non-critical load circuits. TB operates the decoupling of the ELVB from the EEB-UIS network in case of power outages and the transfer to the diesel generator. ELVB supplies seven critical loads. TP4 busbar is the point of common coupling (PCC) interconnecting the PV system to the EEB-UIS network. Table 6 presents the information concerning the busbars of the EEB-UIS network.

Table 6

Busbars of the EEB-UIS electrical network.

Label	Description	Rated capacity
LVSB	Low voltage supply bus, transformer low side; three-phase and neutral.	2000 A
GLVB	General low voltage bus; three-phase and neutral.	800 A
TB	Transfer bus; three-phase and neutral.	700 A
ELVB	Emergency low voltage bus; three-phase and neutral.	160 A
TP	Floor distribution board bus; three-phase and neutral.	100 A
PCC	Point of common coupling; three-phase and neutral.	100 A

The load circuits of the EEB-UIS correspond to the demands of the floorboards (TP), the emergency and the special loads. Table 7 describes their power characteristics. The installed power corresponds to the load inventory by Cortes & Garcia (2018). The maximum power refers to the maximum value measured between May $1^s t$ to May $31^s t$, 2023. Then, Table 8 details the electrical wiring of the EEB-UIS network for the sections that interconnect the main busbars and the distribution boards.

Table 7

Description of the EEB-UIS circuit loads.

Load	Description	Installed power	Maximum power
TAA-1	Air conditioning system 1.	16.81 kW	2.53 kW
TAA-2	Air conditioning system 2.	11.94 kW	2.32 kW
TP1	Distribution board, 1^{st} floor.	12.58 kW	4.46 kW
TP2	Distribution board, 2^{nd} floor.	15.20 kW	2.31 kW
TP3	Distribution board, 3^{rd} floor	6.82 kW	1.23 kW
TP4	Distribution board, 4^{th} floor.	8.41 kW	2.58 kW
TP5	Distribution board, 5^{th} floor.	9.34 kW	2.85 kW
TIE	Emergency lighting distribution board.	4.56 kW	0.00 kW
TR	5^{th} floor regulated voltage circuits.	3.62 kW	1.82 kW
TBH	Hydraulic pump system distribution board.	20.00 kW	0.00 kW
TAUTO	Automation system distribution board.	3.50 kW	0.82 kW
RACK	Cooling systems for computer RACKS.	8.00 kW	7.68 kW
ELEV	Building elevator.	6.86 kW	6.55 kW

4.3 Description of the power backup system

The EEB-UIS has a 260 kVA diesel generator backup system. The genset is the model C200 D6 4 by the Cummins Brazil company. It can operate continuously for 12 hours at prime power. Table 9 shows the main features of the EEB-UIS genset.

4.4 Description of the photovoltaic system

EEB-UIS facility incorporates an on-grid PV system interconnected to the busbar of the 4^{th} floor PCC. Whenever the feeder supply is unavailable, the PV system intelligently ceases power injection into the network, avoiding electrical risk. It has an 11.53 kWp installed capacity enabled by 43 PV panels and 43 microinverters. Each microinverter is dedicated to managing one PV panel and injects the generated power into the network through a two-phase connection. The microinverters are connected in three-phase connection groups (AB, BC and AC), each comprising 14 panel-microinverter sets. This ensures a delta-balanced connection to the PCC. The remaining panel-microinverter set is in a two-phase connection.

Table 8

Electric wire sections of the EEB-UIS network.

Line section	Length	Gauge AWG	Rated current	Resistance [Ω/km]	Reactance [Ω/km]
LVSB–GLVB	5.0 m	300 MCM	285 A	0.144	0.1345
GLVB–TAA-1	51.0 m	$1/0+1/0N$	150 A	0.394/0.394	0.144/0.144
GLVB–TAA-2	28.0 m	$2+2N$	115 A	0.623/0.623	0.148/0.148
GLVB–TP1	13.5 m	$2+4N$	115 A	0.623/1.02	0.148/0.157
GLVB–TP2	17.1 m	$6+8N$	65 A	1.61/2.56	0.167/0.171
GLVB–TP3	20.7 m	$6+8N$	65 A	1.61/2.56	0.167/0.171
GLVB–PCC	24.3 m	$2+4N$	115 A	0.623/1.02	0.148/0.157
PCC–PV	3.0 m	$8+8N$	50 A	2.56/2.56	0.171/0.171
LVSB–TB	8.0 m	$2/0+1/0N$	175 A	0.328/0.394	0.141/0.144
TB–ELVB	3.0 m	$2/0+1/0N$	175 A	0.328/0.394	0.141/0.144
ELVB–TP5	28.0 m	$4+6N$	85 A	1.02/1.61	0.157/0.167
ELVB–TIE	21.0 m	$10+10N$	35 A	3.94/3.94	0.174/0.174
ELVB–TR	30.4 m	$6+6N$	65 A	1.61/1.61	0.167/0.167
ELVB–THB	30.1 m	$2+2N$	115 A	0.623/0.623	0.148/0.148
ELVB–TAUTO	25.0 m	$8+8N$	50 A	2.56/2.56	0.171/0.171
ELVB–RACK	20.0 m	$4+8N$	85 A	1.02/2.56	0.157/0.171
ELVB–ELEV	82.0 m	$6+6N$	65 A	1.61/1.61	0.167/0.167

The PV system integrates 20 Canadian Solar, 13 Trina Solar, 2 Up Solar panels and 37 Emphase M250 and 6 Emphase iQ7+ microinverters. The efficiency of the PV panels and microinverters are approximately 16% and 96%, respectively. Figure 20 shows a top view of the EEB-UIS and the arrangement of the PV system on the rooftop comprising an area of 59.5 m^2. The PV panels' orientation is 10° south facing, strategically capturing sunlight throughout the day for maximum energy generation. Table 10 presents the characteristics of the PV system panels.

4.5 Arrangement of the energy meters

For this research, five smart energy meters are available to measure quality parameters (QPs). Meters are two 2020 AcuRev 2EM, a Acuvim IIW, a Acuvim IIR, and a PQube3. They have been arranged in the GLVB, ELVB and PCC busbars. Table 11 presents the smart meters' description and the measuring points. The smart meters have been set to measure *i)* The volt-

Table 9

Characteristics of the genset backup system of the EEB-UIS.

Parameter	Standby	Prime
Nominal voltage	127/220 V	127/220 V
Nominal frecuency	60 Hz	60 Hz
Rated power	260 kVA	240 kVA
Rated active power	208 kVA	192 kVA
Rated power factor	0.8	0.8
Electric connection	WYE three-phase	

Figure 20

Top view of the PV system on the EEB-UIS rooftop.

age QPs: Voltage (u), frequency (f), total harmonic distortion of voltage ($THDv$), and voltage unbalance factor (VUF). *ii)* The current QPs: Current (I), total harmonic distortion of current ($THDi$), and current unbalance factor (CUF). They were synchronised to record the measurements at the same time. The measurement is recorded with a refreshing time of 10 minutes for 31 consecutive days from May 1^{st} to May 31^{st}, 2023. It corresponds to 4 464 data per QP. Figures 22–21 show the meters coupling to the busbars of the EEB-UIS network.

The voltage QPs measurement is directed by the smart meters. u is the average of the phase voltages. $THDv$ is the average of the phase voltages' total harmonic distortion. VUF is

Table 10

Description of the solar panels of the EEB-UIS PV system.

Brand & Model	Qty.	Rated power	Rated voltage	Rated current	Open circuit voltage	Short circuit current
Trina Solar, TSM-270PD05	13	270 W	30.9 V	8.73 A	38.4 V	9.18 A
Up Solar, UP-M250P	3	250 W	30.6 V	8.17 A	38.0 V	8.50 A
Canadian Solar, CS6P-255P	21	255 W	30.2 V	8.43 A	37.4 V	9.00 A
Jinko Solar, JKM325PP-72	6	325 W	37.6 V	8.66 A	42.7 V	9.10 A

Table 11

Smart meters measuring the EEB-UIS quality parameters.

Meter	Coupling point	Measuring	Current channels	ANCI C 12.20 class	IEC 62053-22 class
AcuRev 2020 2EM	GLVB	TAA-1, TAA-2, TP1, TP2, TP3 and PCC supply.	6, 3-phase	0.5	0.5S
AcuRev 2020 2EM	ELVB	TP5, TIE, TR, TBH, RACK and ELEV.	6, 3-phase	0.5	0.5S
Acuvim IIW	GLVB	GLVB supply.	1, 3-phase	0.5	0.5S
Acuvim IIR	ELVB	ELVB supply.	1, 3-phase	0.5	0.5S
PQube3	PCC	TP4 and PV system.	2, 3-phase	0.5	0.5S

the percentage ratio of the negative and positive sequence voltages. The current QPs measurement is indirect through current transformers. I is the average of the line currents. $THDi$ is the average of the line currents' total harmonic distortion. CUF is the percentage ratio of the negative and positive sequence currents. Moreover, the line power losses (p_{loss}) are calculated with the line currents and the line resistance described in Table 8. The percentage of power loss is the ratio between the line losses and the total power conducted by the line section.

4.6 Chapter contribution

This chapter describes the electrical network of the Electrical Engineering Building (EEB-UIS). It presents the necessary information on the network to develop the comprehensive re-

Figure 21

Arrangement of the meters in the PCC of the EEB-UIS.

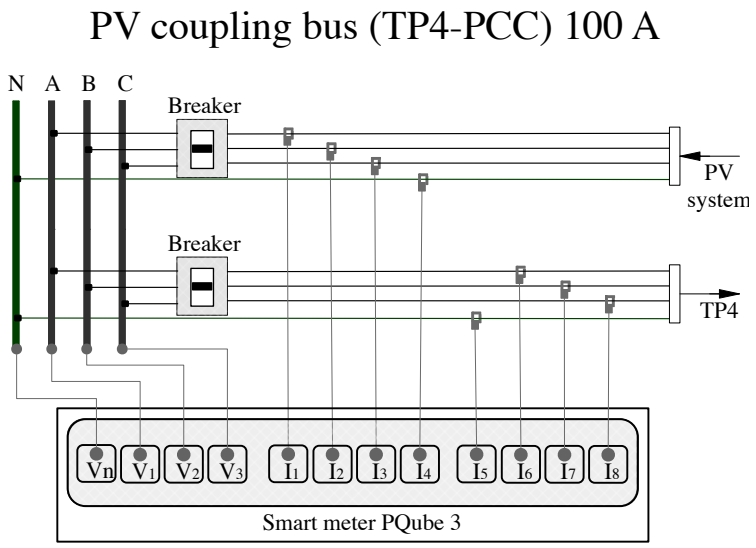

Figure 22

Arrangement of the meters in the GLVB of the EEB-UIS.

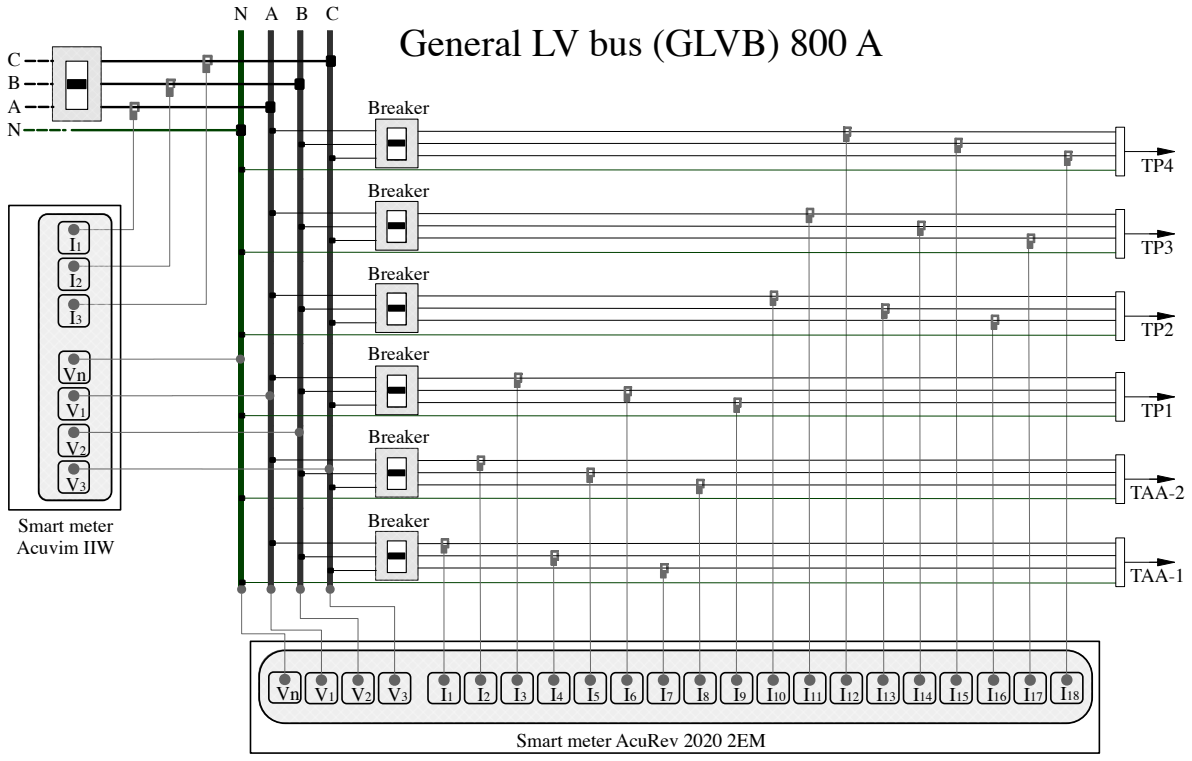

Figure 23

Arrangement of the meters in the ELVB of the EEB-UIS.

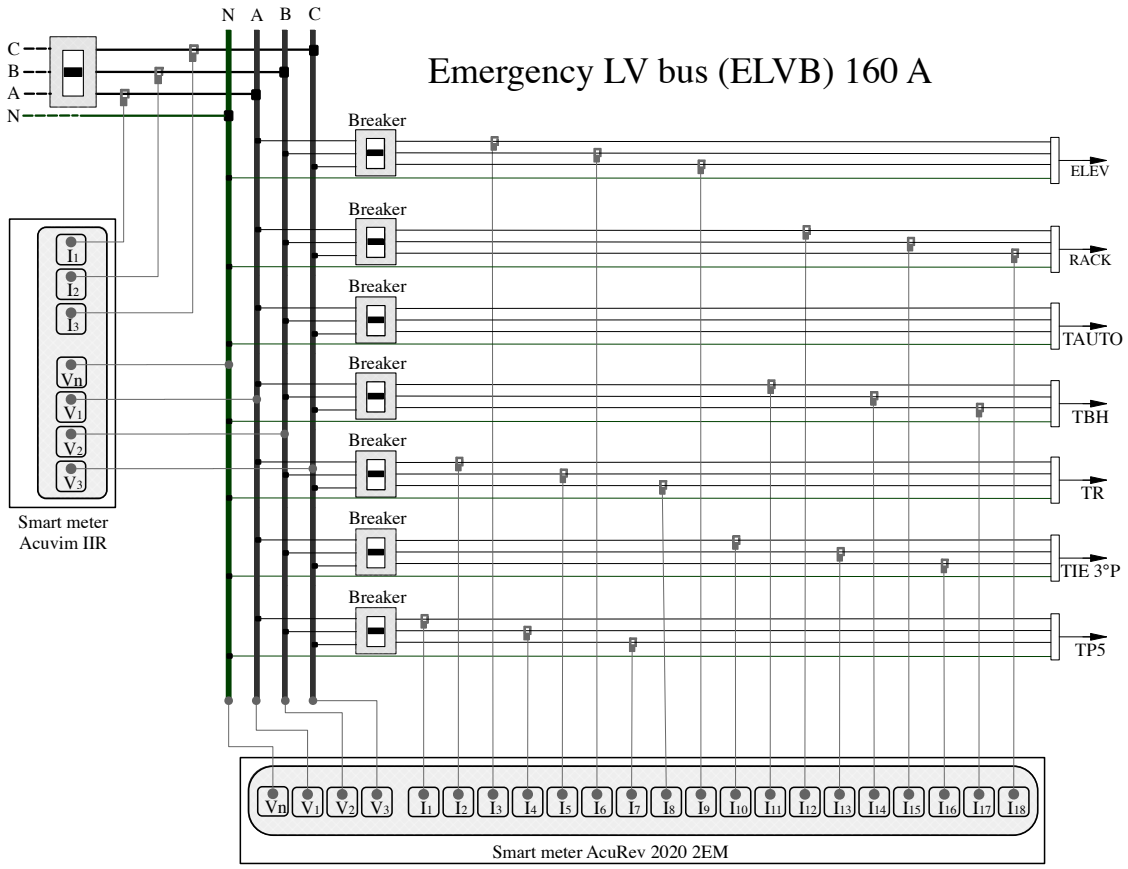

silience (R_{comp}) analysis according to the assessment methodology proposed in Chapter 3. Specific attention has been given to ensuring that the EEB-UIS power grid serves as a suitable case study for this research.

The data described for the type I resilience (R_I) analysis of the EEB-UIS power grid is sourced from the Bucaramanga region, making it applicable to LV networks within the same region. Additionally, outage power information from the medium-voltage (MV) circuit that feeds the EEB-UIS feeder could be used to analyse LV grids supplied by the same MV distribution circuit. Concerning the type III resilience (R_{III}) analysis, it is essential to highlight that this section is exclusively dedicated to the EEB-UIS electrical network. Meticulous efforts have been made to measure the quality parameters of the building's key busbars and load circuits. For this purpose, all available smart meters at the EEB-UIS have been deployed. The meters are set and

synchronised, enabling the continuous record of quality parameter data for an entire month.

This chapter contributes to the third (SO3) and fourth (SO4) specific objectives. The information presented in this chapter corresponds to Part 1 of the electrical resilience assessment methodology. It serves as input for conducting parts 2, 3, 4, and 5 of the R_{comp} assessment of the EEB-UIS. Subsequent chapters focus on utilising the data provided here in the progression of the assessment methodology.

5. Assessing the Electrical Resilience of the EEB-UIS

This chapter exposes the application of the electrical comprehensive resilience (R_{comp}) assessment parts 2 and 3 proposed in Chapter 3. The Electrical Engineering Building (EEB-UIS) has been suitable and characterised for the case study. The EEB-UIS's electrical installation has been involved in several research projects. It has an architecture equivalent to a small-scale low-voltage (LV) network integrating a PV system and a genset backup system. It also has smart metering in the key busbars, allowing the characterisation of its performance operation.

This chapter supports the third specific objective SO3: "Evaluate the effects of the integration of PV generation systems and H_2-ESS on the resilience of a LV electrical network." Furthermore, It contributes to answering research questions RQ2, RQ5 and RQ6. It is organised as follows: Section 5.1 presents remarks to address the evaluation phase of the R_{comp} methodology. Section 5.2 exposes the type I resilience (R_I) assessment in the EEB-UIS. Section 5.3 shows the type II resilience (R_{II}) assessment and Section 5.4 shows type III resilience (R_{III}) characterisation. Then, Section 5.5 presents the R_{comp} analysis. Finally, Section 5.6 sets out the the chapter conclusions.

5.1 Remarks on electrical resilience assessment of the EEB-UIS

This chapter addresses the development of the R_{comp} evaluation phase for EEB-UIS. This

phase consists of parts 2 and 3 of the assessment methodology, as Chapter 3 outlines. Part 2 involves evaluating the type-resiliences, while Part 3 encompasses analysing and integrating these assessments. It is dedicated to analysing the current state of the EEB-UIS electrical network. Figure 24 illustrates the sequence of the R_{comp} evaluation phase's progression. In this context, Part 1 pertains to the information gathering detailed in Chapter 4.

The input for the R_I assessment involves identifying the critical infrastructure (CI) of the EEB-UIS power grid and discerning potential threats to the CI. It has been accomplished through reviewing studies on natural hazards in the EEB-UIS region and investigating electrical CI fragility research. For the R_{II} assessment, the input is the power outage history of the MV circuit supplying the EEB-UIS feeder. This information is sourced from *Electrificadora de Santander S.A E.S.P.* (ESSA-ESP), the local electric utility company. Information about the backup power system is obtained from the EEB-UIS power grid database. Regarding the R_{III} assessment, the input is the electrical network's quality parameters (QP) measurements, as recorded by smart meters in May 2023. Subsequent sections delve into the assessment of EEB-UIS's type-resiliences.

Figure 24

Electrical resilience assessment sequence for the EEB-UIS.

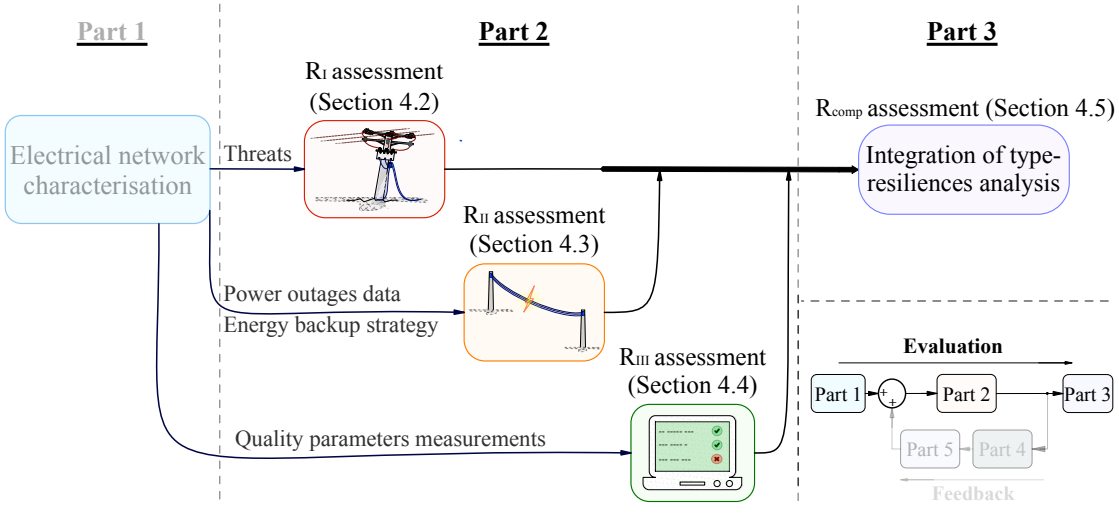

5.2 Type I resilience assessment

The EEB-UIS feeder is in an underground substation and has high protection against natural threats. Then, the critical infrastructure (CI) for the electrical supply of the EEB-UIS is the MV overhead circuit supplying the feeder. It is a 13.2 kV three-phase circuit with 12-meter concrete poles. The R_I assessment is developed for the line and concrete pole supporting the MV circuit that supplies the EEB-UIS feeder.

5.2.1 Determining the HILP risk events

The threat determination is based on the review by Abedi *et al.* (2019) on the vulnerability of electrical power systems. According to their findings, these systems' most remarkable natural threats are hurricanes, earthquakes, and lightning strikes. It is essential to be aware of these potential dangers and determine which could affect the case study. For distribution systems, Li *et al.* (2021) found that gale-force winds usually cause line breaks and pole damage.

Moreover, the research by A. Rodriguez *et al.* (2021) shows that civil constructions in Bucaramanga, Colombia, face risks of rupture by earthquakes. In contrast, flooding does not threaten the power distribution lines in the study area. No information on intentional attacks is reported for the case study location. This way, the potential hazards facing the EEB-UIS's CI are earthquakes and strong winds. Next, they are characterised.

Earthquake characterisation:

The fundamental natural frequency of a 12 m concrete pole is 1.2 Hz (Baghmisheh & Mahsuli, 2021). The National Seismic Hazard Model for Colombia (Arcila *et al.*, 2020) provides the seismic hazard information for Bucaramanga. The mean probability of intensity exceedance data for the 0.7 s oscillation period is used to fit the two-term exponential function shown in Eq. (5.1). Here, Sa is the spectral acceleration as the intensity parameter in g-force. $\rho[E \geq Sa|Sa]$ corresponds to the exceeding probability for each Sa-value of the earthquakes in

one year.

$$\rho[E \geq Sa|Sa] = 0.457 \cdot e^{-383.1 \cdot Sa} + 0.252 \cdot e^{-54.5 \cdot Sa} \tag{5.1}$$

Winds characterisation:

Hourly wind speed data from the last ten years characterises the probability of winds in the case study area. These data were obtained from the NASA Langley Research Center (LaRC) POWER Project funded through the NASA Earth Science/Applied Science Program on 2023/01/20. The data is fitted to a Weibull density function, finding 1.69709 and 1.86989 as the scale and shape parameters, respectively. Here, the intensity parameter is the wind speed measured in m/s. The abscissa is the probability of each wind speed.

5.2.2 Critical infrastructure fragility

Infrastructure fragility could be modeled using a logo-normal cumulative distribution function (CDF) $fr_{[CI|d]} = \Phi(x|\mu_\alpha, \sigma_\alpha)$ (Baghmisheh & Mahsuli, 2021; Sabouhi *et al.*, 2020). Here, x represents the intensity variable of the disruptive event. μ_α and σ_α are the x-log values' mean and standard deviation, respectively. Table 12 presents the characteristic parameters of the EEB-UIS feeder's CI fragility.

The R_I assessment uses the fragility characterisation of 12 m concrete poles before earthquakes by Baghmisheh & Mahsuli (2021). Furthermore, the fragility characterisation of distribution lines in the face of strong wind by Sabouhi *et al.* (2020) and Salman *et al.* (2015). Figure 25 gives the probability of intensity of earthquakes and wind speed for the case study found in the preceding section. Moreover, it shows the characterisation of the CI fragility.

The following section quantitatively evaluates R_I. Here, it can be observed that the probability of occurrence of the threats is greater for intensities that represent a low risk of collapse of the feeder CI. Then, the strong winds and earthquakes are expected not to represent a high impact on the CI in the case study region.

Table 12

Fragility characterisation of the EEB-UIS feeder's CI.

HILP event	Element	μ_α	σ_α	Ref.
Earthquake	12 m pole	-0.772	0.353	Baghmisheh & Mahsuli (2021)
Sa [g-force]	Wire conductor	-0.772	0.353	Baghmisheh & Mahsuli (2021)
Wind [m/s]	12 m pole	4.170	0.112	Salman *et al.* (2015)
	Wire conductor	3.701	0.150	Sabouhi *et al.* (2020)

Figure 25

Fragility function of the EEB-UIS feeder's CI. a) For earthquakes; b) For strong winds.

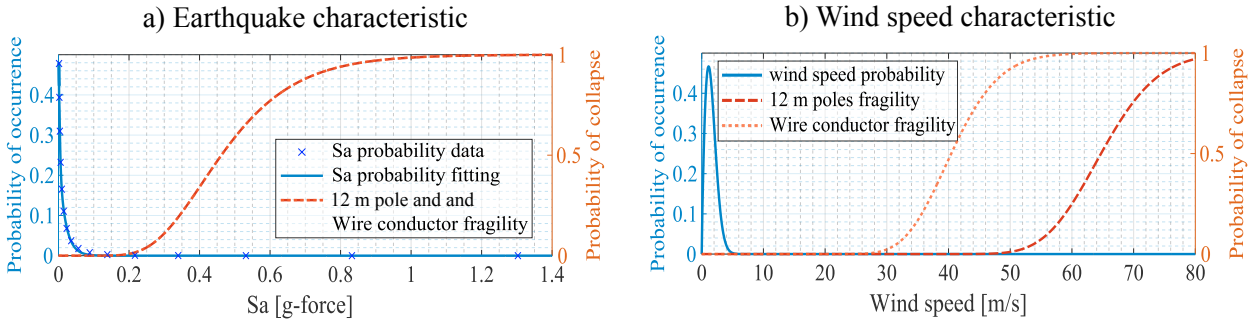

5.2.3 *Integration of stress from HILP risk events*

The methodology proposed in Section 3.3 evaluates R_I. Eq. (3.4) is applied to calculate the stress state probability $SSP_{|quake}$ and $SSP_{|wind}$ according to the CI fragility characterisation. Subsequently, Eq. (3.5) and Eq. (3.6) are employed to determine the total stress state probability $SSP_{|HILP}$, which is instrumental in assessing R_I. Table 13 summarises the results of the R_I assessment. The outcomes indicate an approximate R_I value of 1, which suggests a low likelihood of the feeder's CI collapsing under (HILP) events. This conclusion aligns well with the observations depicted in Figure 25. Notably, earthquakes emerge as the most influential factor contributing to the probability of collapse.

5.3 Type II resilience assessment

The R_{II} assessment is carried out with the collaboration of the local electricity com-

Table 13

Type I resilience assessment results.

HILP event	Pole $\rho[F_p\|d]$	Wire conductor $\rho[F_{ln}\|d]$	Feeder's CI $SSP_{\|d}$
Earthquake	5.77×10^{-9}	1.65×10^{-9}	5.77×10^{-9}
Winds	1.58×10^{-63}	1.20×10^{-31}	1.20×10^{-31}
$SSP_{\|HILP}$		5.77×10^{-9}	

pany *Electrificadora de Santander S.A E.S.P.* (ESSA-ESP), which supplies the electricity to the UIS. ESSA-ESP provided the historical data on power outages for the EEB-UIS feeder's electrical circuit. The information on the power backup capacity is computed from the building's energy backup system and load characteristics.

5.3.1 Power outages characterisation

ESSA-ESP provided the historical data on 2012–2021 power outages for the MV circuit supplying the EEB-UIS feeder. In the ten years, it had 301 outage events from common origin causes. The total duration of the outage is 72.7 hours for 2012–2021. According to (3.7) the outage probability is $\rho_{out} = 8.30 \times 10^{-4}$.

5.3.2 Backup systems reliability

The historical outage data is used to build the cumulative distribution function $CDF(lh_{out})$ described in Section 3.4.2. The CDF fitting found that the Burr Type XII distribution has the best fit with 7.42% mean absolute percentage error (MAPE), followed by the Weibull and Gamma distributions with 8.90% and 17.60% MAPE, respectively. Burr distribution function parameters are $\alpha = 10.910$, $c = 0.516$, and $k = 2.368$. Figure 26 presents the power outage state time per year for the EEB-UIS and the fit of historical outage data to a CDF.

The EEB-UIS has a 250 kVA diesel generator backup system for critical loads. It could supply power for up to 12 continuous hours. The load installed in the emergency busbar is

Figure 26

Historical power outage of the EEB-UIS. a) Annual outage time; b) Cumulative density function fit.

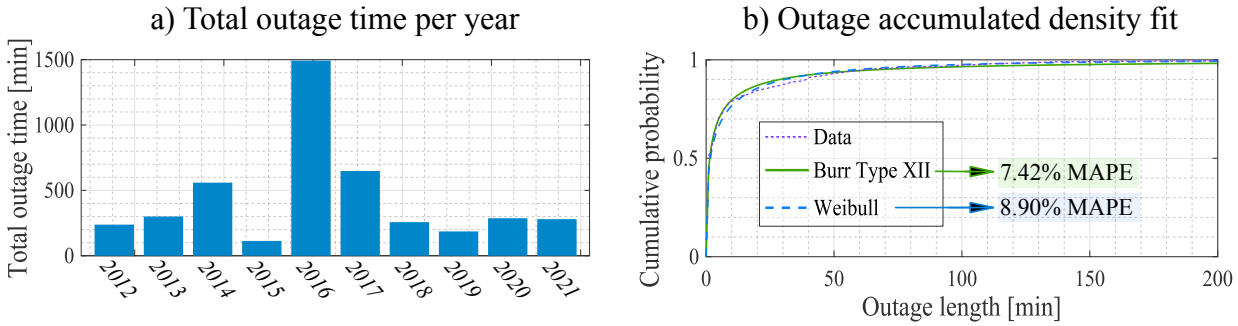

55.88 kW, representing 43.8% of the EEB-UIS installed demand. Then, the backup system offers $TSP = CDF(720) = 0.998$, and $\eta_{bk} = 0.44$.

5.3.3 Supply continuity capacity

R_{II} is evaluated with the procedure proposed in Section 3.4. Eq. (3.9) and (3.10) are applied to characterise the continuity supply capacity. The non-supply probability is $\rho_{off} = 4.65 \times 10^{-4}$. The backup system helps to reduce ρ_{off} by 44%; then, $R_{II} \approx 1$.

5.4 Type III resilience assessment

Smart meters were installed in the main busbars of the EEB-UIS electrical installation to measure the quality parameters (QPs) defined in Section 3.5. An AcuRev 2020 measures the voltage QPs of the general low voltage bus (GLVB) and the current QPs of its branch circuits. An Acuvin IIW measures the current QPs of the wire supplying the GLVB. A second AcuRev 2020 measures the voltage QPs of the emergency low voltage bus (ELVB) and the current QPs of its branch circuits. An Acuvin IIR measures the current QPs of the wire supplying the ELVB. The voltage and current QPs of the PV system point of common coupling (PCC) bus are measured by a PQube3. The meters record data from May 1^{st} to May 31^{st}, 2023, with a 10-minute sampling step. Below is the definition of the nodes, the normalisation of the QPs measurements, and the integration for the R_{III} evaluation.

5.4.1 Defining nodes for evaluation

The EEB-UIS electrical network has three nodes attracting attention for the operation resilience (*OR*) assessment: *i)* The GLVB, it supports 56.2% of the building's installed load. *ii)* The ELVB that supports the critical loads of the network. Furthermore, *iii)* the PCC that interconnects the PV system with the building network. The lines feeding GLVB, ELVB, and PCC nodes; and lines supplying floorboards (TP) and special loads are also of interest for the assessment. Figure 27 shows a single-phase equivalent circuit model of the EEB-UIS illustrating the measurement points in the R_{III} evaluation.

Here, the nodes are numbered for identification. The line impedances are estimated according to the EEB-UIS network characterisation in Section 4.2. The air conditioning and emergency loads are grouped in *TAA* and *Emerg*, respectively. The measurement points correspond to the arrangement of meters. The voltage is measured directly, and the current is measured indirectly through current transformers (CTs). A punctual evaluation is made for the nodes N_2, N_4 and N_8 corresponding to ELVB, GLVB and PCC, respectively. Then, a load quality assessment is made for the floorboard nodes.

Figure 27

Circuit model for the R_{III} assessment of the EEB-UIS.

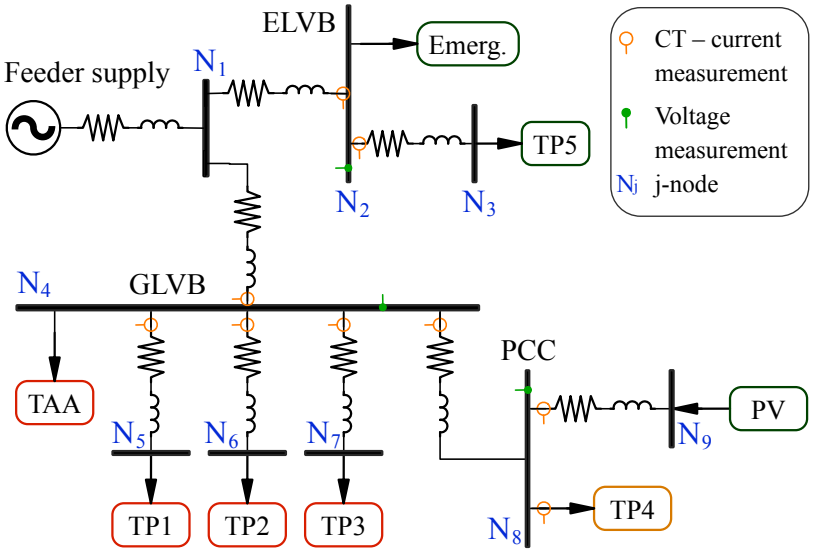

5.4.2 Punctual assessment of the operation resilience

This section develops the voltage (OR_V) and line current (OR_I) operation resilience assessment for the points with QPs measurement. The QPs are normalised according to the transformer operators $\Gamma_k(QP_k)$ defined in Section 3.5.2. The OR indices Φ_k are calculated by Eq. (3.12). The total measurement time corresponds to $T_{meas} = 31\ days$ for this assessment. The nominal voltage values for the case study region are 127/220 V and 60 Hz. The rated current of the line sections corresponds to the conductor size of each section. Table 14 and Table 15 present the results of the OR_V and OR_I indices assessment, respectively.

Table 14

Assessment of the node voltage operation resilience for the EEB-UIS.

Node	Rated power	Voltage resilience index Φ_k				OR_V
		Φ_u	Φ_f	Φ_{VU}	Φ_{HDv}	
N_2 / ELVB	61 kW	0.9456	0.9959	0.9998	0.9687	0.9121
N_4 / GLVB	305 kW	0.9474	0.9958	0.9998	0.9683	0.9133
N_8 / PCC	38 kW	0.9537	0.9941	0.9998	0.9642	0.9139

Results reveal that voltage regulation is the most vulnerable QP. Then, it influences the OR_v behaviour to a significant extent. Any disturbances or deviations in voltage regulation can substantially impact the system's overall resilience. Notably, the resilience indices are close in the three nodes, indicating the network's robustness to maintain voltage conditions in the electrical installation. The resilience voltage indices are in an acceptable range, indicating a strong point of the system's ability to maintain its operational performance even under stress or unfavourable conditions. Results offer reassurance that, despite the vulnerability identified in voltage regulation, the system exhibits satisfactory resilience concerning voltage QPs.

The current operation resilience results indicate favourable line loading and power loss, close to the ideal value, due to the EEB-UIS network operating below the rated conductor load. Critical points are the current's harmonic distortion and unbalance. Line L_{4-5}, feeding TP1, and line L_{1-2}, feeding ELVB, stand out as vulnerable line sections requiring attention due to

Table 15

Assessment of the line current operation resilience for the EEB-UIS.

Line	Rated current	Current resilience index Φ_k				OR_I
		Φ_I	Φ_l	Φ_{CU}	Φ_{HDi}	
L_{1-2}	175 A	0.9998	0.9998	0.9649	0.7656	0.7383
L_{2-3}	85 A	0.9998	0.9998	0.7175	0.9896	0.7097
L_{1-4}	285 A	0.9998	0.9996	0.9173	0.9719	0.8909
L_{4-5}	115 A	0.9998	0.9996	0.8780	0.6585	0.5778
L_{4-6}	65 A	0.9998	0.9996	0.8580	0.9969	0.8547
L_{4-7}	65 A	0.9998	0.9990	0.7814	0.9873	0.7706
L_{4-8}	115 A	0.9998	0.9993	0.9440	0.9221	0.8696
L_{8-9}	50 A	0.9996	0.9994	0.9775	0.9932	0.9699

emergency range conditions. Current unbalance alert pertains to lines feeding TP3, and emergency loads. Contrastingly, line L_{1-4}, supplying GLVB (TAA air-conditioning, TP1 to TP4 circuits), shows acceptable current unbalance and harmonic distortion resilience. It indicates an overall load balance in the phases of the EEB-UIS power grid. Line L_{8-9}, interconnecting the PV system to the PCC, notably has the highest OR_i rating, showcasing proper power balance and low harmonic distortion from the PV installation.

The evaluation of the operation resilience also makes it possible to analyse the evolution of the indices with a refreshing time defined on hourly or daily scales. Knowing the resilience indices development is essential to identify vulnerable issues, apply feedback and strengthen resilience strategies. Figures 28, 29, and 30 present the evolution of the voltage and current operation resilience indices with a one-day refresh time for nodes ELVB, GLVB and PCC, respectively.

Here, it is observed that the PQs exhibiting the highest variation and lowest level of resilience index are voltage regulation, current unbalance and harmonic distortion of current. In the case of OR_V, the monthly average is in the acceptable range; however, there are days when it is in the alert range in the daily evolution. The daily developments of OR_V and OR_I allow for identifying the vulnerabilities of QPs and possible patterns of variations and low values. Tables 16 and 17 present the minimum (min), maximum (max), average ($mean$) and standard

Figure 28

Daily evolution assessment of the operation resilience indices for the ELVB. a) OR_V for the ELVB; b) OR_I for line L_{1-2} supplying the ELVB.

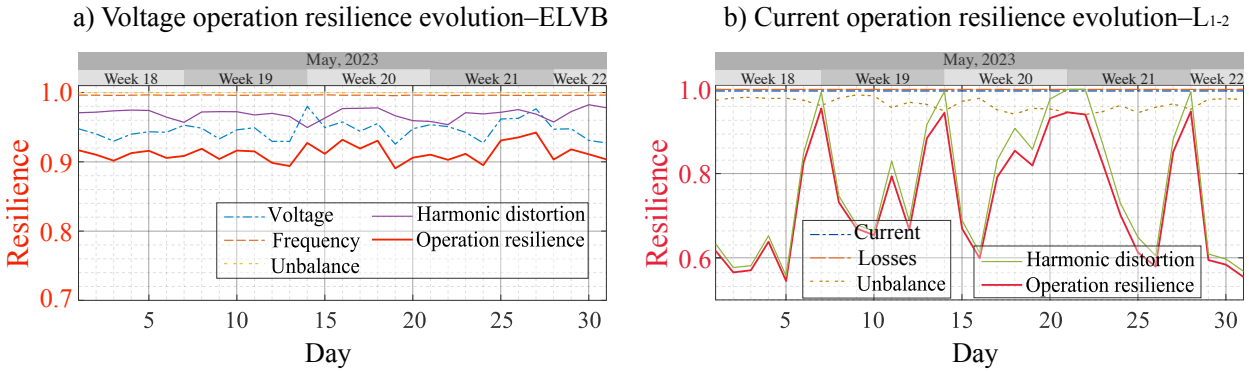

Figure 29

Daily evolution assessment of the operation resilience indices for the GLVB. a) OR_V for the GLVB; b) OR_I for line L_{1-4} supplying the GLVB.

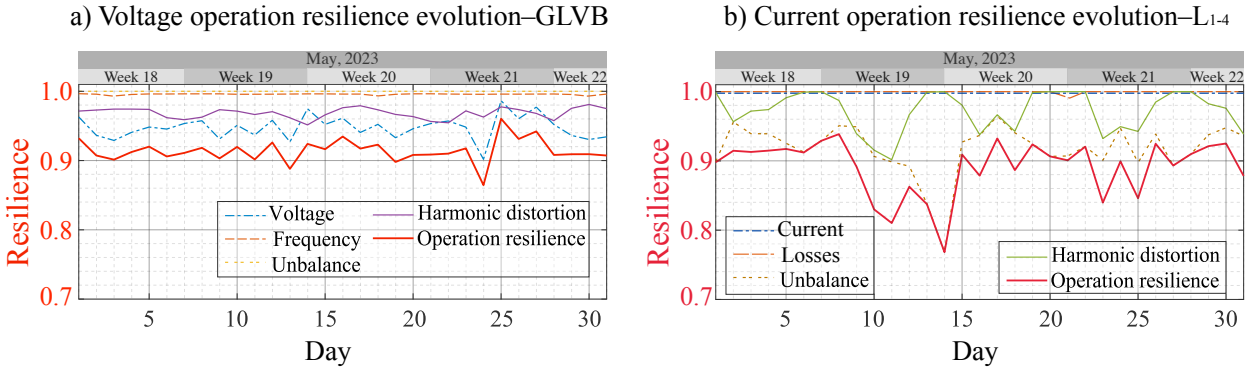

deviation (std) values, for the OR_V and ORI_I of the ELVB, GLVB and PCC busbars.

May 24 is the day that exhibits the lowest OR_V for all busbars. OR_V is 0.8645, 0.8905 and 0.8819 for ELVB, GLVB and PCC, respectively. However, there is no correspondence with the OR_I values. Then, the issue could be due to an overvoltage in the supply through the power distribution network and not to a failure of the EEB-UIS electrical network. The following section develops the overall R_{III} assessment and load quality analysis for the EEB-UIS.

5.4.3 Composite assessment

The composite assessment integrates the individual results of OR_V and OR_I to deter-

Figure 30

Daily evolution assessment of the operation resilience indices for the PCC. a) OR_V for the PCC; b) OR_I for line L_{8-9} interconnecting the PV system to the EEB-UIS network.

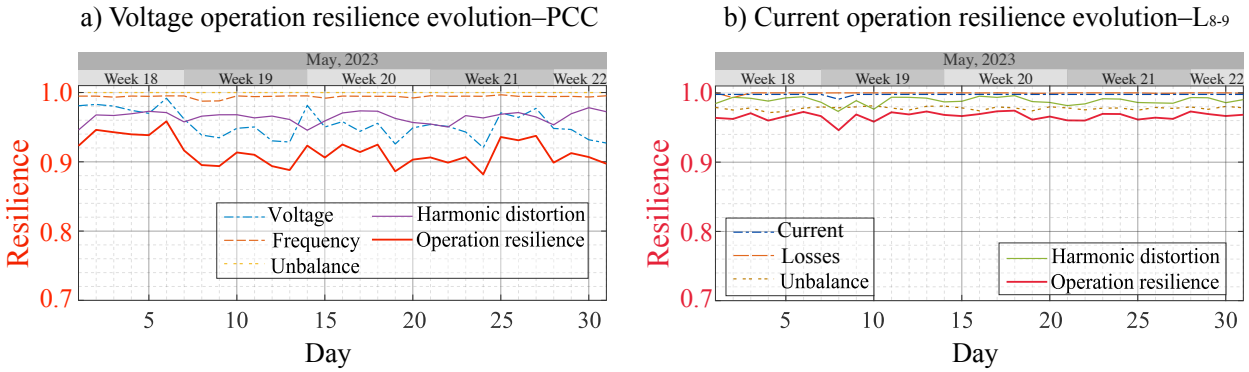

mine R_{III}. The R_{III} resilience of the monitored nodes is determined by the approach of Section 3.5.4. N_2 and N_4 have a single supply line, then, R_{III} is evaluated directly by Eq. (3.15) as the geometric average. N_8 is the PCC and has two supply lines; its current resilience is the weighted additive average between L_{4-8} and L_{8-9}. The quality of the load points is projected through the current resilience operation. Finally, the overall R_{III} resilience of the EEB-UIS is the weighted average of the evaluated nodes' resilience. Table 18 summarises the evaluation results of the R_{III}.

Results indicate $R_{III} = 0.8902$; then, the overall R_{III} resilience of the EEB-UIS is in the alert range. The critical points lie in the quality of the loads. Strengthening strategies could focus on improving the load distribution in the phases and avoiding harmonic distortion. It is also possible to establish measures to correct voltage regulation. The main vulnerability is found in the load of the TP1 and TP5 boards. In addition, the emergency load ($Emerg$) represents a weakness for the operation of the EEB-UIS network and has a direct inference on R_{III}-N_2, therefore, on R_{III}-EEB. The following section compiles the results of the type-resilience assessment by means of the comprehensive resilience (R_{comp}) analysis.

Table 16

Variation of EEB-UIS OR_V indices when considering a one-day update time.

Node	Rate	Voltage resilience index Φ_k				OR_V
		Φ_u	Φ_f	Φ_{VU}	Φ_{HDv}	
ELVB	min	0.9255	0.9955	0.9998	0.9495	0.8095
	max	0.9802	0.9968	0.9998	0.9824	0.9423
	$mean$	0.9474	0.9959	0.9998	0.9687	0.9133
	std	0.0135	0.0003	0.0000	0.0078	0.0125
GLVB	min	0.9018	0.9954	0.9998	0.9515	0.8645
	max	0.9865	0.9965	0.9998	0.9810	0.9604
	$mean$	0.9456	0.9958	0.9998	0.9683	0.9121
	std	0.0168	0.0003	0.0000	0.0077	0.0169
PCC	min	0.9205	0.9875	0.9998	0.9456	0.8819
	max	0.9918	0.9953	0.9998	0.9781	0.9585
	$mean$	0.9537	0.9941	0.9998	0.9642	0.9139
	std	0.0195	0.0018	0.0000	0.0081	0.0196

5.5 Comprehensive resilience

The comprehensive resilience (R_{comp}) integrates the type-resilience assessments to reach conclusions on the electrical resilience of the EEB-UIS. Figure 31 presents a summary of the R_{comp} characterisation for the EEB-UIS; it is equivalent to the split shown in Figure 11. The result indicates that the EEB-UIS is lowly vulnerable to power supply failures due to high-impact natural disturbances. The feeder has high supply reliability under normal operating conditions. EEB-UIS's backup system increases resilience against regular power outages. However, R_{III} indicates an alert regarding the operation's quality. The analysis of the *OR* indicators shows that the EEB-UIS electrical network faces high voltage regulation values and loads with high harmonic pollution. Then, an opportunity to improve the electrical resilience of the EEB-UIS concerns measures to adjust the voltage regulation, the load balance of TP1, TP2 and TP3 circuits and harmonic suppression of emergency and TP1 circuit loads. The following section outlines the contribution of this chapter.

Table 17

Variation of EEB-UIS OR_I indices when considering a one-day update time.

Line	Rate	Current resilience index Φ_k				OR_I
		Φ_I	Φ_l	Φ_{CU}	Φ_{HDi}	
L_{1-2}	*min*	0.9998	0.9998	0.9404	0.5567	0.5450
	max	0.9998	0.9998	0.9869	1.0000	0.9548
	mean	0.9998	0.9998	0.9649	0.7656	0.7383
	std	0.0000	0.0000	0.0142	0.1563	0.1428
L_{1-4}	*min*	0.9998	0.9931	0.7682	0.9017	0.7682
	max	0.9998	1.0000	0.9647	1.0000	0.9387
	mean	0.9998	0.9996	0.9173	0.9719	0.8909
	std	0.0000	0.0012	0.0377	0.0288	0.0402
L_{8-9}	*min*	0.9931	0.9931	0.9714	0.9863	0.9583
	max	1.0000	1.0000	0.9815	0.9970	0.9755
	mean	0.9996	0.9994	0.9775	0.9932	0.9699
	std	0.0012	0.0012	0.0025	0.0022	0.0036

Figure 31

Splitting of the EEB-UIS's electrical resilience assessment.

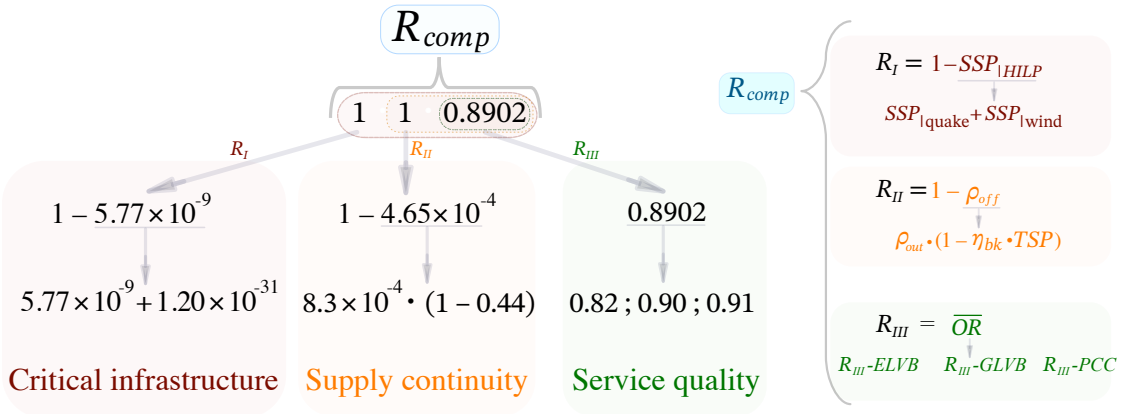

5.6 Chapter conclusions

This chapter exposes the application of the comprehensive electrical resilience (R_{comp}) assessment proposal in the EEB-UIS case study. The EEB-UIS represents a 9-node scale LV distribution network. The local electricity company has provided information on the frequency and duration of power outages of common origin. Five smart energy meters have been installed in the EEB-UIS electrical network to measure the quality parameters required in the

Table 18

Summary of the EEB-UIS type III resilience assessment.

Finding	Value	Description
R_{III}-N_2	0.8206	Operation resilience (R_{III}) at the ELVB node. It is estimated as the geometric average between the OR_V in the ELVB and the OR_I of the line L_{1-2} supplying the ELVB.
R_{III}-N_4	0.9020	R_{III} at the GLVB node. It is estimated as the geometric average between the OR_V in the GLVB and the OR_I of the line L_{1-4} supplying the GLVB.
R_{III}-N_8	0.9069	R_{III} at the PCC node. It is estimated as the geometric average between the OR_V in the PCC and the OR_I of the lines supplying the PCC. OR_I is obtained by the weighted arithmetic average between the OR_I of the lines L_{4-8} and L_{8-9}.
R_{III}-EEB	**0.8902**	**The R_{III} of the EEB-UIS electrical network**. It is calculated by the weighted arithmetic average between R_{III}-N_2, R_{III}-N_4 and R_{III}-N_8.
R_{III}-L_{TP1}	0.5778	The R_{III} projection for the TP1 load. It corresponds to the OR_I of the load line L_{4-5}.
R_{III}-L_{TP2}	0.8547	The R_{III} projection for the TP2 load. It corresponds to the OR_I of the load line L_{4-6}.
R_{III}-L_{TP3}	0.7706	The R_{III} projection for the TP3 load. It corresponds to the OR_I of the load line L_{4-7}.
R_{III}-L_{TP4}	0.8696	The R_{III} projection for the TP4 load. It corresponds to the OR_I of the load line L_{8-10}.
R_{III}-L_{TP5}	0.7097	The R_{III} projection for the TP5 load. It corresponds to the OR_I of the load line L_{2-3}.
R_{III}-L_{Emerg}	0.7383	The R_{III} projection for the emergency loads connected to the ELVB. It corresponds to the OR_I of the line L_{1-2}.

assessment. The case study results indicate that R_I does not require further attention since the CI of the EEB-UIS has a low risk of collapse due to HILP events. R_{II} could be strengthened by increasing the backup system's coverage to the building's non-priority critical loads. R_{III} shows a general alert state for the EEB-UIS network and an emergency state for the TP1 load circuit. Therefore, the EEB-UIS electrical network could require attention to address overvoltage issues, load balance and harmonic distortion of current.

This chapter contributes to the compliance of the third specific objective (SO3). It analyses the effect of the PV systems on electrical resilience. The results in the case study show a positive effect of PV system integration. The OR_I of the PV system line (L8-9) has the best re-

silience rating of the line sections of the EEB-UIS network. Thus, it benefits the overall R_{III}-EEB resilience rating. This effect could be because the EEB-UIS PV system is adequately balanced in power delivery, and the power inverters generate low harmonic pollution. Indeed, it is possible to establish strategies to take advantage of the PV system. It also contributes to answering research questions two (RQ2), five (RQ4) and six (RQ6). R_{III} could be used to evaluate the performance of a PV installation in LV networks since R_{III} analyses the quality of the voltage at the coupling point and the quality of the current delivered by the PV system. Therefore, PV systems could contribute to strengthening LV grids through proper power balancing and delivering current without harmonic distortion. In addition, the R_{III} assessment shows the possibility of constant evolutionary analysis setting an accurate refresh time.

It is possible to analyse the daily fluctuation of the operating quality of an electricity network to identify patterns of poor quality behaviour. Furthermore, an automated operational resilience assessment system could be implemented using smart meter installation and data processing to evaluate the operation resilience for a specific period and plan preventive and corrective actions. The following chapters focus on the resilience feedback phase to develop strengthening strategies. Chapter 6 presents the EEB-UIS electricity grid model for the feedback phase. And Chapter 7 develops the feedback phase.

6. EEB-UIS LV Network Model for the Resilience Feedback Phase

This chapter presents the Electrical Engineering Building (EEB-UIS) LV network model for analysing the feedback phase of electrical resilience. A hydrogen-based energy backup system (H_2-ESS) is proposed as a measure to strengthen resilience. The model is used to simulate power flows, reconfiguration of the point of common coupling (PCC) of the energy resources and implement an energy management strategy (EMS). It facilitates the comparison of resilience-strengthening strategies and implementing sensitivity analysis. The energy macro-

scopic representation (EMR) is used to present the EEB-UIS's electrical network AC and DC components.

This chapter contributes to the development of the third (SO3) and fourth (SO4) specific objectives. The model allows the analysis of the PV and H_2-ESS penetration level, location and effect on the electrical resilience. It allows the simulation of EMS on the EEB-UIS's sources. It also contributes to answering research questions four (RQ4), five (RQ5) and six (RQ6). The remainder of this chapter is organised as follows: Section 6.1 highlights remarks about the EEB-UIS network model and Section 6.2 about its EMR. Section 6.3 presents the model of the AC components. Section 6.4 describes the PV system modelling. Then, Section 6.5 shows the backup system model, and Section 6.6 describes the EL system modelling. Finally, Section 6.7 summarises the chapter's contributions.

6.1 Remarks on the EEB-UIS network model

The electrical resilience assessment's feedback phase requires an EEB-UIS network model. It is also necessary to model the feedback measures and evaluate their effect. This chapter develops the EEB-UIS grid model considering the information detailed in Chapter 4. There are two important remarks in modelling: *i)* The EEB-UIS loads are grouped by priority category. *ii)* The current diesel genset backup system is replaced by an H_2-ESS. The H_2-ESS integrates a fuel cell (FC), a battery bank, an electrolyser (EL) and a tank for the storage of pressurised hydrogen (H_2).

Classifying loads is subject to grouping them into load circuits. Three load categories could be defined for the EEB-UIS regarding their priority:

- L_{CAT1}: Essential loads are the minimum necessary to ensure proper building operation, such as security and emergency loads. They correspond to the TP5 circuit and the loads of the the emergency low voltage bus (ELVB).
- L_{CAT2}: Priority loads contribute to the electrical system's better functioning, but their

absence does not imply a safety risk for the equipment or people. It relates to the TP4 circuit.

- L_{CAT3}: Non-priority loads could not be supplied without causing a significant impact on the operation of the electrical system. They concern the load circuits supplied by the general low voltage bus (GLVB).

Figure 32 presents a schematic of the EEB-UIS LV network equivalent to the diagram shown in Figure 19 of Chapter 4. The network has been simplified into the key nodes highlighting ELVB, GLVB and PCC and the load categories. The H_2-ESS and PV systems have been included as distributed generation (DG) sources. A three-phase model is used for the AC components of the electrical network. It considers the unbalance in voltage and current but not the harmonic distortion. Active and reactive powers are also considered on the AC side. This model is feasible since the strategies analysed in the feedback are focused on improving the network's voltage regulation and the load through the electrical wires.

Figure 32

Diagram of EEB-UIS electrical network integrating DG sources.

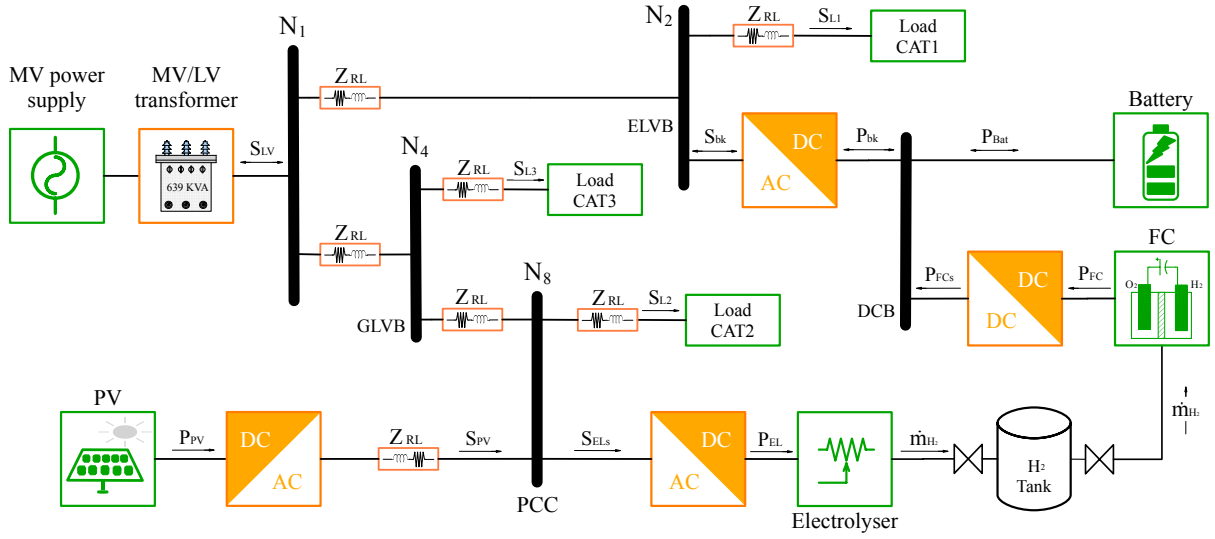

6.2 Using the energy macroscopic representation

The energy macroscopic representation (EMR) presents the EEB-UIS electrical network model interconnecting sources and loads that operate in AC and DC. This formalism facilitates modular modelling of the energy system's elements and systematical interconnection. It also supports understanding and applying control and EMS (Solano *et al.*, 2020). According to the operation of the EEB-UIS network, the feeder imposes the voltage on the supply node. The wires interconnecting elements must respect Ohm's law; thus, there are energy losses and voltage drops. Since line sections are short and the voltage is low, the wires have a resistive-inductive impedance (Z_{RL}). The interconnections between AC and DC elements are through power inverters. The interaction between DC sources requires DC/DC converters. Table 19 presents the EMR elements and their association with components of the EEB-UIS electrical network.

Figure 33 presents the EMR of the EEB-UIS electrical network. The model also integrates a stage of energy measurement and management. This stage is represented with the EMR inversion elements shown in Figure 34. The simulations, power flows and EMS are developed in Matlab and Simulink. Quasi-static power flows are run to estimate the electrical parameters' behaviour over time. Simulations use a 1-minute refresh time and a total simulation time of up to one month. The following sections describe the model of the EEB-UIS's network components.

6.3 AC low-voltage network modelling

The AC grid comprises a feeder, electrical wires, loads, and connection nodes. The feeder and the loads use operation profiles. AC phasor representation is used for voltage and current in vectors of three components representing a three-phase system.

Table 19

EMR elements description for EEB-UIS network.

EMR element	Grid component	Description
Energy source 	Feeder	Set the AC voltage at the supply node. The reaction is the supply current.
	Load demand	Input AC voltage and output current. Constant power model.
	PV and electrolyser	Input DC voltage and output current.
	FC and batteries	Input DC current and output voltage.
Energy conversion 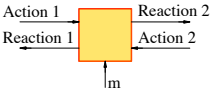	DC/DC converters	FC and Batteries integration.
	DC/AC inverters	Integration of AC and DC equipment.
	AC/DC inverter	One-way AC to DC conversion.
Energy accumulation 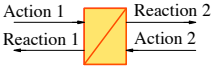	AC wire	Resistance and inductance, constant impedance model.
Energy distribution 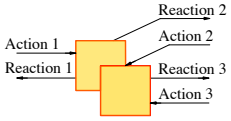	AC node	Circuits and loads branching.
	PCC	Sources coupling points.

Figure 33

Energy macroscopic representation of the EEB-UIS network.

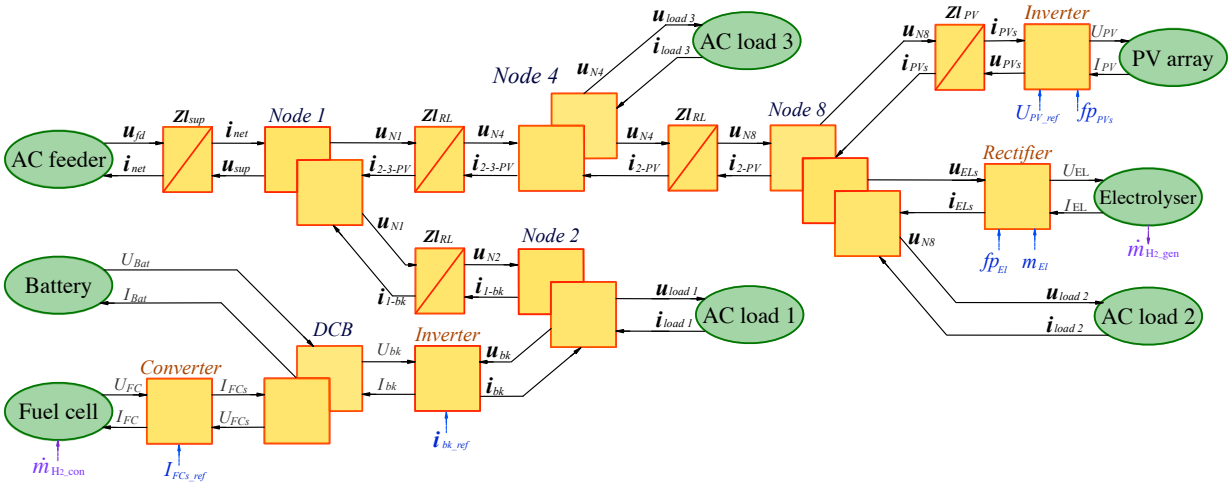

6.3.1 Feeder model

The feeder is modelled as an ideal voltage source supplying the current $\vec{\mathbf{i}}_{net}$ demanded

Figure 34

EMR inversion elements for the measurement and management stage.

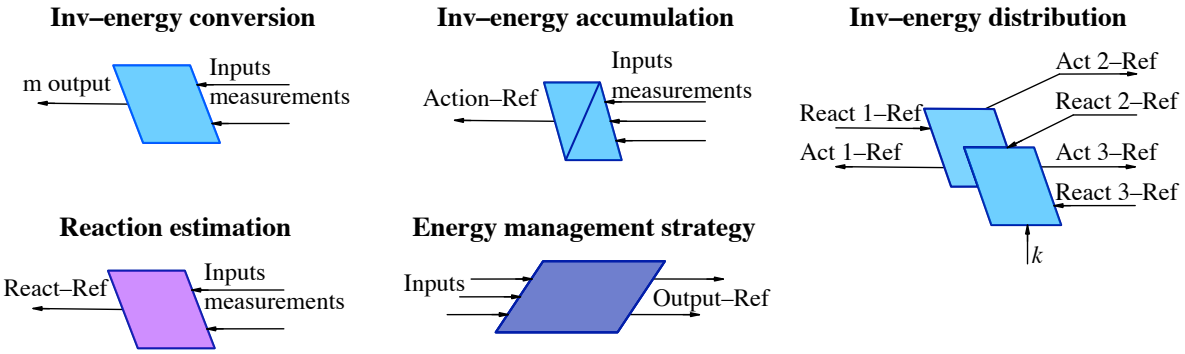

by the electrical system. The voltage profile defines the source root mean square (RMS) voltage values. It is the measurement of the voltage of each phase during May with 10 minutes sampling time. In regular operation with a power supply, the feeder is the reference node for the AC electrical network. In case of a power outage operation, the feeder current is null. Eq. (6.1) presents the structure of the feeder supply voltage $\vec{\mathbf{u}}_{fd}$ and current $\vec{\mathbf{i}}_{net}$. Here, U_A, U_B and U_C are the phase RMS voltages from the voltage profile; θ_A, θ_B and θ_C are their associated phase angles. $\vec{\mathbf{0}}$ is the three-component zero vector.

$$\vec{\mathbf{u}}_{fd} = \begin{bmatrix} U_A \angle \theta_A \\ U_B \angle \theta_B \\ U_C \angle \theta_C \end{bmatrix} \quad \textit{If power supply regular operation}$$

$$\vec{\mathbf{i}}_{net} = \vec{\mathbf{0}} = \begin{bmatrix} 0 \\ 0 \\ 0 \end{bmatrix} \quad \textit{If power outage operation} \tag{6.1}$$

6.3.2 Load model

The load model uses active and reactive power demand profiles. It combines both, obtaining the complex power $\mathbf{S}_\phi$ for each phase. Eq. (6.2) calculate the single-phase load current

$\mathbf{i}_{load\phi}$ and Eq. (6.3) builds the load current vector $\vec{\mathbf{i}}_{load}$. Here, $\mathbf{u}_{load\phi}$ is the single-phase voltage phasor supplying the load of the ϕ-phase. P_ϕ, and Q_ϕ are the single-phase active and reactive power demand profiles for the ϕ-phase, respectively. $\mathbf{i}_{load_A}$, $\mathbf{i}_{load_B}$ and $\mathbf{i}_{load_C}$ are the current phasors calculated by Eq. (6.2) for each load phase.

$$\mathbf{i}_{load\phi} = conj\left\{\frac{P_\phi + \hat{j}Q_\phi}{\mathbf{u}_{load\phi}}\right\} \tag{6.2}$$

$$\vec{\mathbf{i}}_{load} = \begin{bmatrix} \mathbf{i}_{load_A} \\ \mathbf{i}_{load_B} \\ \mathbf{i}_{load_C} \end{bmatrix} \tag{6.3}$$

6.3.3 Wire conductors model

Conductors are modelled as a constant impedance $\mathbf{Z}_l$. The mutual inductive effect of the wire is not considered for power flows in this static model. Eq. (6.4) shows the input-output relationship of a wire. Here, $\vec{\mathbf{u}}_1$ and $\vec{\mathbf{u}}_2$ are the voltage vectors on each side of the wire. $\vec{\mathbf{i}}_1$ is the vector of the current that goes through the wire. R_l and X_l are the wire's total resistance and inductive reactance, respectively.

$$\begin{aligned} \vec{\mathbf{i}}_1 &= \frac{\vec{\mathbf{u}}_1 - \vec{\mathbf{u}}_2}{(R_l + \hat{j}X_l)} \\ \vec{\mathbf{i}}_2 &= \vec{\mathbf{i}}_1 \end{aligned} \tag{6.4}$$

6.3.4 Connection node model

The purpose of the nodes is to interconnect the branches. The node voltage is set by the main branch. The current through the main branch is the sum of the currents of the secondary branches. Eq. (6.5) relates to energy distribution. Here $\vec{\mathbf{u}}_1$ and $\vec{\mathbf{i}}_1$ are the node voltage and the primary branch current, respectively. $\vec{\mathbf{u}}_2$ and $\vec{\mathbf{u}}_3$ are the node voltages referring to the branch

branches. $\vec{\mathbf{i}}_2$ and $\vec{\mathbf{i}}_3$ are the branch currents. Figure 35 summarises the model of the AC LV network's elements.

$$\begin{aligned} \vec{\mathbf{u}}_3 &= \vec{\mathbf{u}}_2 = \vec{\mathbf{u}}_1 \\ \vec{\mathbf{i}}_1 &= \vec{\mathbf{i}}_2 + \vec{\mathbf{i}}_3 \end{aligned} \tag{6.5}$$

Figure 35

AC LV electrical network model.

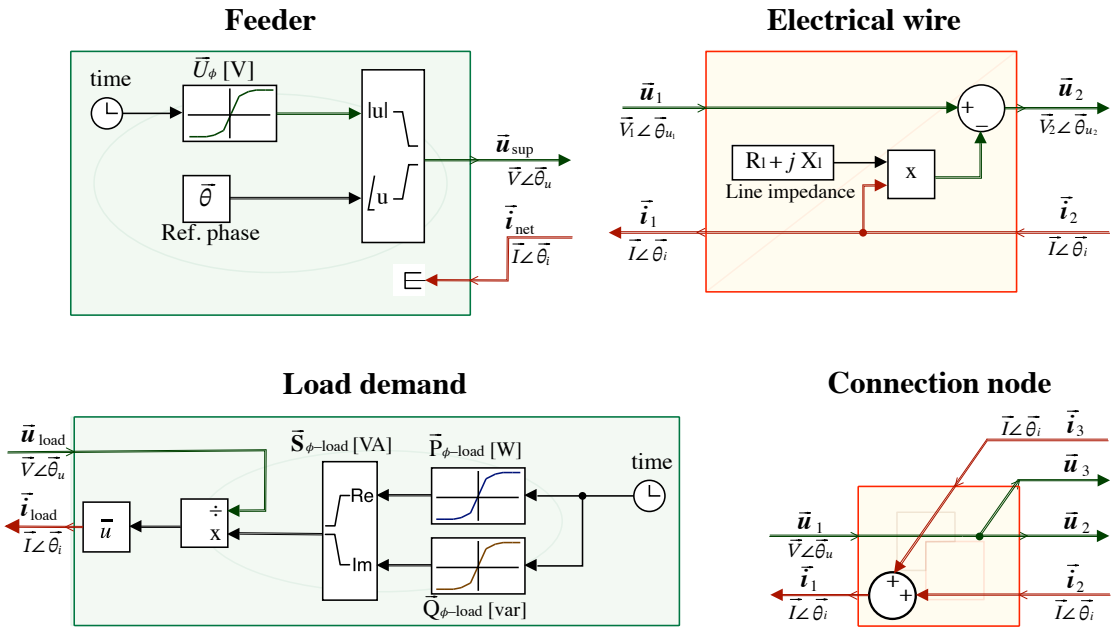

6.4 Photovoltaic generation system modelling

A PV generation system comprises an array of PV modules, a DC/AC inverter and connection wires. Next, the components model is described.

6.4.1 PV array model

The model for solar cell simulations proposed by Gow & Manning (1999) is used. Despite it being an old model, it is used in several current researches such as Hassan *et al.* (2023);

Yaqoob *et al.* (2022); Fahim *et al.* (2022). It corresponds to the saturation one-diode circuit model. Eq. (6.6) to Eq. (6.8) relate the voltage and current of the solar cell.

$$\begin{aligned} I_c &= I_{ph} - I_d - \frac{U_d}{R_{sh}} \\ I_{ph} &= \frac{G}{G_a} \cdot [I_{sc} + k_i \cdot (T - 298.15)] \end{aligned} \tag{6.6}$$

$$I_d = I_0 \cdot \left[e^{\frac{U_d}{U_T}} - 1 \right] \tag{6.7}$$

$$I_0 = \frac{I_{sc} + k_i \cdot (T - 298.15)}{e^{\left[\frac{U_{oc} + k_v \cdot (T - 298.15)}{U_T}\right]} - 1}$$

$$\begin{aligned} U_d &= U_c + R_s \cdot I_c \\ U_T &= \frac{n \cdot k_B \cdot T}{q} \end{aligned} \tag{6.8}$$

Here, U_c and I_c are the solar cell's voltage and current, respectively. I_d is the diode's saturation current, and U_d is its voltage. R_{sh} and R_s are the cell's parallel and series resistance, respectively. I_{ph} is the solar-induced current. G_0 is the standard irradiance (1 000 W/m^2). G and T are the irradiance and temperature perceived by the cell in W/m^2 and Kelvin, respectively. The current and voltage temperature coefficients are K_i and k_v, respectively. I_{sc} and U_{oc} are the cell's short circuit current and open circuit voltage, respectively. U_T is the thermal voltage. n, k_B and q are the diode emission coefficient, the Boltzmann constant, and the elementary charge on an electron, respectively.

All the above parameters correspond to a single solar cell. A solar module comprises n_s cells in series and n_p in parallel. A PV system integrates N_{ar} arrays parallel of N_{st} modules in series. Eq. (6.9) relates the module's open circuit voltage U_{oc_mod} to U_{oc} and the module's short circuit current I_{sc_mod} to I_{sc}. Eq. (6.10) links the module voltage U_{mod} to U_c and the current I_{mod} to I_c. Eq. (6.11) ties the array PV's voltage U_{PV} and current I_{PV} with U_{mod} and I_{mod}, respectively.

$$\begin{aligned} U_{oc} &= \frac{U_{oc\_mod}}{n_s} \\ I_{sc} &= \frac{I_{sc\_mod}}{n_p} \end{aligned} \tag{6.9}$$

$$\begin{aligned} U_{mod} &= U_c \cdot n_s \\ I_{mod} &= I_c \cdot n_p \end{aligned} \tag{6.10}$$

$$\begin{aligned} U_{PV} &= U_{mod} \cdot N_{st} \\ I_{PV} &= I_{mod} \cdot N_{ar} \end{aligned} \tag{6.11}$$

6.4.2 PV power inverter model

A power inverter interconnects the PV array to the AC electrical network. The inverter's AC voltage $\vec{\mathbf{u}}_{PVs}$ is synchronised with the voltage of the interconnection point to inject the generated PV power into the grid. The inverter associates a maximum power point tracking (MPPT) algorithm to maximise the PV array power. Thus, the voltage U_{PV} of the inverter DC side is given by Eq. (6.12) and Eq. (6.13) develops the AC power of the PV system. The model is that the PV system delivers balanced power to the AC grid. Therefore, the single-phase powers are equal in value. Here, P_{PVs} is the power of the PV system. $P_{\phi PVs}$, $Q_{\phi PVs}$ and $\mathbf{S}_{\phi PVs}$ are the single-phase active, reactive and complex power of the PV system, respectively. η_{inv_PV} is the efficiency of the inverter. fp_{PVs} is the power factor set for the inverter.

$$U_{PV} = U_{PV\_ref} = f_{|MPPT}\left(U_{PV}\ ,\ I_{PV}\right) \tag{6.12}$$

$$\begin{aligned} P_{PVs} &= \eta_{inv\_PV} \cdot U_{PV} \cdot I_{PV} \\ P_{\phi PVs} &= \frac{P_{PVs}}{3} \\ Q_{\phi PVs} &= P_{\phi PVs} \cdot \frac{\sqrt{1-fp_{PV}^2}}{fp_{PVs}} \\ \mathbf{S}_{\phi PVs} &= P_{\phi PVs} + \hat{j} Q_{\phi PVs} \end{aligned} \tag{6.13}$$

A single-phase current $\mathbf{i}_{\phi PVs}$ is defined by Eq. (6.14) and the structure of the PV system

current vector $\vec{\mathbf{i}}_{PVs}$ by Eq. (6.15). Here, $\mathbf{u}_{\phi PVs}$ represents the single-phase voltage at the inverter of the PV system. $\mathbf{i}_{PVs_A}$, $\mathbf{i}_{PVs_B}$ and $\mathbf{i}_{PVs_C}$ are the single-phase current components of $\vec{\mathbf{i}}_{PVs}$. $\mathbf{u}_{PVs_A}$, $\mathbf{u}_{PVs_B}$ and $\mathbf{u}_{PVs_C}$ are the single-phase voltage components of $\vec{\mathbf{u}}_{PVs}$.

$$\mathbf{i}_{\phi PVs} = conj\left\{\frac{\mathbf{S}_{\phi PVs}}{\mathbf{u}_{\phi PVs}}\right\} \tag{6.14}$$

$$\vec{\mathbf{i}}_{PVs} = \begin{bmatrix} \mathbf{i}_{PVs_A} \\ \mathbf{i}_{PVs_B} \\ \mathbf{i}_{PVs_C} \end{bmatrix} = \begin{bmatrix} conj\left\{\frac{\mathbf{S}_{\phi PVs}}{\mathbf{u}_{PVs_A}}\right\} \\ conj\left\{\frac{\mathbf{S}_{\phi PVs}}{\mathbf{u}_{PVs_B}}\right\} \\ conj\left\{\frac{\mathbf{S}_{\phi PVs}}{\mathbf{u}_{PVs_C}}\right\} \end{bmatrix} \tag{6.15}$$

6.4.3 Connection wire model

The wire connects the PV system with the electrical network. Eq. (6.16) relates the voltage drop in the conductor. Here R_{l_PV} is the resistance of the wire, and X_{l_PV} is the inductive reactance. $\vec{\mathbf{u}}_{PCC}$ is the voltage at the point of coupling. Figure 36 summarises the PV system model.

$$\vec{\mathbf{u}}_{PVs} = \vec{\mathbf{u}}_{PCC} - (R_{l\_PV} + \hat{j}X_{l\_PV}) \cdot \vec{\mathbf{i}}_{PVs} \tag{6.16}$$

6.5 Fuel cell-battery backup system modelling

The energy backup system comprises a proton exchange membrane fuel cell (PEMFC) and a lead-acid battery pack. They are coupled on the DC side through a DC/DC converter associated with the FC. Then, a DC/AC inverter couples the backup set to the AC side. The components model is described below.

6.5.1 Fuel cell array model

The FC polarisation model described by Kandidayeni *et al.* (2020) is used. The voltage

Figure 36

Photovoltaic system model.

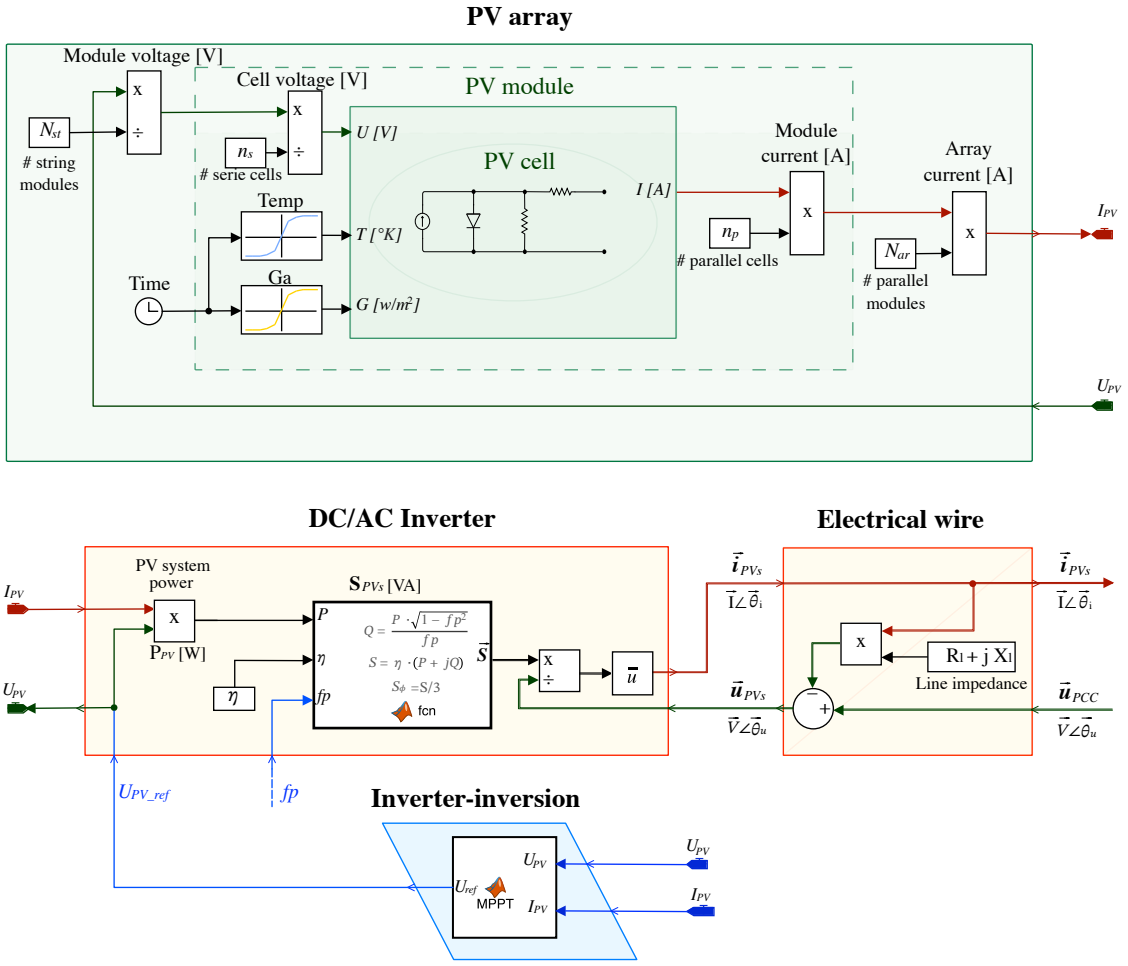

of a single-cell U_{fc} is given by Eq. (6.17) and Eq. (6.18) estimated the H_2 consumption $\dot{m}_{H_2\_fc}$.

$$U_{fc} = U_{OCV} - \eta_{act} - \eta_{conc} - \eta_{ohm} \tag{6.17}$$

$$\dot{m}_{H_2\_fc} = \dot{m}_{OC} + m_{H_2} \cdot I_{fc} \tag{6.18}$$

Here, I_{fc} is the operating current of a single cell, and U_{OCV} is the internal induced voltage of the cell assumed constant. η_{act}, η_{conc} and η_{ohm} are the activation, concentration, and ohmic voltage drops, respectively. They are defined in Eq. (6.19). Here, $\dot{m}_{H_2\_con}$ is in kg/s. $\dot{m}_{OC}$ is open circuit H_2 flow, and m_{H_2} is the H_2 consumption factor.

$$\begin{aligned} \eta_{act} &= C_{act} \cdot log_{10}(I_{fc}) \\ \eta_{conc} &= C_{conc} \cdot I_{fc}^{k_{sq}} \cdot ln\left(1 - \frac{I_{fc}}{J_{max}}\right) \\ \eta_{ohm} &= r_{cell} \cdot I_{fc} \end{aligned} \tag{6.19}$$

Furthermore, C_{act} and C_{conc} are activation and concentration constants, respectively. k_{sq} is the concentration exponent. J_{max} is the cell's maximum density current. Moreover, r_{cell} is the single-cell equivalent resistance. These parameters characterise the FC. The FC pack's current I_{FC} and Voltage U_{FC} depend on the number of cells in series N_{S_fc} and the parallel branches N_{P_fc} as Eq. (6.20) shows. Then, Eq. (6.21) presents the total FC's H_2 consumption.

$$\begin{aligned} U_{FC} &= U_{fc} \cdot N_{S\_fc} \\ I_{FC} &= I_{fc} \cdot N_{P\_fc} \end{aligned} \tag{6.20}$$

$$\dot{m}_{H_2\_con} = N_{S\_fc} \cdot N_{P\_fc} \cdot \dot{m}_{H_2\_fc} \tag{6.21}$$

6.5.2 FC converter model

The converter couples the FC array with the battery pack. The input voltage and output current are related to the current reference for the FC system I_{FCs_ref} as Eq. (6.22) shows.

$$\begin{aligned} P_{FC\_ref} &= \frac{U_{FCs} \cdot I_{FCs\_ref}}{\eta_{conv}} \\ I_{FC} &= f_{I|P}\left(P_{FC\_ref}\right) \end{aligned} \tag{6.22}$$

Here P_{FC_ref} is the power reference for the FC array. U_{FCs} is the FC system voltage and η_{conv} is the converter's efficiency. I_{FC} is the operating current the inverter imposes on the FC. $f_{I|P}$ is a lookup table of FC current as a function of FC power including a current saturation stage. Then, U_{FC} depends on I_{FC}, as introduced before. Eq. (6.22) presents the calculation of the FC system's current I_{FCs}. Here, P_{FC} is the FC array power, and U_{FCs} is the FC system voltage.

$$\begin{aligned} P_{FC} &= I_{FC} \cdot U_{FC} \\ I_{FCs} &= \frac{\eta_{conv} \cdot P_{FC}}{U_{FCs}} \end{aligned} \tag{6.23}$$

6.5.3 *Battery pack model*

The battery static model described by Moubayed *et al.* (2008) is implemented. Eq. (6.24) shows the voltage U_b and the state of charge SOC_b of a single battery.

$$\begin{aligned} U_b &= E_m - I_b \cdot R_{int} \\ SOC_b &= \frac{1}{Cap_b} \cdot \int_0^t I_b \cdot dt \end{aligned} \tag{6.24}$$

Here, I_b is the current of a single battery. Cap_b is the storage capacity of a single battery. E_m and R_{int} are the battery open-circuit voltage and internal resistance, respectively. They are functions of SOC_b as Eq. (6.25) presents. The voltage U_{Bat} and current I_{Bat} of the battery pack relate to the number of batteries in series N_{b_s} and the number of branches N_{b_p} as Eq. (6.26) present.

$$\begin{aligned} E_m &= f_{U|SOC}\,(SOC_b) \\ R_{int} &= f_{R|SOC}\,(SOC_b) \end{aligned} \tag{6.25}$$

$$\begin{aligned} U_{Bat} &= N_{b_s} \cdot U_b \\ I_{Bat} &= N_{b_p} \cdot I_b \end{aligned} \tag{6.26}$$

6.5.4 *DC coupling model*

The FC system and the battery pack require a coupling. The battery pack does not have a converter; it imposes the voltage U_{BK} on the DC node. Then, the DC current I_{BK} of the backup system is the sum of the currents of the battery pack and the FC system. Eq. (6.27) shows the relationship described.

$$\begin{aligned} U_{BK} &= U_{FCs} = U_{Bat} \\ I_{BK} &= I_{FCs} + I_{Bat} \end{aligned} \tag{6.27}$$

6.5.5 DC/AC coupling model

A power inverter couples the DC and AC sides. It is based on the current reference vector $\vec{\mathbf{i}}_{bk\_ref}$ to define the AC current $\vec{\mathbf{i}}_{bk}$ delivered by the backup system. The backup system supplies adequate current to each phase. Thus $\vec{\mathbf{i}}_{bk\_ref}$ contains references per phase $\mathbf{i}_{bk_{A}\_ref}$, $\mathbf{i}_{bk_{B}\_ref}$ and $\mathbf{i}_{bk_{C}\_ref}$ as shown in Eq. (6.28). During operation with regular supply power, the voltage of the inverter $\vec{\mathbf{u}}_{inv}$ is synchronised with the voltage of the coupling point. In case of a power outage, the inverter of the backup system imposes the voltage and is the reference of the AC grid. It is presented in Eq. (6.29). Here, U_N is the nominal voltage of the EEB-UIS network.

$$\vec{\mathbf{i}}_{bk} = \vec{\mathbf{i}}_{bk\_ref} = \begin{bmatrix} \mathbf{i}_{bk_{A}\_ref} \\ \mathbf{i}_{bk_{B}\_ref} \\ \mathbf{i}_{bk_{C}\_ref} \end{bmatrix} \tag{6.28}$$

$$\vec{\mathbf{u}}_{inv} = \begin{bmatrix} U_N \angle 0 \\ U_N \angle -\frac{2\pi}{3} \\ U_N \angle -\frac{4\pi}{3} \end{bmatrix} \quad \textit{If power outage operation} \tag{6.29}$$

The AC operating power of the backup system is obtained by the product of its voltage and current. The DC side current I_{BK} is the ratio between the active backup power P_{bk} and the efficiency of the inverter η_{inv}. Eq. (6.30) sets the operating parameters of the inverter. Here, $\vec{\mathbf{u}}_{inv}$ is the voltage on the AC side of the inverter. Furthermore, $\bullet$ is the vectors' scalar product operator, and the $real\{\,\}$ operator returns the real part of a value. Figure 37 summarises the FC-battery backup system model.

$$\begin{gathered} \mathbf{S}_{bk} = \vec{\mathbf{u}}_{inv} \bullet conj\left\{\vec{\mathbf{i}}_{bk}\right\} \\ I_{BK} = \frac{real\{\mathbf{S}_{bk}\}}{\eta_{inv} \cdot U_{BK}} \end{gathered} \tag{6.30}$$

Figure 37

FC-battery backup system model.

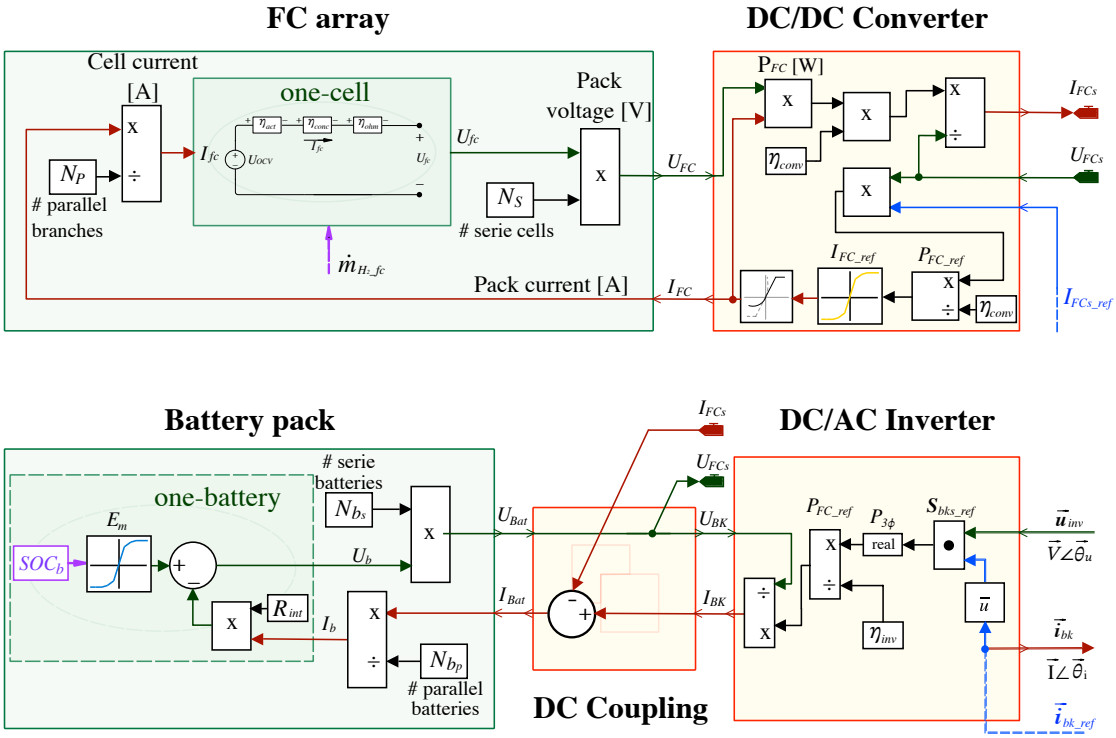

6.6 Electrolyser system modelling

The electrolyser (EL) system comprises an alkaline EL and a voltage inverter. The inverter interconnects the EL to the AC power grid. The model of the EL system is described below.

6.6.1 Alkaline electrolyser model

The empirical polarisation model described by Ulleberg (2003) is used for the alkaline electrolyser. Eq. (6.31) presents the relationship between the voltage of an EL cell U_{el} and its current I_{el}.

$$U_{el} = U_{rev} + r_{el} \cdot \frac{I_{el}}{A} + s \cdot ln\left(\tau \cdot \frac{I_{el}}{A} + 1\right) \tag{6.31}$$

Here, U_{rev} is the reversible voltage of the water. r_{el} is the equivalent resistance of a

single cell depending on the EL's temperature T. A is the electrode area in m^2. s and τ are the activation overpotential parameters. U_{rev} can be determined from the Gibbs energy ΔG for water splitting as Eq. (6.32) shows.

$$U_{rev} = \frac{\Delta G}{z \cdot F} = \frac{\Delta H - T \cdot \Delta S}{z \cdot F} \tag{6.32}$$

Here, z is the number of electrons transferred per reaction; it equals 2. F is Faraday's constant. T is the water temperature in kelvin. ΔH and ΔS are the enthalpy and entropy change in the reaction, respectively. The total energy demanded ΔH is related to the cell thermoneutral voltage U_{tn} by (6.33). At standard conditions (25 °C, 1 bar), $\Delta G = 237\ kJ/mol$, $U_{rev} = 1.229\ V$, and $U_{tn} = 1.482\ V$.

$$U_{tn} = \frac{\Delta H}{z \cdot F} \tag{6.33}$$

Ulleberg (1997) proposed modelling the effect of EL's temperature T_{EL} on r_{el} and τ by Eq. (6.34). Here, r_1 and r_2 are the ohmic resistance parameters. τ_1 , τ_2 and τ_3 are overvoltage on electrodes parameters. These parameters are obtained empirically by characterising the EL $I-U$ saturation curve at different temperatures. The EL's temperature T_{EL} is given by Eq. (6.35).

$$\begin{aligned} r_{el} &= r_1 + r_2 \cdot T_{EL} \\ \tau &= \tau_1 + \frac{\tau_2}{T_{EL}} + \frac{\tau_3}{T_{EL}^2} \end{aligned} \tag{6.34}$$

$$T_{EL} = T_{ini} + \frac{\Delta t}{C_t} \cdot \left(\dot{Q}_{gen} - \dot{Q}_{loss} - \dot{Q}_{cool}\right) \tag{6.35}$$

Here, T_{ini} is the initial temperature. Δt is the time interval. C_t is the overall thermal capacity of electrolyser in JK_{-1}. $\dot{Q}_{gen}$, $\dot{Q}_{loss}$ and $\dot{Q}_{cool}$ are the heat transfer rate in W calculated by Eq. (6.36).

$$\begin{aligned} \dot{Q}_{gen} &= N_c \cdot U_{el} \cdot I_{el} \cdot \left(1 - \eta_e\right) \\ \dot{Q}_{loss} &= \frac{1}{R_t} \cdot (T_{EL} - T_a) \\ \dot{Q}_{cool} &= UA_{HX} \cdot LMTD \end{aligned} \tag{6.36}$$

Here, N_c is the total number of EL cells. η_e is the EL energy effiency defined by Eq. (6.37). R_t is the EL overall thermal resistence in $W^{-1}K$. T_a is the room temperature. UA_{HX} is the heat transfer coefficient-area product for the heat exchanger in WK^{-1}. Moreover, $LMTD$ is the log mean temperature difference. Q_{cool} could assume a constant cooling value when T_{EL} exceeds a critical temperature T_{crit}.

$$\eta_e = \frac{U_{tn}}{U_{el}} \tag{6.37}$$

Finally, Eq. (6.38) presents the relationship of the EL stack's voltage U_{EL} and current I_{EL} with the number of cells in series N_{S_el} and the number of branches in parallel N_{P_el}.

$$\begin{aligned} U_{EL} &= N_{S\_el} \cdot U_{el} \\ I_{EL} &= N_{P\_el} \cdot U_{el} \end{aligned} \tag{6.38}$$

6.6.2 Hydrogen production model

According to Farady's law, the rate H_2 production $\dot{m}_{H_2\_gen}$ is directly proportional to the transfer of electrons. Hance, $\dot{m}_{H_2\_gen}$ could be expressed with Eq. (6.39). Here, η_F is the Faraday efficiency representing the ratio between the actual and theoretical maximum amount of H_2 production. According to Ulleberg (2003) η_F could be expressed empirically by Eq. (6.40) depending on I_{el}. Here, the parameters of Faraday's efficiency are f_1 and f_2. At nominal current η_F is around 0.95.

$$\dot{m}_{H_2\_gen} = \eta_F \cdot \frac{N_c \cdot I_{el}}{z \cdot F} \tag{6.39}$$

$$\eta_F = \frac{(I_{el}/A)^2}{f_1 + (I_{el}/A)^2} \cdot f_2 \tag{6.40}$$

6.6.3 Voltage inverter model

The inverter couples the EL stack with the AC grid. The inverter model uses a reference current vector $\vec{\mathbf{i}}_{ELs\_ref}$ to define its operation. It sets the reference current for each phase. The grid provides the operating voltage. Eq. (6.41) and Eq. (6.42) give the EL inverter's reference current $\vec{\mathbf{i}}_{ELs\_ref}$ and voltage $\vec{\mathbf{u}}_{ELs}$, respectively. Here, $\mathbf{i}_{ELs_A\_ref}$, $\mathbf{i}_{ELs_B\_ref}$ and $\mathbf{i}_{ELs_C\_ref}$ are the reference currents per phase. $\vec{\mathbf{u}}_{PCC\_EL}$ is the voltage vector at the coupling point of the EL system, and $\mathbf{u}_{PCC_A\_EL}$, $\mathbf{u}_{PCC_B\_EL}$ and $\mathbf{u}_{PCC_C\_EL}$ are their voltages per phase.

$$\vec{\mathbf{i}}_{ELs\_ref} = \begin{bmatrix} \mathbf{i}_{ELs_A\_ref} \\ \mathbf{i}_{ELs_B\_ref} \\ \mathbf{i}_{ELs_C\_ref} \end{bmatrix} \tag{6.41}$$

$$\vec{\mathbf{u}}_{ELs} = \vec{\mathbf{u}}_{PCC\_EL} = \begin{bmatrix} \mathbf{u}_{PCC_A\_EL} \\ \mathbf{u}_{PCC_B\_EL} \\ \mathbf{u}_{PCC_C\_EL} \end{bmatrix} \tag{6.42}$$

The reference for the AC power consumption of the EL system is defined in Eq. (6.43). Here, $\mathbf{S}_{ELs\_ref}$ and fp_{ELs_ref} are the complex power and power factor references for the EL system, respectively. $abs\{\}$ operator returns the magnitude of a value.

$$\begin{aligned} \mathbf{S}_{ELs\_ref} &= \vec{\mathbf{u}}_{ELs} \bullet conj\{\vec{\mathbf{i}}_{ELs\_ref}\} \\ fp_{ELs\_ref} &= \frac{real\{\mathbf{S}_{ELs\_ref}\}}{abs\{\mathbf{S}_{ELs\_ref}\}} \end{aligned} \tag{6.43}$$

Then, Eq. (6.44) presents the reference power P_{EL_ref} and the current I_{EL} for the EL stack. Here, η_{INV} is the overall inverter efficiency. $f_{I|P,T}$ is a lookup table relating the EL's power and temperature with the current I_{EL}.

$$\begin{aligned} P_{EL\_ref} &= \eta_{INV} \cdot real\{\mathbf{S}_{ELs\_ref}\} \\ I_{EL} &= f_{I|P,T}\left(P_{EL\_ref}\right) \end{aligned} \tag{6.44}$$

To define the AC side operating power, Eq. (6.45) defines the power ratio factor $\vec{\mathbf{s}}_{EL_\phi}$. It is a vector where each component defines the ratio of power for each phase to the total EL system power $\mathbf{S}_{ELs}$ defined in Eq. (6.46).

$$\vec{\mathbf{S}}_{ELs\_ref} = \begin{bmatrix} \mathbf{u}_{ELs_A} \cdot conj\{\mathbf{i}_{ELs_{A\_ref}}\} \\ \mathbf{u}_{ELs_B} \cdot conj\{\mathbf{i}_{ELs_{B\_ref}}\} \\ \mathbf{u}_{ELs_B} \cdot conj\{\mathbf{i}_{ELs_{B\_ref}}\} \end{bmatrix} \tag{6.45}$$

$$\begin{aligned} \vec{\mathbf{s}}_{EL_\phi} &= \frac{\vec{\mathbf{S}}_{ELs\_ref}}{\mathbf{S}_{ELs\_ref}} \\ P_{ELs} &= \frac{U_{EL} \cdot I_{EL}}{\eta_{INV}} \\ Q_{ELs} &= P_{ELs} \cdot \frac{\sqrt{1-fp^2_{ELs\_ref}}}{fp_{ELs\_ref}} \\ \mathbf{S}_{ELs} &= P_{ELs} + \hat{j} Q_{ELs} \end{aligned} \tag{6.46}$$

Finally, Eq. (6.47) defines the EL system power per phase $\vec{\mathbf{S}}_{ELs}$. And, the EL system current $\vec{\mathbf{i}}_{ELs}$ is given by Eq. (6.48). Figure 38 summarises the EL system model.

$$\vec{\mathbf{S}}_{ELs} = \begin{bmatrix} \mathbf{S}_{ELs_A} \\ \mathbf{S}_{ELs_B} \\ \mathbf{S}_{ELs_C} \end{bmatrix} = \mathbf{S}_{ELs} \cdot \vec{\mathbf{s}}_{EL_\phi} \tag{6.47}$$

$$\vec{\mathbf{i}}_{ELs} = \begin{bmatrix} conj\left\{\frac{\mathbf{S}_{ELs_A}}{\mathbf{u}_{ELs_A}}\right\} \\ conj\left\{\frac{\mathbf{S}_{ELs_B}}{\mathbf{u}_{ELs_B}}\right\} \\ conj\left\{\frac{\mathbf{S}_{ELs_C}}{\mathbf{u}_{ELs_C}}\right\} \end{bmatrix} \tag{6.48}$$

Figure 38

Electrolyser system model.

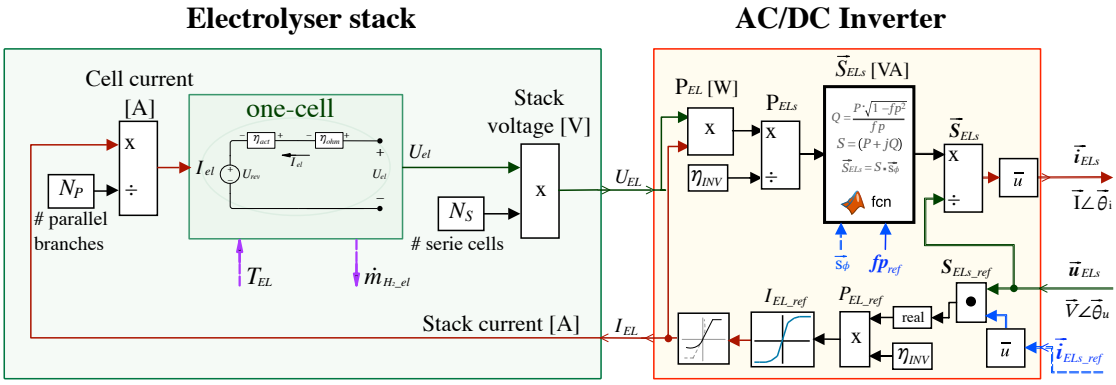

6.7 Summary of contributions

This chapter presents the modelling of the EEB-UIS's electrical networks to analyse the strengthening of electrical resilience. The model is shown using the EMR formalism. The EEB-UIS's AC side uses the phasor representation. This chapter contributes to the third (SO3) and fourth (SO4) specific objectives. The proposed modelling integration allows measuring or estimating the parameters of the electrical network. Then, it is possible to analyse the effect of the energy sources' operation mode and the quality parameters' behaviour. It also allows analysing strategies to strengthen electrical resilience and compare their effectiveness.

This chapter also contributes to answering research questions four (RQ4), five (RQ5) and six (RQ6). The modelling allows testing EMS. It is compatible with the electrical resilience assessment proposal. It allows determining if a H_2 backup system increases the resilience of the electrical network. It also allows the evaluation of the electrical network's resilience evolution through simulations and determining a systematic analysis of the resilience level. The following chapter implements the EEB-UIS LV network model in the electrical resilience feedback analysis.

7. Resilience Feedback Analysis

This chapter focuses on the feedback phase of the electrical resilience for the EEB-UIS case study. It corresponds to the development of parts 4 and 5 of the comprehensive resilience (R_{comp}) assessment methodology proposed in Chapter 3. Here, the results of Chapter 5 are considered to propose strategies to strengthen the EEB-UIS resilience. Results indicate potential for strengthening R_{II} and R_{III}. Then, it addresses two strategies: *i)* Increase the supply continuity capacity in power outages. And, *ii)* implementing an energy management strategy (EMS) for the EEB-UIS sources to strengthen the operation quality. In this sense, it is proposed to define an hydrogen-based energy storage system (H_2-ESS) as a backup system for the EEB-UIS and associate an EMS to address the two approaches.

This chapter completes the third specific objective SO3: "Evaluate the effects of the integration of PV generation and H_2-ESS on the resilience of a LV electrical network." Furthermore, it outlines the achievement of the SO4: "Analyse the sensitivity of the resilience of a LV network to variations in the level of penetration and location of the PV systems and the H_2-ESS and the application of EMS." It also contributes to answering research questions RQ2, RQ4, and RQ6. This chapter is organised as follows: Section 7.1 describes the remarks on the resilience feedback phase. Section 7.2 develops the H_2-ESS sizing. Section 7.3 concerns strengthening the R_{II}. Section 7.4 focuses on the R_{III} feedback. Then, Section 7.5 performs a sensitivity analysis regarding the R_{III} strengthening. Finally, Section 7.6 provides the chapter's conclusions.

7.1 Remark on the feedback phase of the EEB-UIS electrical resilience

The electricity resilience feedback consists of an analysis of the vulnerability of the electricity system in order to develop strategies for strengthening it. Then, a new R_{comp} assessment allows quantifying the improvement. This phase refers to parts 4 and 5 of the methodology pre-

sented in Chapter 3. Figure 39 places the feedback within the resilience assessment. Here, the EEB-UIS type resilience results in Chapter 5 are analysed to determine the vulnerabilities to be addressed and then plan improvement strategies.

Figure 39

Sequence of electrical resilience feedback for the EEB-UIS.

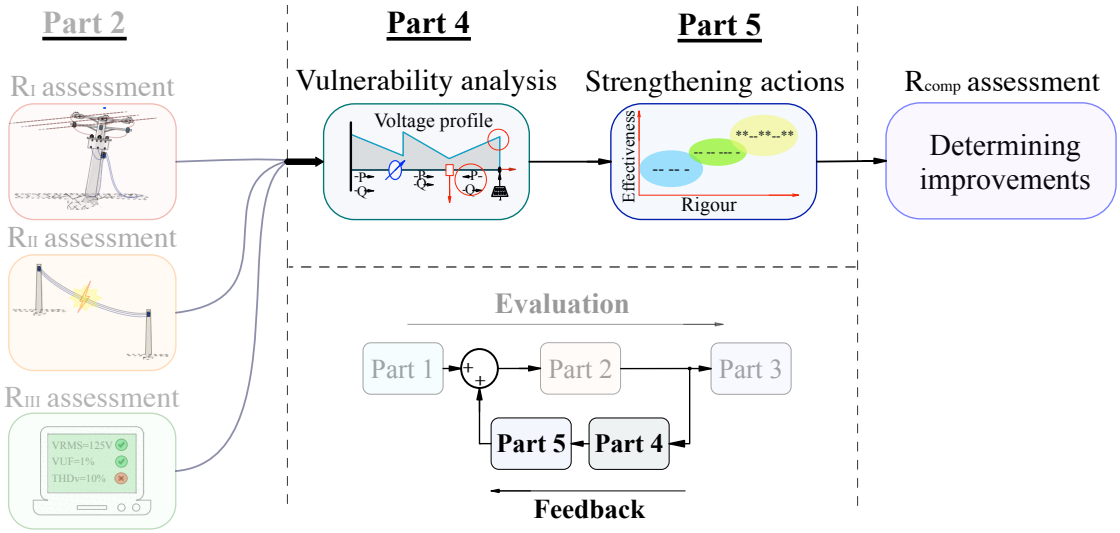

Results in Chapter 5 show a low probability of collapse for the CI of the EEB-UIS. In addition, interventions on the MV circuit feeding the EEB-UIS feeder concern the local electricity operator. Therefore, resilience feedback does not cover the strengthening of type I resilience (R_I) for the EEB-UIS-specific case. In cases where R_I is on alert, it would be recommended to strengthen the civil structure of the MV circuit that supplies the feeder. Poles with greater resistance to earthquakes and strong winds would be recommended.

Regarding the strengthening of R_{II}, two approaches have been identified: *i)* increasing the supply reliability; and *ii)* improving energy backup during power outages. Once again, the first one concerns the electricity operator. The second one could be addressed by the electricity installation itself. In the same vein, the strengthening of R_{III} has several approaches to improve the quality of the electrical system operation. In this way, the EEB-UIS resilience feedback focuses on R_{II} and R_{III}. This thesis proposes a hybrid resilience improvement measure linking supply robustness and operational flexibility by integrating two stages: *i)* The sizing of

an H_2-ESS as a backup system for the EEB-UIS. The R_{II} feedback analyses the implications of the H_2-ESS backup system on the reliability of the EEB-UIS power grid. It then estimates the increase in its supply continuity capacity.

Moreover, *ii)* the feedback considers the application of a EMS to strengthen R_{III}. According to the R_{III} assessment, the voltage regulation and current unbalance are the quality parameters (QPs) demanding the most attention. This stage focuses on improving them through the energy management of the projected H_2-ESS. EMS performance and power quality measurement are developed through simulations in the Matlab & Simulink environment. The EEB-UIS network model developed in Chapter 6 is used here. The analysis is developed based on the voltage supply and load demand profiles logged by the smart meters during May 2023. A local sensitivity analysis is also carried out concerning the rated power and connection point of the H_2-ESS and PV systems. The following sections present the development of electrical resilience feedback.

7.2 Sizing of the hydrogen-based backup system

This section describes the sizing of the H_2-ESS backup system for the EEB-UIS. The sizing methodology uses the total supply probability (TSP) index proposed in Section 3.4.2 as a decision parameter. It focuses on the history of power outages to fit a probability function and determine the appropriate survival time based on the categorisation of the loads. The H_2-ESS is composed of a fuel cell (FC) stack, a battery pack, an electrolyser (EL) and a hydrogen (H_2) tank. It also integrates voltage converters and power inverters to interconnect the sources. It is intended to strengthen the survival of the EEB-UIS loads in case of power outages. The EL is meant to absorb the excess power generated by the PV system, generating green H_2.

The next sections develop the sizing of the H_2-ESS backup system. Section 7.2.1 presents the sizing methodology. Section 7.2.2 describes the H_2-ESS sizing applied to the EEB-UIS. Then Section 7.2.3 shows a 48-hour extended power outage test.

7.2.1 Sizing methodology

The sizing proposal is supported by research (R. Rodriguez *et al.*, 2022). This work considers that the FC supplies the energy, and the battery pack supports the power peaks. It also defines the best economic benefit of generating green H_2 or buying it. The H_2-ESS sizing is developed for the EEB-UIS considering its electrical network description in Chapter 4 and modelling in Chapter 6. The methodology comprises five steps: *i)* The model of the electrical network and sources. *ii)* The load categorisation. *iii)* The definition of the total supply probability (TSP). *iv)* The cost function. And *v)* the sources dispatch strategy. They are described below:

Modelling

The EEB-UIS model has already been presented in Chapter 6. It should focus on the scenario where the H_2-ESS supports power outages. Four remarks are defined in the event of an outage: *i)* The feeder is not available to supply power. *ii)* The H_2-ESS sets the voltage at the emergency low voltage bus (ELVB). *iii)* The ELVB is the reference node of the electrical system. Furthermore, *iv)* the PV system injects power into the grid. Thus, the EEB-UIS network diagram is arranged as shown in Figure 40.

Figure 40

Diagram of EEB-UIS network in power outage state

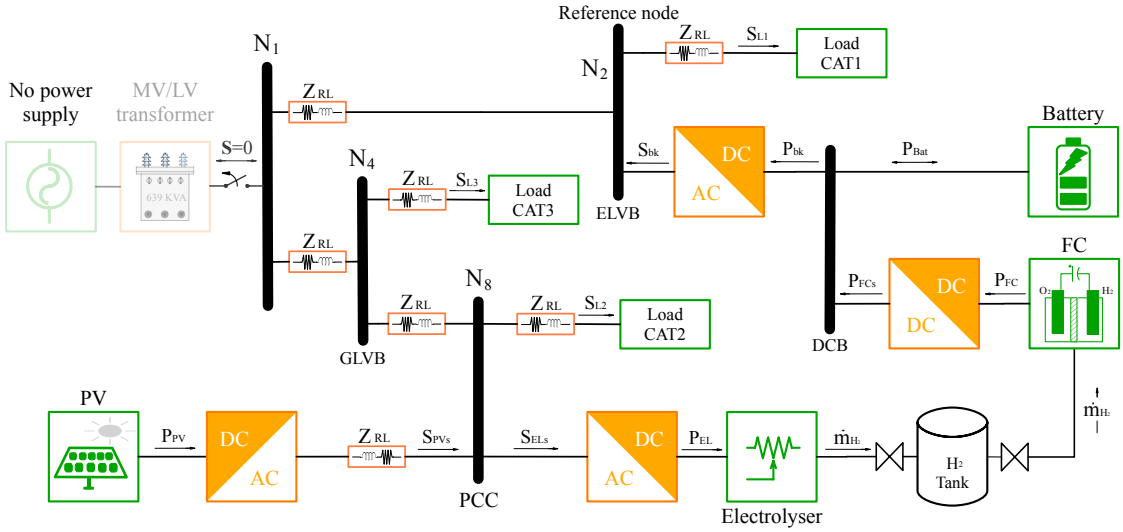

This way, the H_2-ESS current $\vec{\mathbf{i}}_{bk}$ corresponds to the network load demand as shown in Eq. (7.1). Here, $\vec{\mathbf{i}}_{bk\_out}$ is the backup current demanded by the EEB-UIS electrical network in the outage state. The H_2-ESS inverter sets the voltage $\vec{\mathbf{u}}_{ELVB}$ of the ELVB as presented in Eq. (7.2). Here, $\vec{\mathbf{u}}_{inv}$ is the voltage on the AC side of the H_2-ESS inverter. It is assumed that the inverter provides a balanced voltage. U_N is the nominal voltage of the EEB-UIS network. The model is implemented in the Matlab & Simulink environment running quasi-static power flows.

$$\vec{\mathbf{i}}_{bk} = \vec{\mathbf{i}}_{bk\_out} \tag{7.1}$$

$$\vec{\mathbf{u}}_{ELVB} = \vec{\mathbf{u}}_{bk} = \begin{bmatrix} U_N \angle 0 \\ U_N \angle -\frac{2\pi}{3} \\ U_N \angle -\frac{4\pi}{3} \end{bmatrix} \tag{7.2}$$

Load categorisation

The EEB-UIS load circuits are categorised as presented in Section 6.1. Table 20 outlines the categorisation.

Table 20

Categorisation of the EEB-UIS load.

Category	Description	Circuits
L_{CAT1}	Essential loads	TP5, TIE 3P, TR, TBH, RAC, ELV
L_{CAT2}	Priority loads	TP4
L_{CAT3}	Non-priority loads	TP1, TP2, TP3, TAA-1, TAA-2

Loss of power supply probability and total supply probability

The lost of power supply probability (LPSP) could be defined as the percentage of unmet

load given by Eq. (7.3) (Attemene *et al.*, 2020). Here $P_{def}(t)$ is the unserved power and $P_{load}(t)$ is the power demand by the network integrating L_{CAT1}, L_{CAT2}, and L_{CAT3}. The LPSP The allows for a priori estimation of the power rate of the backup system with a focus on defining an admissible unmet demand.

$$LPSP = \frac{\sum_{t=0}^{T} P_{def}(t) \cdot dt}{\sum_{t=0}^{T} P_{load}(t) \cdot dt} \tag{7.3}$$

The total supply probability (TSP) introduced in Section 3.4.2 is defined as a complementary criterion for the sizing. It is the probability of supplying the load demand during a T_{TSP}-duration outage. It would allow defining the minimum survivability required to satisfy the target TSP. The length data history of the EEB-UIS power outages is used to determine T_{TSP}. From this data, its probability density function (PDF) and cumulative distribution function (CDF) are fixed. The distribution function with the lowest mean absolute percentage error (MAPE) is used for sizing. Figure 41 presents the procedure to determine T_{TSP}.

Figure 41

Process for determining survival time to satisfy a target TSP.

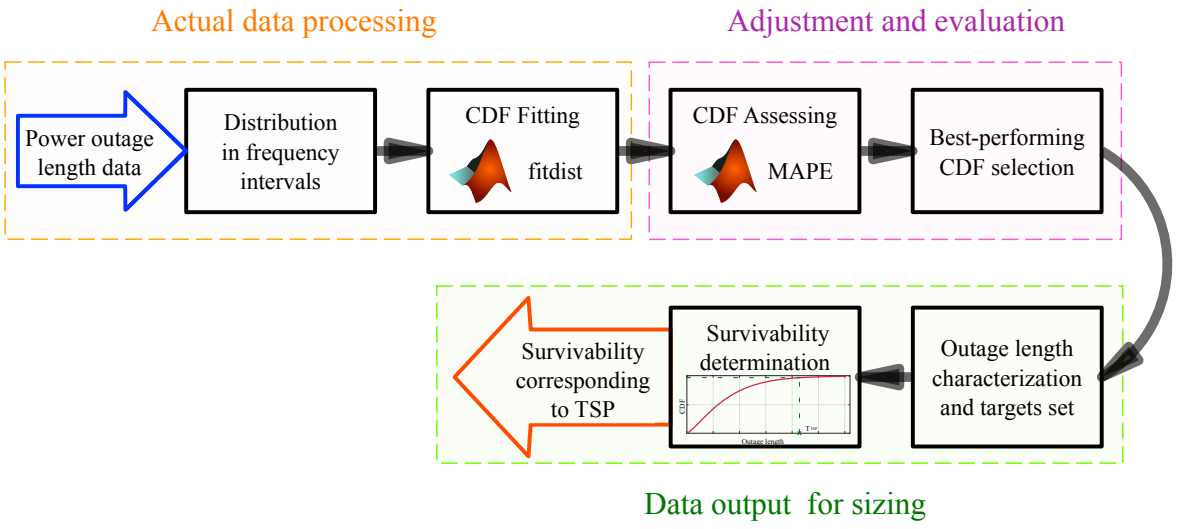

The sizing of the H_2-ESS must satisfy the energy backup criteria for each load category.

For L_{CAT1}, it should be guaranteed to supply the entire load as many times as power outages. Consequently, LPSP must be the minimum possible and TSP the maximum possible. Similarly, for L_{CAT2} and L_{CAT3}, TSP and LPSP should be guaranteed according to the load priority. Then, L_{CAT2} would have more support than L_{CAT3}. Table 21 shows the proposed LPSP and TSP criteria. The LPSP values correspond to those suggested by Ayop *et al.* (2018). The TSP values are proposed by R. Rodriguez *et al.* (2022) for the EEB-UIS load categories.

Table 21

LPSP and TSP criteria for sizing the backup system.

Category	LPSP	TSP
L_{CAT1}	$\approx 0\%$	$> 95\%$
L_{CAT2}	$< 10\%$	$> 70\%$
L_{CAT3}	$< 50\%$	$> 40\%$

These criteria refer to a typical operating scenario covering regular outages. The backup system should supply L_{CAT1} as much as possible during an extraordinary outage, such as a natural disaster or large-scale equipment damage.

Cost function

The H_2-ESS is intended to supply the power of the building in an outage. It should satisfy the power balance as Eq. (7.4) shows. Here, $P_{FC}(t)$, $P_{Bat}(t)$ and $P_{PVs}(t)$ are the power of FC, batteries, and PV system, respectively. $P_{L_{CAT1}}(t)$, $P_{L_{CAT2}}(t)$ and $P_{L_{CAT3}}(t)$ are the power of loads L_{CAT1}, L_{CAT2} and L_{CAT3} respectively. $P_{loss}(t)$ corresponds to the resistance and conversion loss power. Moreover, $P_{def}(t)$ represents the unsupplied load power. Proper sizing must ensure that $P_{def}(t)$ is null. Additionally, the H_2-ESS must ensure the energy balance shown Eq. (7.5).

$$P_{FC}(t) + P_{Bat}(t) + P_{PVs}(t) = P_{L_{CAT1}}(t) + P_{L_{CAT2}}(t) + P_{L_{CAT3}}(t) + P_{loss} - P_{def}(t) \tag{7.4}$$

$$\sum_{t=0}^{T_{total}} \left(P_{FC}(t) + P_{Bat}(t) + P_{PVs}(t) - P_{loss} + P_{def}(t)\right) \cdot dt = \sum_{t=0}^{T_{TPS1}} P_{L_{CAT1}}(t) \cdot dt + \sum_{t=0}^{T_{TPS2}} P_{L_{CAT2}}(t) \cdot dt + \sum_{t=0}^{T_{TPS3}} P_{L_{CAT3}}(t) \cdot dt \tag{7.5}$$

Here T_{total} is the total time of the outage issue. T_{TSP1}, T_{TSP2}, and T_{TSP3} are the survival times determined for each load category account for total supply probabilities TSP_1, TSP_2, and TSP_3, respectively. The cost function is defined by the annualised total cost C_{total} of the H_2-ESS. C_{total} considers the acquisition cost C_{acq}, and operation and maintenance cost $C_{O\&M}$. Here, $C_{O\&M}$ is assumed as a percentage of the C_{acq} for each source. Also, the operation considers the cost of purchasing H_2 from an external source. Eq. (7.6) presents the cost function subject to TSP and LPSP.

$$\begin{aligned} min: & \sum_{s=1}^{N} (CRF_s \cdot NC_s \cdot C_s) + \sum_{s=1}^{N} \left(C_{M_s} \cdot NC_s\right) + m_{H_2}^{Ext} \cdot C_{H_2} \\ s.t.: \quad & TSP \\ & LPSP \end{aligned} \tag{7.6}$$

Here, NC_s, C_s, and C_{Ms} are the nominal capacity, acquisition cost per unit of capacity and maintenance cost per unit of capacity, respectively, for each s-component. $m_{H_2}^{Ext}$ is the amount of H_2 supplied by the external source and C_{H_2} is the cost per kg of H_2. CRF_s is the capital recovery factor shown in Eq. (7.7). Here, r is the annual rate of return, and N_{Ls} is the lifetime years of each component.

$$CRF_s = \frac{r \cdot (r+1)^{N_{LS}}}{(r+1)^{N_{LS}} - 1} \tag{7.7}$$

Table 22 presents acquisition and O&M costs for H_2-ESS components. The sizing is implemented in the Matlab & Simulink environment. The PSO algorithm solves the optimisation problem involving Eq. (7.6). Here, the particles of the PSO algorithm are in the form $[N_{S_{fc}}, N_{P_{fc}}, N_{S_b}, N_{P_b}, N_{S_{el}}, N_{P_{el}}]$, including the combination of series and parallel modules for

FC, EL and battery systems. It represents an integer linear optimisation problem.

Table 22

Cost characteristics for the H_2-ESS components.

Component	Acquisition cost C_{acq}	O&M cost $C_{O\&M}$	Lifetime
Batteries (Kosmadakis *et al.*, 2021)	250 €/kWh	2% of C_{acq}	6 years
Fuel cell (Timilsina, 2021)	2500 €/kW	3% of C_{acq}	5 years
Electrolyser (Attemene *et al.*, 2020)	1700 €/kW	4% of C_{acq}	8 years
H_2 tank (Attemene *et al.*, 2020)	990 €/kg	1.2% of C_{acq}	20 years
Converters (Attemene *et al.*, 2020)	200 €/kW	1% of C_{acq}	15 years
Green hydrogen (IRENA, 2020)	6 €/kg	−−−	−−−

Source dispatch strategy

A rule-based dispatch strategy is proposed to determine the energy participation of FC and batteries. It attempts to keep the batteries state of charge $SOC_b(t)$ within the operating values SOC_b^{min} and SOC_b^{max}. $P_{FC}(t)$ is set at the rated power P_{FC}^{max} as possible. If $SOC_b(t)$ exceeds a cut-off limit SOC_b^{cut}, $P_{FC}(t)$ must drop to the minimum value P_{FC}^{min}. FC is disconnected in the undesirable case that $SOC_b(t)$ exceeds the maximum value. Algorithm 1 presents the dispatch strategy.

7.2.2 Results of the H_2-ESS backup system for the EEB-UIS

The above methodology is applied to size the EEB-UIS's H_2-ESS backup system. The local electricity distribution operator provided the historical data on power outages for the MV circuit supplying the EEB-UIS feeder. The following sections describe the outage characterisation, the LPSP and TSP target set and the H_2-ESS size.

Power outages characterisation

The power outage history related to EEB-UIS is sourced from *Electrificadora de Santander S.A E.S.P.* (ESSA-ESP), the local electric utility company. ESSA-ESP provided historical

Algorithm 1: Rules-based dispatch strategy for the H_2-ESS

Data: SOC_b^{min} , SOC_b^{max} , SOC_b^{cut} , P_{FC}^{max} , P_{FC}^{min}
Input: $SOC_b(t)$, $P_{load}(t)$
Result: $P_{FC}(t)$, $P_{Bat}(t)$
initialization;
if $SOC_b(t) < SOC_b^{max}$ **then**
  while $SOC_{Bat}(t) \geq SOC_{Bat}^{min}$ **do**
    if $SOC_b(t) < SOC_b^{cut}$ **then**
      $P_{FC}(t) = P_{FC}^{max}$;
    else
      $P_{FC}(t) = P_{FC}^{min}$;
    end
    $P_{Bat}(t) = P_{load}(t) - P_{FC}(t)$;
  end
else
  $P_{FC}(t) = 0$;
  $P_{Bat}(t) = P_{load}(t)$;
end

data on outages for 2012–2021. The processing of this information has been presented in Section 5.3.1 to determine the actual TSP of the EEB-UIS network. For the backup system sizing, the inverse CDF is calculated, determining the target backup time for the load categories. Figure 42 Presents the fit of historical outage data to a CDF and its inverse function.

Figure 42

CDF fit for the EEB-UIS outage length.

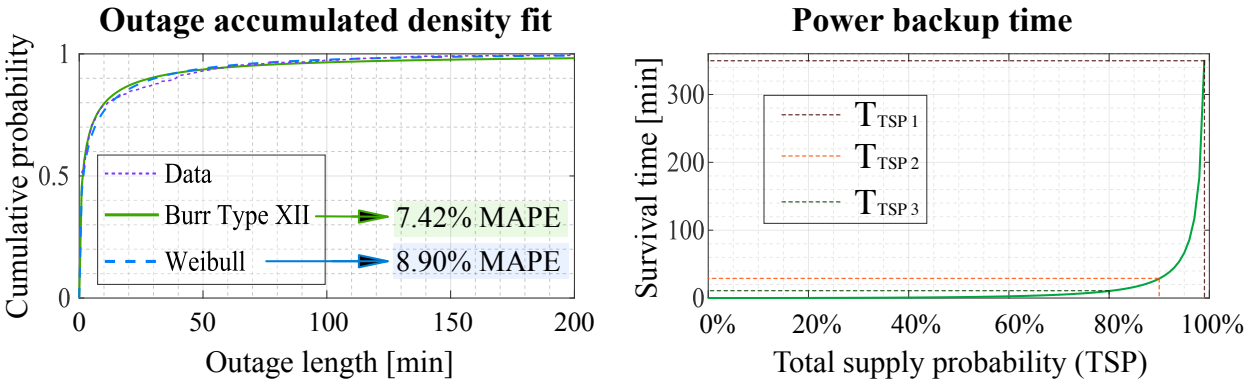

Here, the Burr Type XII distribution has the best fit with 7.42% MAPE, followed by the

Weibull and Gamma distributions with 8.90% and 17.60% MAPE, respectively. Burr distribution function parameters are $\alpha = 10.910$, $c = 0.516$, and $k = 2.368$. T_{TSP1}, T_{TSP2} and T_{TSP3} are the survival time for L_{CAT1}, L_{CAT2} and L_{CAT3}, respectively. They are calculated from the TSP target in Table 21.

Survival time by load category

The loads are grouped according to their priority as presented by Section 7.2.1. The survival time for each load category is calculated by applying the inverse of the CDF fixed to the TSP percentages. Table 23 shows the survival time results for the EEB-UIS load categories. Here, the power and energy values correspond to the demand profile proposed by R. Rodriguez *et al.* (2022) for sizing a backup system for the EEB-UIS. Then, Figure 43 shows the demand profile with the survival time cut-off.

Table 23

Survival time for the EEB-UIS loads.

Category	Circuits	LPSP target	TSP target	Minimum survivability	Energy demand	Maximum power
L_{CAT1}	TP5, TIE 3P, TR, TBH, RAC, ELV	0%	99%	351 min	34.62 kWh	18.0 kW
L_{CAT2}	TP4	0%	90%	29 min	0.61 kWh	2.6 kW
L_{CAT3}	TP1, TP2, TP3, TAA-1, TAA-2	0%	80%	10 min	0.35 kWh	16.0 kW

Backup system sizing

The sizing involves determining the number of cells in series and parallel for the FC and EL stacks and the battery pack's number of modules. Therefore, a single unit for each source is used. Table 24, Table 25 and Table 26 present the characteristics of the reference single FC, single battery, and single EL, respectively. Then, Table 27 shows the searching range used for the

Figure 43

Load demand profile for the sizing of the EEB-UIS backup system. a) Power profile; b) Energy demand.

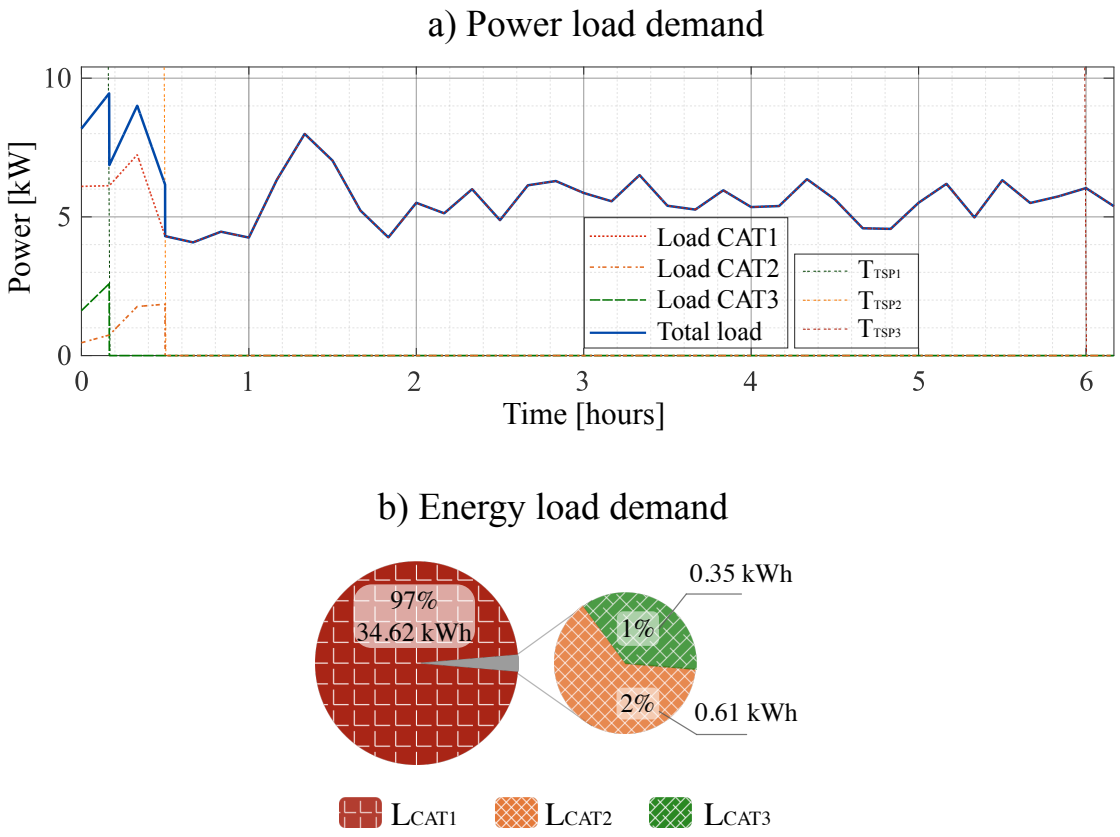

number of series and parallel modules. The sizing is developed in Matlab using the PSO optimisation algorithm. PSO particles are in the form $[N_{S_{fc}}, N_{P_{fc}}, N_{S_b}, N_{P_b}, N_{S_{el}}, N_{P_{el}}]$ including the combination of series and parallel modules for FC, EL and battery systems. The initial population consists of 50 best-performing particles from a population of 1 000 randomly distributed sizing solutions in the search range. The particle redirection has a unitary inertial factor and random local and global position weights in the range $[0, 1]$. The algorithm performs 50 iterations.

The sizing solution is the combination $[N_{S_{fc}}, N_{P_{fc}}]$, $[N_{S_b}, N_{P_b}]$, and $[N_{S_{el}}, N_{P_{el}}]$ with the best performance in the last iteration. The power flows are run in Simulink, implementing the dispatch strategy presented in Algorithm 1. It determines the system performance for each PSO particle. The simulation time relates to $T_{TSP}(99\%) = 351\ min$. The limit state of charges

Table 24

Parameters of an FC single-cell used for sizing.

Parameter	Description	Value
P_{fc}^{rat}	Rate power	150 W
U_{OCV}	Internal voltage induced	0.8834 V
$\dot{m}_{OC}$	H_2 mass flow in open circuit operation	$1.39X10^{-8}$ kg/s
m_{H_2}	H_2 consumption factor	$9.71X10^{-9}$ $kg/s\ A^{-1}$
C_{act}	Activation constant	0.0278
C_{conc}	Concentration constant	$-5.6403X10^{-11}$
k_{sq}	Concentration exponent	3
J_{max}	Maximum current	250 A
r_{cell}	Single-cell equivalent resistance	0.5973 $m\Omega$

Table 25

Parameters of a single-battery used for sizing.

Parameter	Description	Value
Cap_b	Energy storage capacity	110 Ah
U_b^{rat}	Rated voltage	12.8 V
I_{max}	Maximum current	150 A
r_{cell}	Battery equivalent resistance	6 $m\Omega$
U_b^{min}	Minimum permissible voltage	10 V
SOC_b^{min}	Minimum permissible SOC	0.30
SOC_b^{max}	Maximum permissible SOC	0.95

Table 26

Parameters of an EL single-cell used for sizing.

Parameter	Description	Value
P_{el}^{rat}	Rate power	400 W
I_{max}	Maximum current	150 A
A_{el}	Electrode area of a single cell	575 cm^2
U_{rev}	Reversible voltage of the water	1.23 V
U_{tn}	Thermoneutral cell voltage	1.23 V
r_{el}	Single-cell equivalent resistance	1.2 $m\Omega$

Table 27

Search range for the number of source modules used in H_2-ESS sizing.

System	Searching range	
	Series cells/modules	Parallel branches
FC stack	[0 , 60]	[1 , 10]
Battery pack	[0 , 50]	[1 , 10]
EL stack	[0 , 60]	[1 , 10]

$SOC_b^{min} = 0.40$, $SOC_b^{cut} = 0.90$, and $SOC_b^{max} = 0.95$ are fixed for the battery pack. The acquisition cost uses $r = 9\%$ as the annual return rate. The PSO algorithm found that the solution with the lowest annualised cost integrates an FC and a battery bank. The solution satisfies the power, energy, LPSP and TSP requirements. It shows that using an electrolyser to support power outages makes no sense since the power surplus of the PV system is stored by the batteries and returned at peak demand. Thus, purchasing H_2 is more convenient in outages; if stored hydrogen is available, it could be used to reduce the operation cost.

In this sense, two solutions are proposed for the H_2-ESS backup system of the EEB-UIS: *i)* The solution determined in the PSO algorithm, which does not include an electrolyser and an H_2 tank. It is focused only on supporting power outages. Furthermore, *ii)* a complementary solution that proposes to add an electrolyser and an H_2 tank to support the operation of the EEB-UIS during the regular power supply by the feeder. Solution two is used in detail to develop the R_{III} resilience-strengthening strategies in the subsequent sections. For this purpose, a 6 kW electrolyser equivalent to the peak power surplus of the PV system and a 20 kg H_2 tank by rounding down the hydrogen consumption of the H_2-ESS in a 351 min outage have been considered. Table 28 summarises the description of the backup system and the costs for a 351 min power outage scenario. Here, the complementary solution is shaded to highlight its additional focus on regular non-outage operation. The following section presents the performance of the H_2-ESS backup system in case of an extended 48-hour power outage.

Table 28

Characteristics and costs of the H_2-ESS sizing for the EEB-UIS.

Component	Rated value	Description and configuration	C_{acq} cost	$C_{O\&M}$ cost
Fuel cell	5.6 kW	Energy source. 37 cells of 150 W rated power in series.	€ 3 567	€ 416
Batteries	22.5 kWh 31 kW	Power source. 4 branches of 4 batteries in series of 12.8 V and 110 Ah.	€ 1 255	€ 113
DC/AC inverter	35 kW	Inverter interconnecting the backup system with the EEB-UIS network.	€ 867	€ 70
DC/DC converter	5.6 kW	Converter interconnecting the FC with the batteries.	€ 139	€ 11
Hydrogen	23.2 kg	Purchased hydrogen from an external source.	€ 139	−−−
Total annualised cost–Solution 1			**€ 6 576**	
Electrolyser	6 kW	Manageable load. 15 cells of 400 W rated power in series.	€ 1 843	€ 408
Hydrogen tank	20 kg	Pressurised reservoir for storing the green H_2 generated.	€ 2 169	€ 238
AC/DC inverter	6 kW	Voltage inverter interconnecting the EL system with the EEB-UIS network.	€ 150	€ 12
Total annualised cost–Solution 2			**€ 11 398**	

7.2.3 Operation in a long power outage scenario

A performance test of the H_2-ESS in an unusual power outage scenario lasting 48 hours is made. Here, L_{CAT2} and L_{CAT3} should be supplied 30 minutes and 10 minutes, respectively; and L_{CAT1} the test's total time. For this test, 48 hours of peak demand is sought for the EEB-UIS during May 2023. The period found is from 10^{th} May at 6:00 a.m. to 12^{th} May at 5:50 a.m., 2023. This test implements solution 1, where hydrogen is purchased from an external source. In the test, the H_2-ESS supplies the demand, guaranteeing the LPSP and TSP criteria for this scenario. Here, the hydrogen consumption cost amounts to € 1 170. Figure 44 presents the power demanded by the EEB-UIS and the power supplied by each source. Figure 45 shows the

SOC of the batteries SOC_b. The maximum power demand is in the first 30 minutes of the test when the full load of the EEB-UIS is supplied. Furthermore, the EEB-UIS load shows that the critical hours of demand are from 6:00 a.m. to 7:00 p.m. during regular working hours.

Concerning the source operation, the FC increases the power up to the rated value when the batteries SOC_b tends to decrease. The PV system meets the load and recharges the batteries during sunny hours. The batteries supply the remaining power peak load demand. SOC_b is kept in the appropriate range. The essential load L_{CAT1} has the higher energy demand because it is supplied the entire time. The demand for the building in the 48-hour outage test is 196 kWh. The FC supplies most of the load demand, followed by the PV system. Batteries cause 1.9 kWh of energy demand as the SOC_b increases 7.6% at the test's end. The results show 12.2 kWh losses between the conversion device and the grid wires. Then, the electrical efficiency is 94.2% for this outage test. Figure 46 shows the energy distribution of the EEB-UIS for the 48-hours test. The following sections address the enhancement of the electrical resilience of the EEB-UIS by the energy management of the H_2-ESS backup system.

7.3 Strengthening type II resilience to regular outages

This strategy involves the H_2-ESS backup system to strengthen the support of EEB-UIS loads in the event of a power outage. Section 7.2 has already detailed the sizing of the H_2-ESS based on the TSP criteria. The TSP has been defined for each load category in Table 23 as follows: *i)* L_{CAT1}: TSP of 99% equivalent to 351 minutes survival time. *ii)* L_{CAT2}: non-essential priority load, TSP of 90% corresponding to 29 minutes of survivability. And *iii)* L_{CAT3}: non-priority load, TSP of 80% representing 10 minutes of survival time. The strategy is to extend the coverage of backup power to non-essential loads. Although the survival time defined for L_{CAT2} and L_{CAT3} represents 8.3% and 2.8%, respectively, concerning the survival time of L_{CAT1}, the EEB-UIS would be able to support its entire load in 80% of power outage events.

In this way, it is possible to increase the backup power reliability of the EEB-UIS. The H_2-ESS could give a higher benefit than the current diesel generator (genset). Table 29 com-

Figure 44

EEB-UIS Power distribution in an adverse scenario of a 48-hour power outage.

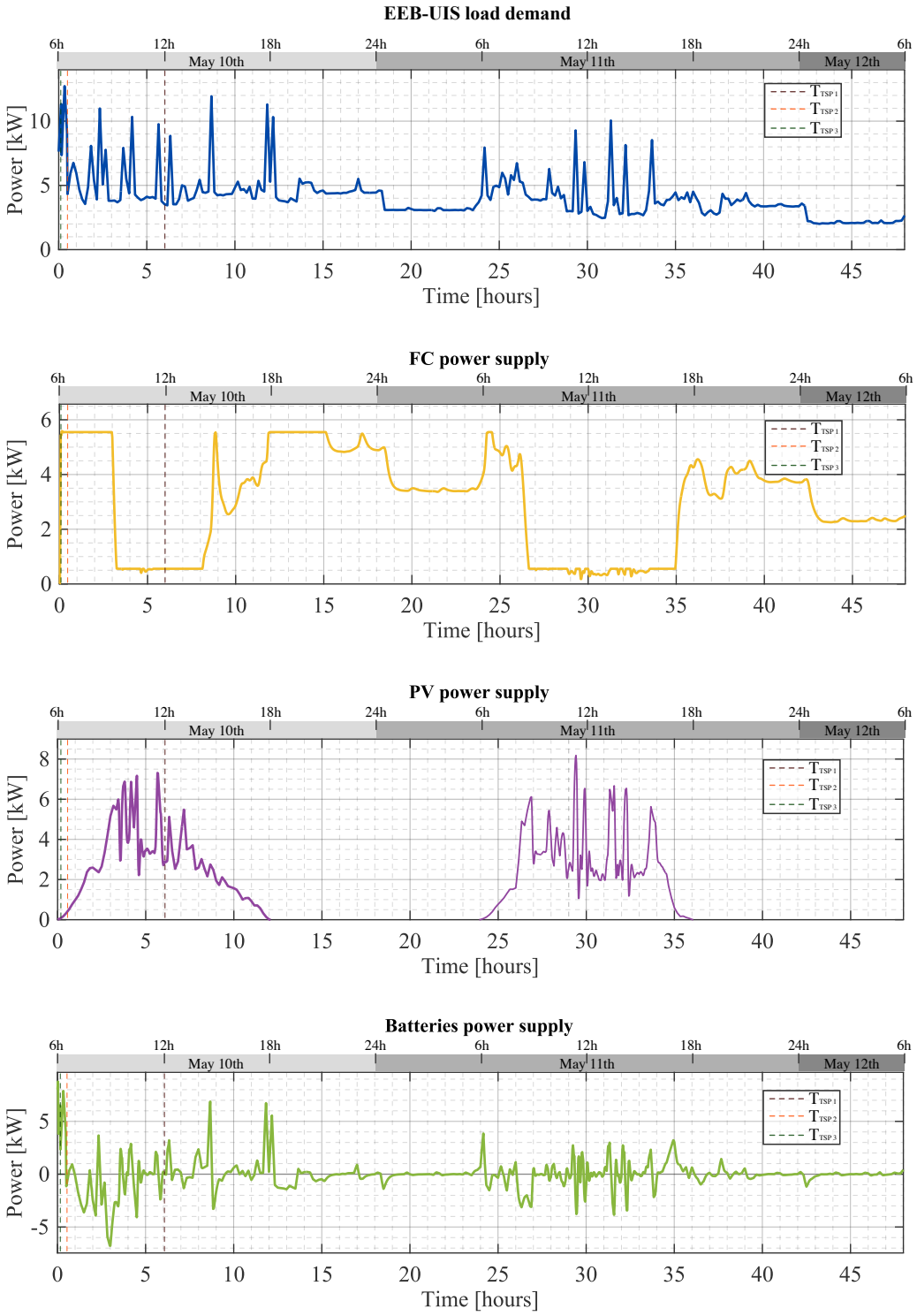

Figure 45

Batteries state of charge in a 48-hour power outage scenario.

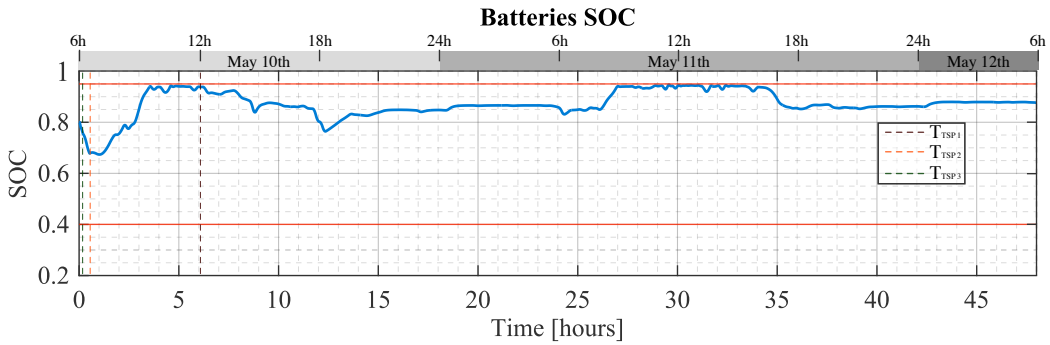

Figure 46

Energy participation in a 48-hour power outage scenario.

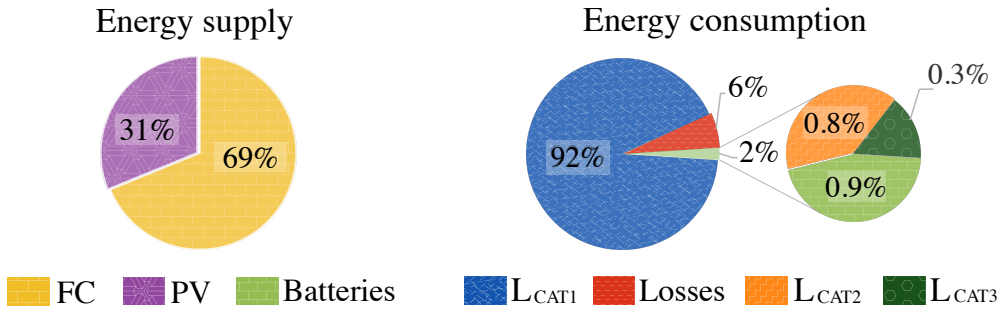

pares the two energy backup systems and the contribution to R_{II}. Here, η_{bk} and BC are the backup factor and backup contribution per load category, respectively. η_{bk} has been defined in Section 3.4.2 and BC corresponds to the product between TPS and η_{bk}. The H_2-ESS reduces the probability of non-supply ρ_{off} by 80%. This benefit is achieved by extending power backup coverage to loads L_{CAT2} and L_{CAT3}.

It is important to note that increasing the backup power coverage with another backup system, such as the genset, is possible. However, considering H_2-ESS as a backup system helps develop strategies to strengthen the quality of operation. This strategy is discussed in the next section.

7.4 Enhancing operational quality resilience R_{III}

Table 29

Contribution of the backup systems to the backup network reliability.

Load	Power	Genset				H_2-ESS			
		T_{bk}	TSP	η_{bk}	BC	T_{bk}	TSP	η_{bk}	BC
L_{CAT1}	55.9 kW	720 min	99.8%	0.44	43.9%	351 min	99%	0.44	43.6%
L_{CAT2}	8.4 kW	0 min	0%	0.00	0.0%	29 min	90%	0.06	5.4%
L_{CAT3}	63.4 kW	0 min	0%	0.00	0.0%	10 min	80%	0.50	40.0%
Backup factor		0.439				0.890			
ρ_{off}-EEB		4.65×10^{-4}				9.13×10^{-5}			

The feedback of the R_{III} consists of using the H_2-ESS with an electrolyser system to improve the EEB-UIS electrical network performance. For this purpose, the battery bank and the EL stack are used as dispatchable power sources. The feedback is developed for the monitored EEB-UIS nodes (GLVB, ELVB and PCC) in May 2023. It matches the resilience evaluation in Chapter 5. The analysis performs power flow and EMS simulations via Matlab & Simulink, implementing the model of the EEB-UIS network presented in Chapter 6 for operation with regular power supply through the feeder.

Simulations use the supply and load demand profiles logged by the smart meters. The simulation time is 31 days with 1 second refresh rate. The QPs measurement covers voltage regulation, voltage and current unbalance, wire current and power losses. This approach involves five issues about the H_2-ESS: *i)* The feeder supply is available and is the reference of the electrical system. *ii)* The operation of the FC system is avoided. *iii)* The EL system uses power from the PV system to generate green H_2. *iv)* Green H_2 is intended to supply the FC system in outage states. And, *v)* the FC could generate power to avoid excess of green H_2. The following sections expand on this feedback strategy.

7.4.1 Strategy to strengthen the EEB-UIS type III resilience

This thesis proposes an energy management strategy (EMS) for the H_2-ESS to strengthen the operation of the EEB-UIS power grid. Here, the EL seeks to generate H_2 from PV system power, avoiding reverse power flows and overvoltages at supply nodes. It is coupled to the PV

system's point of common coupling (PCC) to absorb power when needed. The FC-battery system is connected to the emergency low voltage bus (ELVB). It is mainly to supply emergency loads in a power outage. However, It could support the ELVB voltage regulation in regular operation. In this instance, the batteries absorb or supply power as needed. Figure 47 shows the arrangement of the EEB-UIS network for the resilience feedback analysis to apply the EMS. Decision parameters and EMS by source are described below.

Figure 47

Arrangement of EEB-UIS network for the electrical resilience feedback analysis.

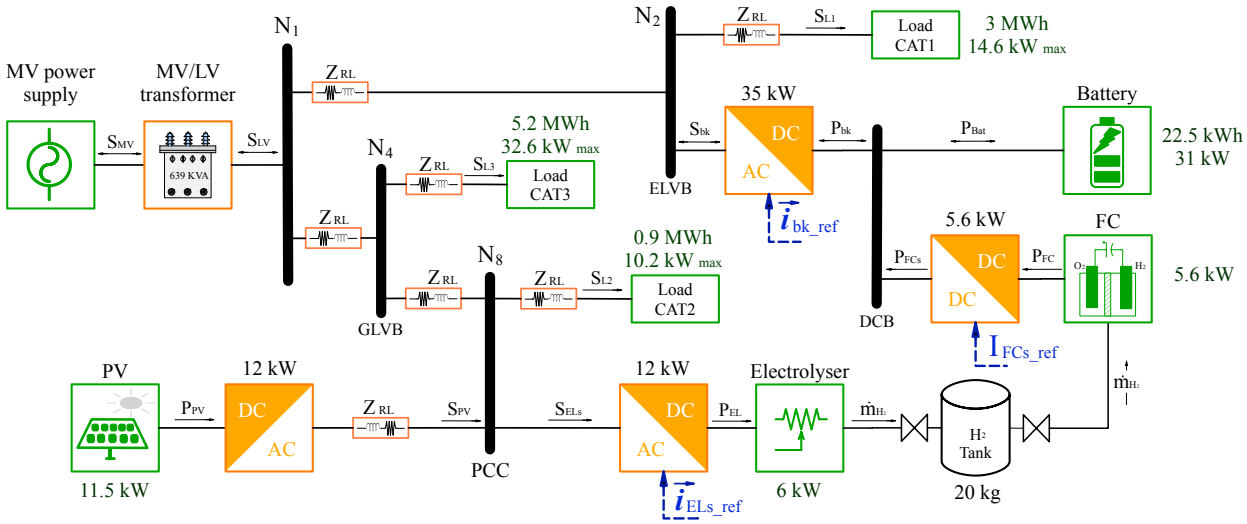

7.4.2 Decision and control parameters

The characterisation of R_{III} for the EEB-UIS shows that Φ_u is a vulnerable index. Then, ϕ_u-N_2, ϕ_u-N_4 and ϕ_u-N_8 could be defined as the decision parameters. Improving them could have a positive effect on the other resilience indices. The control parameters are the currents $\vec{\mathbf{i}}_{bk}$, $\vec{\mathbf{i}}_{ELs}$ and I_{FCs} corresponding to the H_2-ESS, EL and FC systems respectively. They seek to regulate the voltage at the connection nodes and also contribute to alleviating the load on the supply lines. $\vec{\mathbf{i}}_{bk}$ and $\vec{\mathbf{i}}_{ELs}$ are current phasor vectors integrating a magnitude and an angle per fase. I_{FCs} is a DC current. The EMS to define the control references is described below.

7.4.3 H_2-ESS energy management

The EMS of the H_2-ESS system seeks to regulate the connection point voltage in case of overvoltage or undervoltage. This EMS considers that the batteries absorb or deliver power to the ELVB during day-to-day operation. The contribution of reactive power and the current unbalance are also considered. The H_2-ESS could supply part of the reactive power demanded by L_{CAT1} and relieve the phases with the highest load. Algorithm 2 presents the EMS for the H_2-ESS. It determines the control reference current $\vec{\mathbf{i}}_{bk\_ref}$ for the backup system. In this sense, if the backup system is required to operate, it generates an unbalanced power directly proportional to the unbalance of the L_{CAT1} load. It injects more power to the phase that demands more power and less power to the phase that requires less power. As a result, it improves the load balance on line L_{1-2}. If the batteries absorb power, the unbalance is inversely proportional to the unbalance of the L_{CAT1} load. Here P_{bk_max} is the H_2-ESS inverter's nominal power. pf_{bk_min} and pf_{bk_max} are the allowable limits of inverter power factor, leading and lagging, respectively. u_n is the nominal voltage of the EEB-UIS electrical network. SOC_b^{ref} is the reference batteries SOC pack set to 0.8. P_b^{ch} is the suggested power rating for charging the battery pack. It is equivalent to 10% of its rated power.

$\vec{\mathbf{u}}_{N_2}$ is the vector of the voltage measured at the ELVB. $\mathbf{S}_{L_{CAT1}}$, $\vec{\mathbf{S}}_{L_{CAT1}}$ and $fp_{L_{CAT1}}$ are the complex power, the complex power vector and the power factor of the L_{CAT1} load, respectively. Furthermore, u_{N_2} is the average magnitude of the ELVB voltage and ϕ_u-N_2 is the resilience index corresponding to u_{N_2}. $\vec{\mathbf{1}}$ and $\vec{\mathbf{0}}$ are the three-component vector of ones and the zeros, respectively. The $conj\{\}$ operator returns the conjugate of a complex number. The operator ./ is the component-by-component division between two vectors of the same dimension. The DC side of the H_2-ESS integrates a battery and an FC system. The FC is intended to recharge batteries during power outages. SOC_b must be sufficient to deal with an emergency. Then, an FC system's hysteresis control EMS is defined for regular operation with the feeder supply. If SOC_b drops below 35%, the FC turns on at an optimal power for hydrogen consumption. When the SOC_b reaches 70%, the FC returns to the off state. Algorithm 3 presents the EMS for the FC system.

Algorithm 2: Backup system EMS

Data: Backup system parameters
Data: P_{bk_max} , pf_{bk_max} , pf_{bk_min}, u_n, SOC_b^{ref}, P_b^{ch}
Result: Backup system reference current, $\vec{\mathbf{i}}_{bk\_ref}$

initialisation;
Measure→ $\vec{\mathbf{u}}_{N_2}$, $\mathbf{S}_{L_{CAT1}}$ $\vec{\mathbf{S}}_{L_{CAT1}}$, $fp_{L_{CAT1}}$;
Calculate→ u_{N_2} , ϕ_u-N_2; – Eq. (3.11);

while ϕ_u-$N_2 < 0.95$ **do**
  if $u_{N_2} \leq u_n$ **then**
    ▷ Undervoltage case;
    if ϕ_u-$N_2 \geq 0.70$ **then**
      $P_{bk} = \left[\left(\frac{-1}{0.95-0.70}\right)\cdot(\phi_u\text{-}N_2) + \frac{0.95}{0.95-0.70}\right]\cdot P_{bk\_max}$;
    else
      $P_{bk} = P_{bk\_max}$;
    end
    $fp_{bk} = fp_{L_{CAT1}}$;
    $\vec{\mathbf{s}}_\phi = \frac{\vec{\mathbf{S}}_{L_{CAT1}}}{\mathbf{S}_{L_{CAT1}}}$; ▷ *Load balancing vector*;
  else
    ▷ Overvoltage case;
    if $SOC_b \leq SOC_b^{ref}$ **then**
      $P_{bk} = -P_b^{ch}$;
    else
      $P_{bk} = 0$;
    end
    $fp_{bk} = 1$;
    $\vec{\mathbf{s}}_\phi = \frac{1}{2}\cdot\left[\vec{\mathbf{I}} - \frac{\vec{\mathbf{S}}_{L_{CAT1}}}{\mathbf{S}_{L_{CAT1}}}\right]$; ▷ *Load balancing vector*;
  end
end

while ϕ_u-$N_2 \geq 0.95$ **do**
  ▷ Acceptable voltage regulation ;
  $P_{bk} = 0$;
  $fp_{bk} = 1$;
  $\vec{\mathbf{s}}_\phi = \vec{\mathbf{0}}$;
end

$Q_{bk} = P_{bk}\cdot\frac{\sqrt{1-fp_{bk}^2}}{fp_{bk}}$;
$\vec{\mathbf{S}}_{bk} = [P_{bk} + \hat{j}Q_{bk}]\cdot\vec{\mathbf{s}}_\phi$;
$\vec{\mathbf{i}}_{bk} = conj\{[\vec{\mathbf{S}}_{bk}] \ ./ \ [\vec{\mathbf{u}}_{N_2}]\}$;

Here, I_{FCs_ref} is the reference current for the FC system. P_{FC_opt} and η_{FC} are the FC's power and efficiency at optimal operation. U_b is the battery pack voltage.

Algorithm 3: Fuel cell EMS

Data: Backup system parameters
Data: P_{FC_opt} , η_{FC}
Result: Fuel cell system reference current, I_{FCs_ref}

initialisation;
Measure→ SOC_b , U_b;
if $SOC_b < 0.35$ **then**
    ▷ *Charging batteries*;
    while $SOC_b \leq 0.7$ **do**
        $P_{FC} = P_{FC\_opt}$;
    end
else
    $P_{FC} = 0$;
end
$P_{FCs\_ref} = \eta_{FC} \cdot P_{FC}$;

7.4.4 Electrolyser energy management

The EL system is intended to improve voltage regulation at the PCC in the event of overvoltage. It could absorb power generated by the PV system. It could also contribute by supplying part of the reactive power demanded by L_{CAT2}. This way, the EMS generates a reference current $\vec{\mathbf{i}}_{ELs\_ref}$ for the EL system proportional to the power injected by the PV system. The proportionality is related to the voltage index ϕ_u-N_8. Algorithm 4 shows the EMS for the EL system. Here P_{ELs_max} is the nominal power of the EL system inverter. pf_{ELs_max} is the allowable limits of the inverter power factor. Moreover, SOC_{H_2} represents the filling state of the H_2 tank with respect to the maximum storage capacity. $SOC_{H_2}^{max}$ is the maximum recommended filling state for the H_2 tank. u_n is the nominal voltage of the EEB-UIS electrical network. $\vec{\mathbf{u}}_{N_8}$ is the voltage at the PCC. $fp_{L_{CAT2}}$ is the power factor of the L_{CAT2} load. P_{PVs} is the power generated by the PV system. u_{N_8} is the average magnitude of the PCC voltage and ϕ_u-N_8 is the resilience index corresponding to u_{N_8}. The $abs\{\}$ operator returns the magnitude of a value. The following section presents the results of this EMS approach to strengthening the EEB-UIS R_{III}.

7.4.5 Results of the EMS approach on type III resilience

The EMS is applied to the EEB-UIS electrical network for its operation between May 1^{st}

Algorithm 4: Electrolyser system EMS

Data: Electrolyser system parameters
Data: P_{ELs_max} , pf_{ELs_max} , u_n , $SOC_{H_2}^{max}$
Result: Electrolyser system reference current, $\mathbf{i}_{ELs\_ref}$

initialisation;
Measure→ $\vec{\mathbf{u}}_{N_8}$, P_{PVs} , $Q_{L_{CAT2}}$, $fp_{L_{CAT2}}$, SOC_{H_2};
Calculate→ u_{N_8} , ϕ_u-N_8; – Eq. (3.11);
while ϕ_u-$N_8 \leq 0.95$ & $u_{N_8} \geq u_n$ & $SOC_{H_2} < SOC_{H_2}^{max}$ **do**
  ▷ Overvoltage case;
  if ϕ_u-$N_8 \geq 0.70$ **then**
    $P_{ELs} = \left[\left(\frac{-1}{0.95-0.70}\right)\cdot\left(\phi_u\text{-}N_8\right) + \frac{0.95}{0.95-0.70}\right]\cdot P_{PVs}$;
  else
    $P_{ELs} = P_{PVs}$;
  end
  $fp_{ELs} = fp_{L_{CAT2}}$;
end
while ϕ_u-$N_2 > 0.95$ **do**
  ▷ Acceptable voltage regulation ;
  $P_{ELs} = 0$;
  $fp_{ELs} = 1$;
end
if $P_{ELs} < P_{L_{CAT2}}$ **then**
  $Q_{ELs} = P_{ELs}\cdot\frac{\sqrt{1-fp_{ELs}^2}}{fp_{ELs}}$;
else
  $Q_{ELs} = Q_{L_{CAT2}}$
end
$\vec{\mathbf{s}}_{P\phi} = \frac{1}{2}\cdot\left[\vec{\mathbf{1}} - \frac{\vec{\mathbf{P}}_{L_{CAT2}}}{P_{L_{CAT2}}}\right]$; ▷ *Load balancing vector for active power*;
$\vec{\mathbf{s}}_{Q\phi} = -\frac{\vec{\mathbf{Q}}_{L_{CAT2}}}{abs\{Q_{L_{CAT2}}\}}$; ▷ *Load balancing vector for reactive power*;
$\vec{\mathbf{S}}_{ELs} = P_{ELs}\cdot\vec{\mathbf{s}}_{P\phi} + Q_{ELs}\cdot\vec{\mathbf{s}}_{Q\phi}$;
$\vec{\mathbf{i}}_{bk} = conj\{[\vec{\mathbf{S}}_{ELs}]\ ./\ [\vec{\mathbf{u}}_{N_8}]\}$;

and May 31st, 2023. The feeder voltage supply and load demand values relate to the measured profiles logged by smart meters. Power flow simulations do not consider harmonic current and voltage distortion. Then, the R_{III} post-feedback evaluation assumes that Φ_f, Φ_{HDv} and Φ_{HDi} do not change with respect to the results presented in Section 5.4.2. The other operation resilience indices are calculated according to the results of the power flow simulation by the methodology described in Section 3.5.4. Table 30 shows the comparison of the actual EEB-UIS

electrical network's R_{III} assessment to the results of the resilience improvement simulation.

Table 30

Impact of the EMS on EEB-UIS type III resilience.

Index	Actual system	EMS simulation	Index	Actual system	EMS simulation
Φ_I-L_{1-2}	0.9998	0.9999	Φ_u-N_2	0.9456	0.9458
Φ_l-L_{1-2}	0.9998	0.9999	Φ_{VU}-N_2	0.9998	0.9999
Φ_{CU}-L_{1-2}	0.9649	0.9657	Φ_u-N_4	0.9474	0.9474
Φ_I-L_{1-4}	0.9998	0.9999	Φ_{VU}-N_4	0.9998	0.9999
Φ_l-L_{1-4}	0.9996	0.9999	Φ_u-N_8	0.9537	0.9542
Φ_{CU}-L_{1-4}	0.9173	0.9229	Φ_{VU}-N_8	0.9998	0.9999
Φ_I-L_{4-8}	0.9998	0.9999	R_{III}-N_2	0.8206	0.8213
Φ_l-L_{4-8}	0.9993	0.9997	R_{III}-N_4	0.9020	0.9052
Φ_{CU}-L_{4-8}	0.9440	0.9670	R_{III}-N_8	0.9069	0.9149
			R_{III}-EEB	0.8902	0.8935

Results show that the proposed EMS provides benefits to strengthen R_{III}. The main benefit is the improvement of the operation resilience of the EL system's coupling node, PCC/Node 8. An increase of 2.4% in the current unbalance index (Φ_{CU}-L_{4-8}) of the wire supplying the PCC is evidenced. There is also a slight improvement in the PCC voltage regulation index (Φ_u-N_8), which is accompanied by a 31% decrease in the standard deviation of the Φ_u-N_8, representing an additional benefit. Figure 48 shows the evolution of the Φ_u and Φ_{CU} resilience indices of the PCC with a daily assessment refresh. The other resilience indices do not show a remarkable change. This fact could be because the EMS is focused on the quality operation of PCC and ELVB Nodes. The EL system records operation during the 31 days of the test, absorbing power from the PV system at peak generation times. Over the fedback test, the EL system generates 5.33 kg of green H_2, which could then be used to support power outages. In contrast, the FC-Battery system only registers operation on day 1 of the test, when the battery pack take power until it is recharged to the set limit. Figure 49 shows the energy participation of the EEB-UIS's sources and loads in the 31-day R_{III} feedback test.

In the 31-days test, the EEB-UIS load demand is 9.32 MWh. The FC system does not

Figure 48

Evolution of the Φ_u-N_8 and Φ_{CU}-L_{4-8} indices in the R_{III} feedback test.

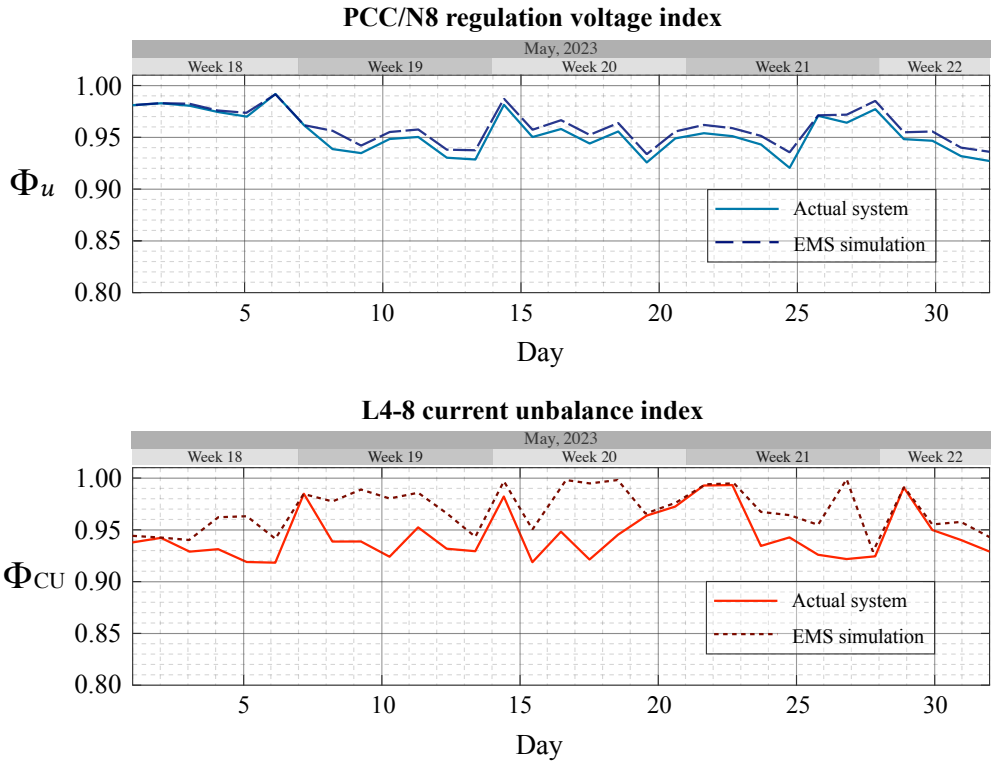

Figure 49

Energy participation of the EEB-UIS sources in the 31-day feedback test.

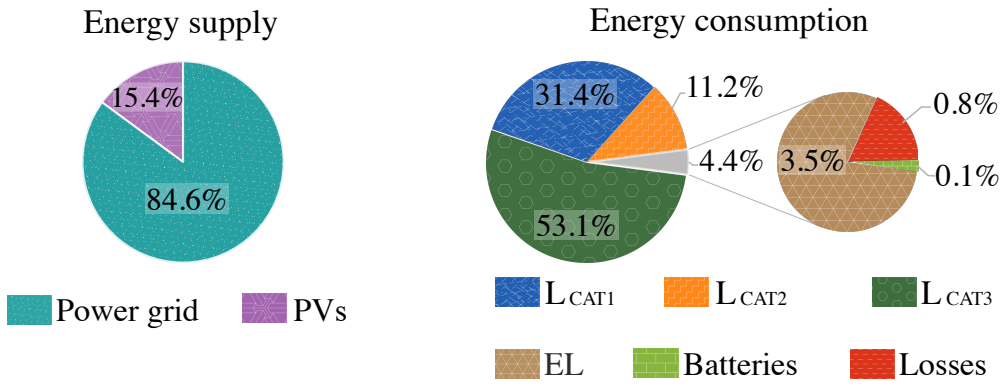

generate power since its connection point (Node 2) does not register undervoltage issues. On the other hand, Node 2 experiences slight overvoltage events; thus, the batteries absorb energy until their preferred SOC_b is reached. The EL system absorbs energy from the PCC supporting its voltage regulation. The PV system generates 1.5 MWh, of which 22.7% is used for electroly-

sis. In overvoltage events at the ELVB, the H_2-ESS absorbs 10.2 kWh to recharge the batteries. The power supply grid provides 8.25 MWh to meet the power demand. The following figures present the operating power of the load and energy sources of the EEB-UIS in the R_{III} feedback test and the voltage profile of the analysed nodes. Figure 50 shows the EEB-UIS power demand profile for May 2023. It notes that the peaks of demand are during working hours which is because the EB-UIS is a building for academic activities. In the evening hours it generally only attends to building management and security loads. The PV system injects peak power at the hours of maximum solar irradiance around midday as Figure 51 shows.

Following Figure 52 presents the per unit voltage behaviour of the PCC and ELVB nodes. It is evident that the PCC voltage is always above the nominal value and the voltage increases when the PV system injects power. In such a case the EL system absorbs power contributing to the normalisation of the voltage regulation. Similarly, the ELVB voltage tends to lie above the nominal value. However, the FC-Batteries system is limited to absorb power by the energy storage capacity of the batteries. Then, the batteries absorb power at a constant recharging power until the SOC_b limited by the EMS is reached. Figure 53 shows the behaviour of the SOC_b during the first 6 hours of the R_{III} feedback test.

Figure 50

Load demand profile of the EEB-UIS in may.

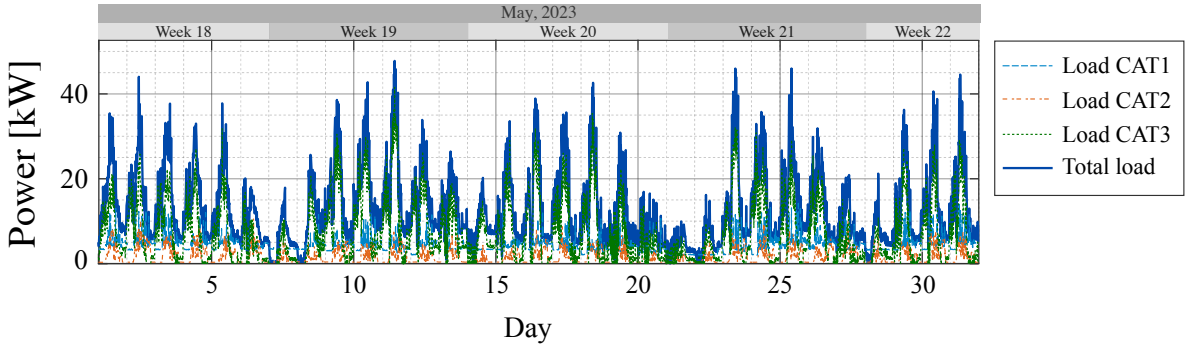

Here the initial SOC_b is set to 0.35 on purpose to appreciate the performance of the EMS. In hour 4 the batteries reach an SOC_b equal to 0.8 and remain at the same charge level until the end of the test. The feedback from R_{III} reflects that an accurate EMS could help to strengthen

Figure 51

Power performance of PV and EL systems in the R_{III} feedback test.

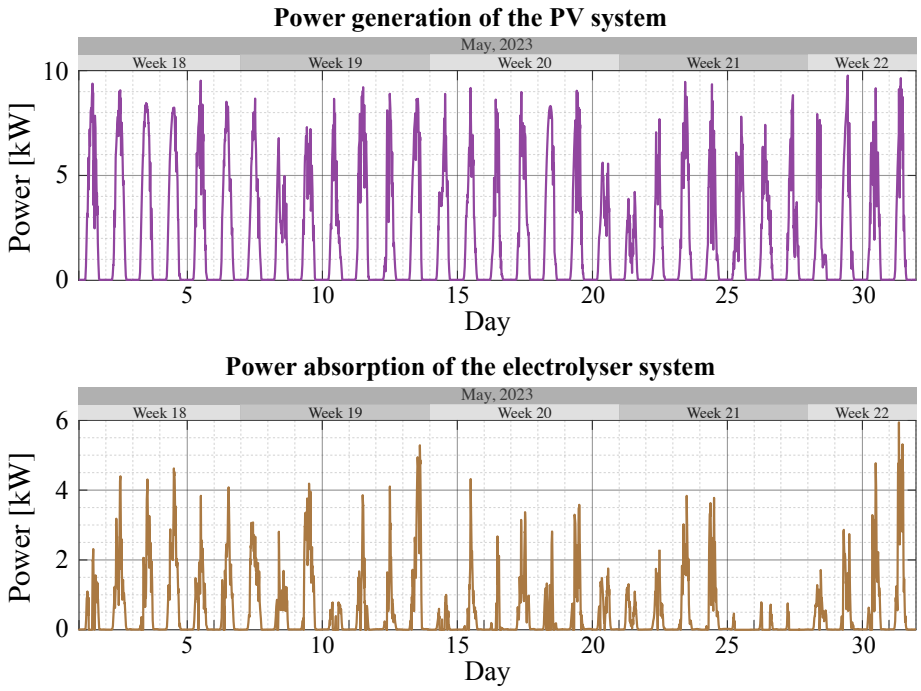

Figure 52

Voltage performance of ELVB and PCC in the R_{III} feedback test.

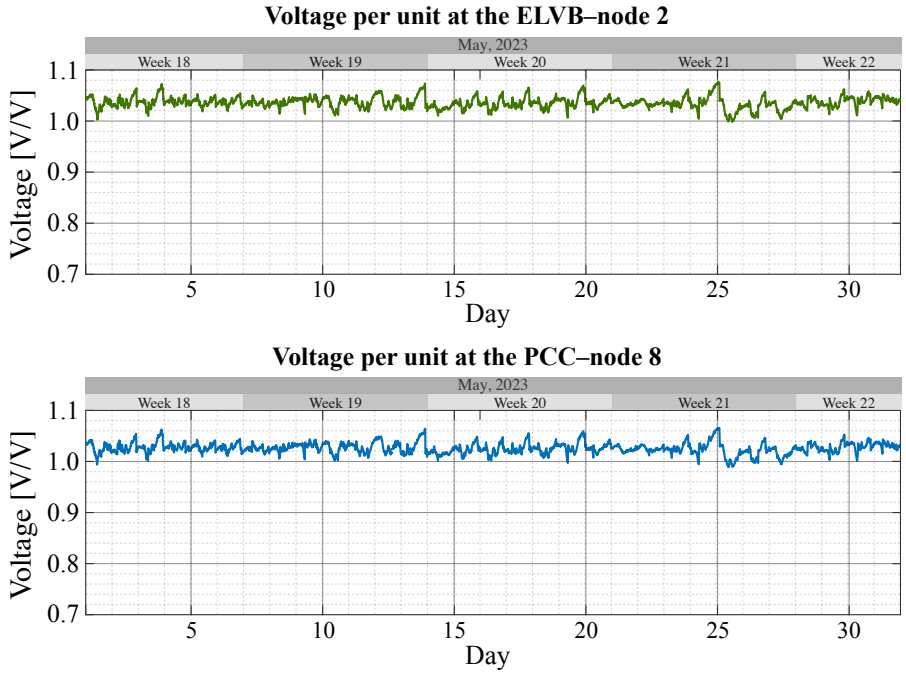

Figure 53

Battery state of charge performance in the first 6 hours of the feedback test.

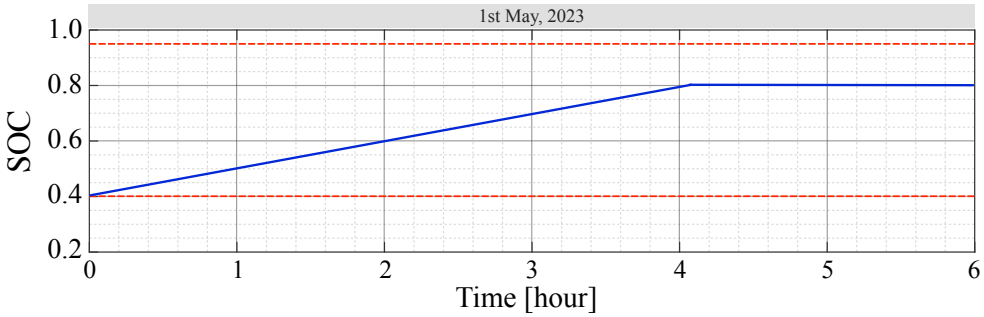

the operation resilience by mitigating the negative issues generated by PV systems, overvoltage and undervoltage events. The following section develops a sensitivity analysis of the size and connection point of the PV and EL systems.

7.5 Sensitivity analysis regarding type III resilience

A local sensitivity analysis is performed to analyse the effect of the size and conection point of the DER. It considers two scenarios: *i)* The EEB-UIS network with the PV system without the H_2-ESS system. The connection point of the PV system is changed between the nodes N_2, N_4 and N_8. The installed PV power is fixed by ±10%, ±20% and ±50% in each node. *ii)* The EEB-UIS network with the PV system and the H_2-ESS system. The connection point of the EL system is changed between the nodes N_2, N_4 and N_8. The maximum power of the EL is fixed in ±10%, ±20% and ±50%. The size of PV, FC Batteries and EMS do not change. The result of the sensitivity analysis is shown below.

7.5.1 Sensitivity analysis for the PV system

Figure 54 shows the result of the local sensitivity analysis for the PV system. It evidences a negative effect on the electrical resilience R_{III} as the installed PV power increases. However, the effect is less when the PV is installed in GLVB than the one with higher power capacity.

Figure 54

Sensitivity of R_{III} against the size and location of the PV system in the EEB-UIS.

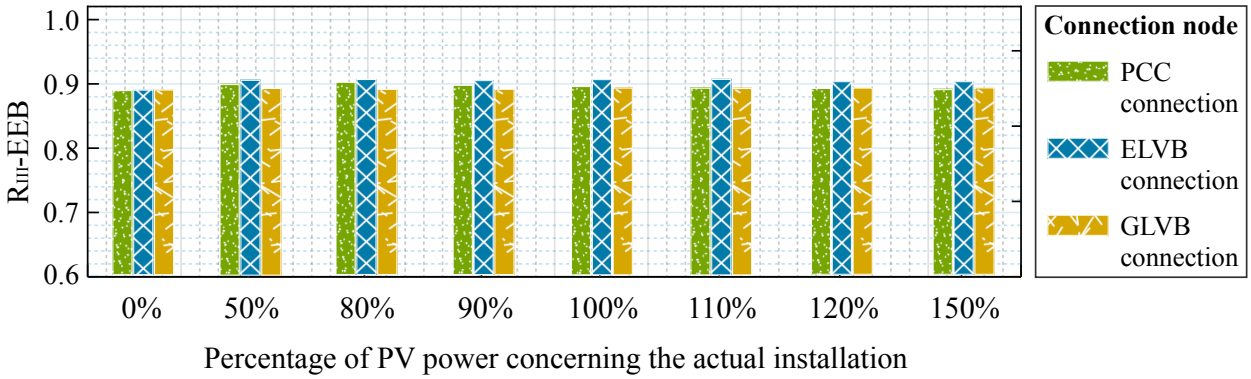

7.5.2 Sensitivity analysis for the EL system

Figure 55 presents the sensitivity analysis result for the EL system. It shows that the EL contributes to strengthening R_{III}. The contribution is higher when the system is installed in the PCC. Although the EL power increases, the EMS restricts its consumption to the generated PV power to generate green H_2. According to the established EMS, an EL power greater than the installed PV power does not significantly strengthen R_{III}. Note that the result could change if another EMS is used. The following section summarises the conclusions of this chapter.

Figure 55

Sensitivity of R_{III} against the size and location of the EL system in the EEB-UIS.

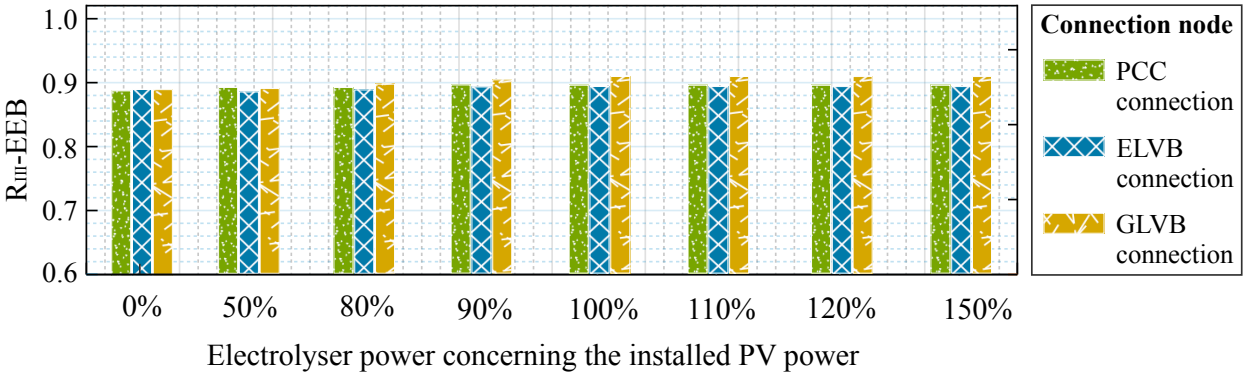

7.6 Chapter conclusions

This chapter develops the feedback on the electrical resilience of the EEB-UIS according to the results of Chapter 5. The resilience evaluation phase identifies that R_I does not require further attention since the CI of the EEB-UIS has a low risk of collapse due to HILP events. R_{II} could be strengthened by increasing the backup system's coverage to the building's non-priority critical loads. R_{III} shows a state of emergency requiring attention to address overvoltage issues. The feedback phase is implemented to determine strategies to strengthen R_{II} and R_{III}. It integrates an H_2-ESS backup system, strengthening backup supply capacity during power outages. Furthermore, the application of EMS on the projected H_2-ESS to improve operation resilience.

In this approach, this chapter develops a methodology to size an H_2-ESS as a backup system for the EEB-UIS. The EEB-UIS load is grouped into three categories: *i)* L_{CAT1}, essential load; *ii)* L_{CAT2}, priority load; and *iii)* L_{CAT3}, non-priority load. The proposal uses historical power outage data to adjust a probability density function and define the backup time for the load categories. The sizing is addressed as an optimisation problem subject to the lost of power supply probability (LPSP) and total supply probability (TSP) criteria. The optimisation is carried out in the Matlab & Simulink environment for a simulation time of 351 minutes. Then, a test is made for an unusual 48-hour power outage using a peak demand period corresponding to May 2023. The sized H_2-ESS meets the EEB-UIS demand and satisfies the TSP and LPSP conditions.

The second part of this chapter deals with analysing strategies for strengthening the electrical resilience of the EEB-UIS. This case study shows that the proposed H_2-ESS increases the EEB-UIS's supply capacity regarding power outages from 44% to 89% compared to its current situation, thereby improving R_{II} resilience. This achievement is reached by extending backup coverage to non-priority loads of the grid strategically. Furthermore, it is proposed to add an electrolysis system to deal with surplus power from the PV system, to support voltage regulation at the common coupling points and to generate green H_2. This approach is tested in a simu-

lation of the EEB-UIS grid electrical operation for the whole month of May. It also implements an energy management strategy focused on regulating the voltage level of the nodes interconnecting power sources and mitigating their load demand unbalance. Simulation results show an appropriate performance of the H_2-ESS system with electrolyser to support resilient operation with the addition of the possibility to generate green H_2, which is stored for later use in the event of an outage.

This chapter ensures the fulfilment of the third (SO3) and fourth (SO4) specific objectives. It sizes an accurate H_2-ESS for the EEB-UIS case study, allowing the application of energy management strategies. Then, it analyses the effect of H_2-ESS and PV systems on electrical resilience. These systems strengthen the R_{II} by increasing survivability during a power outage. Regarding R_{III}, the PV system could be counterproductive for networks with voltage regulation problems and high line impedance. On the other hand, the H_2-ESS could be used to establish EMS focused on dealing with voltage regulation issues. Additionally, the sensitivity analysis shows greater electrical resilience when the PV systems are installed in nodes with higher power capacity. A more significant benefit is when the H_2-ESS electrolyser is installed on the same node as the PV system.

It answers research questions three (RQ3) and four (RQ4); it also contributes to answering RQ5 and RQ6. R_{III} could be used to evaluate the performance of EMS in LV networks since R_{III} is directly related to the representative operation quality parameters. Likewise, the H_2-ESS contribute a double benefit to strengthening electrical resilience. They support the supply in power outages and could address service quality issues. Finally, the R_{III} assessment shows the possibility of constant evolutionary analysis. In this way, it is possible to study the improvements or declines in the electrical network when an intervention is made and compare the evolution of the network. An automated operational resilience assessment system could be implemented using smart meter installation and data processing.

8. Contribution and General Conclusions

This chapter delves into the contribution of the thesis. It describes the achievement of the proposed objectives and their correspondence with the results. It is organised as follows: Section 8.1 remarks on the achievement of the thesis objectives. Section 8.2 emphasises the thesis' contributions and products. Then, Section 8.3 presents the general conclusions. Finally, Section 8.4 focuses on future work.

8.1 Achievement of objectives

The doctoral thesis development has allowed the achievement of the objectives set. The specific objectives (SO) and their declaration for fulfilment are outlined below.

- ***SO1.*** *Determining the resilience evaluation indices for a low-voltage (LV) electrical network that allows analysing the performance of the integration of photovoltaic (PV) generation and hydrogen-based energy storage system (H_2-ESS).*

A bibliographic review had been carried out to identify the electrical resilience evaluation approaches that cover LV networks. The main effects of the interconnection of PV systems in LV networks have also been identified. Chapter 2 presents the breakdown of the bibliographic review. The results show that three approaches to resilience apply to the thesis field. Each approach associates indices for the evaluation of resilience.

i) The critical infrastructure (CI) approach: The indices are the probability of occurrence of catastrophic events, the probability distribution of event intensity and the CI fragility of the electrical network. This approach is general for physical systems that associate civil infrastructure and, therefore, at all levels of electrical networks.

ii) The reliability of the electrical supply: This approach highlights the probability of an outage state of an electrical network. Then, a historical record compilation of the frequency and

length of power outages is vital to characterise the network's reliability. Since LV electrical networks are generally supplied by a feeder with radial topology, the feeder reliability characterises the supply's resilience. On the other hand, energy backup systems could increase electrical resilience. Therefore, the backup factor is also an index considered in this approach.

iii) The supply quality approach: It focuses on the probability that an electrical network loses supply continuity due to poor quality. Resilience indices are related to supply voltage parameters such as voltage regulation, frequency, and voltage unbalance. However, networks involving distributed energy sources should consider additional indices related to power flows and voltage at other nodes in the network, even those without measurements. In the case of PV systems, the literature finds that they could cause overvoltage in the PCC, reverse power flows, and current unbalance. Then, the resilience indices in this approach relate to voltage regulation, frequency, current level, voltage and current harmonic distortion, voltage and current unbalance, and power losses for the supply node and nodes interconnecting energy sources.

- ***SO2.*** *Establish a procedure to assess the resilience of low-voltage (LV) electrical networks with the injection of power from PV systems and H_2-ESS.*

A methodology for evaluating the electrical resilience of LV networks is proposed in Chapter 3. This methodology has considered the resilience analysis approaches and the evaluation indices described in the bibliographic review. It proposes three resilience classifications according to approaches. R_I resilience for electrical CI in the face of high-impact events. R_{II} resilience for the local electrical network in the face of regular power outages. Furthermore, R_{III} resilience for the network operation against events that alter the supply quality. The R_I, R_{II} and R_{III} resilience indicators provide information on the capacity of the electrical network to face disruptive events. They allow for identifying the events for which the network is vulnerable and affect the supply capacity. R_I helps to know infrastructural changes that could improve the robustness of the feeder and the related circuit before HILP events. It focuses on network operators responsible for the feeder circuit's electrical infrastructure. R_{II} also allows the identification of the continuity of supply before outages of common origin. On the one hand, the

local network operator could improve supply reliability by including assets. Also, the user could analyse the contribution of an energy backup system and plan its appropriate sizing, finding a tradeoff between the investment for the backup system and the contribution to resilience. R_{III} allows knowing the quality of the service and identifying how likely it is to incur a violation of the quality parameters. It also defines the feasibility of including new energy sources or loads by analysing their effect on R_{III}.

- ***SO3.*** *Evaluate the effects of the integration of PV generation systems and H_2-ESS on the resilience of a LV electrical network.*

This objective is addressed by applying the proposed methodology for resilience assessment in the electrical networks of the Electrical Engineering Building (EEB-UIS) as a case study. Chapter 5 details the development of the electrical resilience analysis in the EEB-UIS and its findings. Chapter 7 develops the design of an H_2-ESS as a backup system for power outages, provides feedback on the resilience evaluation results and proposes strategies to strengthen the EEB-UIS electrical resilience. The resilience results of the EEB-UIS show that integrating PV systems does not affect R_I since these systems are not considered CI. Regarding R_{II}, the H_2-ESS increase the reliability of the electrical network representing a benefit for R_{II}. Using the PV system to contribute energy to the backup system in a power outage is also possible. In the case of the EEB-UIS network, an H_2-ESS sized as a backup system could contribute R_{II} by increasing the capacity to supply load demand in the event of a power outage. The PV could contribute up to 31% of the demand in a 48-hour outage.

The H_2-ESS and PV systems have a more significant effect on R_{III} since they interfere with the quality of the operation. Depending on the operating conditions, they could benefit or harm the network. In the case of the EEB-UIS, the PV system generates slight overvoltage in the point of common coupling (PCC) in the hours of high solar intensity, affecting the R_{III}-PCC resilience in the PCC. Simulations of an H_2-ESS integration show that it is possible to improve the performance of the electrical operation, thus contributing to the strengthening of R_{III}. Then, an optimised EMS could offer more benefits.

- ***SO4.*** *Analyse the sensitivity of the resilience of a LV electrical network to variations in the level of penetration and location of the PV systems and the H_2-ESS and the application of EMS.*

Chapter 7 also details a sensitivity analysis of the location and size of the electrolyser (EL) and PV systems for the EEB-UIS network. The analysis varies the installed PV power by ±10%, ±20% and ±50% concerning the actual PV installed power. The interconnection point is also tested in three nodes of the EEB-UIS network. The nodes analysed are the emergency low voltage bus (ELVB), the general low voltage bus (GLVB) and the point of common coupling (PCC) of the actual PV system. The same conditions are analysed for the EL system. The simulations implement a rule-based EMS defining the H_2-ESS participation. The results show that the EEB-UIS could increase the installed PV power by 50% without the operation resilience R_{III} of the EEB-UIS falling into a state of emergency. Also, changing the interconnection point of the EL system to the general bus and the emergency bus would result in a slight increase of R_{III}. In the same vein, the use of the EL system to regulate the intermittence of the PV power would produce benefits in R_{III}. The best interconnection point for the EL system is the same coupling point of the PV system.

8.2 Contributions and products

The development of this thesis contributes to the definition and application of electrical resilience for LV networks. Likewise, it tends to plan resilient LV networks before the integration of DG systems, mainly H_2-ESS and PV systems. Additionally, this thesis has allowed the publication of five papers directly related to the thesis and two complementary papers. The development of the thesis also allowed the co-direction of an undergraduate project and a master project. The contributions and products achieved are detailed below.

8.2.1 Thesis contributions

The main contributions of this thesis are:

- *Setting a definition of electrical resilience for LV networks.* This thesis developed a bibliographic review identifying the approaches to evaluating electrical resilience in LV networks. It classified the approaches into three type-resilience and identified their interactions. Then, this thesis provides a comprehensive definition of the resilience of LV power grids.

- *A comprehensive methodology for assessing the electrical resilience of the LV networks integrating PV generation.* This thesis proposes an original methodology to assess the electrical resilience of LV networks incorporating PV generation. The methodology is comprehensive, addressing three distinctive categories of disturbances that power systems may face: *i)* High-impact, low-probability disturbances. *ii)* Disturbances causing power outages with prompt recovery. And *iii)* permanent supply quality disturbances. It establishes a procedure for each type-resilience evaluation. It emphasises operation resilience, where the integration of PV systems has the most significant impact. Then, it proposes resilience evaluation indices adjusted to LV networks that integrate PV systems. This research implements the comprehensive electrical resilience assessment in the EEB-UIS network and exemplifies the analysis of the three types of resilience and their integration.

- *Providing information for optimising and improving electrical resilience in LV Networks with PV Integration.* The implementation in the case study develops an analysis of the benefits of an H_2-ESS backup system. The H_2-ESS could serve as a backup system in case of an outage, increasing the resilience of the continuity of supply. It could also associate EMS to mitigate overvoltage and reverse power flows given the PV system, strengthening the operation resilience. Likewise, this thesis develops a sensitivity analysis of the connection point and size of the H_2-ESS electrolyser. The work includes power flow simulations allowing a detailed analysis of the influence of H_2-ESS and EMS on the electrical resilience of the grid in the case studied. It analyses the use of H_2-ESS and EMS to improve the resilience of LV networks, and it provides crucial information for the optimisation and

improvement of electrical resilience in similar scenarios.

8.2.2 Products achieved in the thesis

The development of this thesis has reached the production of five peer–reviewed articles:

- *Electrical resilience assessment for low-voltage buildings. In Energy & Buildings,* (R. Rodriguez *et al.*, 2024). It exposes the application of a comprehensive electrical resilience analysis for a university building. It proposes a resilience assessment methodology and then applies it in the EEB-UIS. The research has progressed until reaching the proposal presented in this thesis to evaluate the electrical resilience of LV networks.

- *Sizing of a fuel cell–battery backup system for a university building based on the probability of the power outage length. In Energy Reports,* (R. Rodriguez *et al.*, 2022). It proposes the sizing of backup systems based on the history of the power outage length. It applies the proposed methodology to sizing an H_2-ESS for the EEB-UIS. This research focuses on strengthening the resilience of supply continuity for LV networks.

- *Assessment of power quality parameters and indicators at the point of common coupling in a low voltage power grid with photovoltaic generation emulated. In Electric Power Systems Research,* (Pinzon *et al.*, 2022). It emulates the injection of PV power in an LV network, evaluating the influence on the quality of the voltage and power in the PCC. The emulation uses the EPH3 equipment of Lucas Nülle and a PQube3 smart meter. Fifteen scenarios are emulated, considering the reduction of active power, the percentage of shadow on the surface of the PV panel and the number of shaded PV panels.

- *A framework for the resilience of LV electrical networks with photovoltaic power injection. In Tecnura,* (R. Rodriguez *et al.*, 2021). It develops a literature review on the operational resilience approach for LV networks. It applies the findings to characterise the voltage resilience index for the EEB-UIS network.

- *Resilience assessment in a low-voltage power grid with photovoltaic generation in a university building. In International Review of Electrical Engineering*, (Parrado *et al.*, 2021). It proposes a resilience index approach to quantify PV systems' impacts on the LV networks' operation quality. The evaluation of the resilience scheme is applied to the EEB-UIS and its PV system. The test followed up 31 days of measuring the quality parameters of the EEB electrical network, with data acquisition every 10 minutes.

Additionally, this thesis contributed to the co-direction of two degree–projects:

- *Proposal for an evaluation scheme of the electrical resilience of low-voltage networks with integration of photovoltaic generation - operating condition in stable state.* Master thesis, *Universidad Industrial de Santander*, Colombia, 2020.

- *Resilience assessment of a low voltage electrical network with the integration of photovoltaic generation in the Lucas Nülle EPH3 equipment.* Undergraduate project, *Universidad Industrial de Santander*, Colombia, 2021.

8.3 General conclusions

This thesis proposes a methodology for assessing the electrical resilience of LV networks. It focuses on networks integrating PV generation systems. The approaches available in the literature to address electrical resilience have been categorised according to the type of disturbing event the LV network could face. Then, It proposes resilience indices and an assessment methodology for each type of event. *i)* Type I resilience (R_I) to high-impact low-probability (HILP) events assesses the ability of the LV network's critical infrastructure (CI) to withstand natural disasters. *ii)* Type II resilience (R_{II}) to low-impact high-probability (LIHP) events assesses the capability of the LV network to recover from common cause outages. R_{II} also considers the contribution of energy backup systems to support priority loads. *iii)* Type III resilience (R_{III}) analyses the service quality provided to users. Then, the three types of resilience are integrated to achieve an comprehensive resilience (R_{comp}) analysis. Additionally, the proposed

methodology includes a feedback phase focused on identifying the network's weak points and strengthening electrical resilience.

The proposed electrical resilience assessment has been implemented in the Electrical Engineering Building (EEB-UIS) as a case study. EEB-UIS meets the criteria for developing a R_{comp} analysis. It has an electrical network designed to implement academic and research practices. Its topology is equivalent to a 9-nodes LV radial distribution network. Also, it integrates an on-grid PV system and a diesel generator backup system. Furthermore, a smart metering system monitors the electrical variables of the EEB-UIS nodes. It has made it possible to measure and record the quality parameters of the EEB-UIS electrical operation. The application in the EEB-UIS exemplifies the procedure for the R_{comp} analysis and is consistent with the findings in the literature. It finds R_I and R_{II} close to the maximum value, and R_{III} shows vulnerability in the supply quality. The main parameter to strengthen is voltage regulation followed by current unbalance. It should be noted that the R_I evaluation is valid for the region of the case study, R_{II} covers the LV networks fed by the same MV distribution circuit. However, the R_{III} assessment is exclusive to the EEB-UIS network.

The application of R_{comp} in the case study shows the versatility of the proposal to be applied in LV networks that integrate PV generation. This proposal covers the R_I resilience of the CI that could be affected by HILP events causing intense damage to the electrical infrastructure of a region, interrupting the electrical supply. R_I could expand to the entire region with the same risk events condition. The particularity of the analysis is the CI set integrating the feeder. R_{II} covers recurring power outages that the local network operator quickly overcomes. These incidents are recorded in the MV circuits supplying the feeders of the LV networks. Then R_{II} could address the LV networks supplied by the MV circuit or by a common feeder. The particularity is in the energy backup systems integrating the analysed LV network. R_{III} focuses on quality of service, and it strongly depends on the supply voltage quality. However, R_{III} could be affected by the characteristics of the studied LV network and its associated loads. The application in the case study also finds it more feasible to improve R_{II} and R_{III} with infrastructure and

energy management strategies. For this case, the integration of an H_2-ESS has been proposed as a backup system that could increase the supply capacity for EEB-UIS loads in the event of power outages. It also showed a benefit in supporting voltage regulation at the coupling nodes and reducing the power imbalance of the grid. However, it is possible to implement backup systems of other natures or EMS for the sources already installed in the study network.

In synthesis, this thesis focuses on assessing electrical resilience in LV power grids with photovoltaic systems in warm tropical climates, but its methodology could be applied to various LV grids. For the future, the expansion of this methodology to MV distribution networks and the development of tools to assess the real-time performance of electrical systems is envisaged, as well as the definition of energy management strategies to integrate distributed generation and energy storage systems, strengthening electrical resilience at local and regional levels in different climatic contexts. The lines of future work identified are described in the following section.

8.4 Future work

Future work is framed to expand and adapt the electrical resilience assessment methodology developed in this thesis to MV and LV distribution networks and electrical installations in a generalised way. Strategies to effectively integrate distributed generation and energy storage systems, together with energy management strategies, should be explored to increase the reliability of electrical grids in different disruptive situations. Four main lines have been identified for the continuation of the research line of this doctoral thesis. They are outlined below.

Adaptation to different climatic conditions. The methodology developed in this thesis, originally applied to low voltage grids with PV systems in warm tropical climates, has the potential to be extended to other low voltage grids with different climatic conditions. Adaptation to different climatic scenarios could strengthen electrical resilience in a broader context. The tropical weather conditions could relate to the high-impact low-probability events, posing a threat to the studied region. Then, identifying risk events and the critical infrastructure fragility

characterisation could be adjusted to an electrical grid in another type of weather. Likewise, the characterisation of power outages depends on the history of common outages of the power supply circuits. Generalising the R_{III} assessment requires more attention concerning the type of load demand of the electrical grid and the distributed generation systems involved.

Extending the methodology to medium voltage grids. In order to obtain a more comprehensive view of electrical resilience in distribution systems, the extension of the developed methodology to cover MV distribution networks is envisaged. This approach will allow for a more comprehensive understanding of electrical resilience in the entire distribution system. In addition, practical tools will be explored to assess in real-time the performance of both MV and LV electrical networks, which will facilitate the identification of areas for improvement in the electricity distribution chain. This development will significantly strengthen electricity resilience at the local and regional levels.

Advanced integration of distributed generation and energy storage. The case study results show that H2ESS and PV systems can strengthen electrical resilience by increasing the reliability of the electrical system and supporting the quality of the service. Along this path, it is advisable to explore the analysis of the integration of other sources of distributed generation and ESS at the LV and MV levels. Likewise, energy management strategies focus on the control and optimisation of the operation of electrical networks. Likewise, energy management strategies focus on the control and optimisation of the operation of electrical networks. It is also advisable to develop systematic strategies for the financial evaluation of resilience-strengthening strategies to balance the cost and the benefit obtained.

Resilience analysis of special electrical networks. In future research, it is essential to identify appropriate weights for evaluating resilience depending on the type of load analysed. For example, a university building has different characteristics than a shopping centre, a residential building or a hospital. They require special consideration in the analysis. That could be addressed by weighting resilience indices based on load criticality. It is also essential to make a detailed analysis of the normalisation functions of the quality parameters in the assessment of

R_{III}. Verify the correspondence between the QP ranges according to the quality standards and the resilience conditions. Also, verify if the piecewise linear correspondence is the best normalisation alternative or if a non-linear correspondence performs better. On the other hand, the case study benefited from a smart metering system facilitating R_{III} resilience assessment and feedback strategies analysis. However, LV power grid installations often have basic energy meter equipment, creating a gap in the method to carry out the resilience study when energy measurement is limited. Identifying the minimum parameters necessary for an adequate comprehensive resilience analysis is crucial to address in future work.

References

Abdeltawab, H. H., & Mohamed, Y. A. R. I. (2016). Robust energy management of a hybrid wind and flywheel energy storage system considering flywheel power losses minimization and grid-code constraints. *IEEE Transactions on Industrial Electronics*, *63*, 4242-4254. doi: 10.1109/TIE.2016.2532280

Abedi, A., Gaudard, L., & Romerio, F. (2019). Review of major approaches to analyze vulnerability in power system. *Reliability Engineering and System Safety*, *183*, 153-172. doi: 10.1016/j.ress.2018.11.019

Agathokleous, R. A., & Kalogirou, S. A. (2020). Status, barriers and perspectives of building integrated photovoltaic systems. *Energy*, *191*. doi: 10.1016/j.energy.2019.116471

Aleem, S. A., Hussain, S. M. S., & Ustun, T. S. (2020). A review of strategies to increase PV penetration level in smart grids. *Energies*, *13*, 1-28. doi: 10.3390/en13030636

ANSI C84.1. (2016). Electric power systems and equipment-voltage ratings. *American National Standards Institute*, 1-123.

Arcila, M., Garcia, J., Montejo, J., Eraso, J., Valcarcel, J., Mora, M., ... Diaz, F. (2020). National seismic hazard model for Colombia. *Bogota: Colombian Geological Service and Global Earthquake Model Foundation, Special Geological Publications*, *43*, 1-310. doi: 10.32685/9789585279469

Ates, Y., Uzunoglu, M., Karakas, A., Boynuegri, A. R., Nadar, A., & Dag, B. (2016). Implementation of adaptive relay coordination in distribution systems including distributed generation. *Journal of Cleaner Production*, *112*, 2697-2705.

Attemene, N. S., Agbli, K. S., Fofana, S., & Hissel, D. (2020, 2). Optimal sizing of a wind, fuel cell, electrolyzer, battery and supercapacitor system for off-grid applications. *International Journal of Hydrogen Energy*, *45*, 5512-5525. doi: 10.1016/j.ijhydene.2019.05.212

Ayop, R., Isa, N. M., & Tan, C. W. (2018, 1). Components sizing of photovoltaic stand-alone system based on loss of power supply probability. *Renewable and Sustainable Energy Reviews*, *81*, 2731-2743. doi: 10.1016/j.rser.2017.06.079

Baghmisheh, A. G., & Mahsuli, M. (2021). Seismic performance and fragility analysis of power distribution concrete poles. *Soil Dynamics and Earthquake Engineering*, *150*, 1-15. doi: 10 .1016/j.soildyn.2021.106909

Bajaj, M., Singh, A. K., Alowaidi, M., Sharma, N. K., Sharma, S. K., & Mishra, S. (2020). Power quality assessment of distorted distribution networks incorporating renewable distributed generation systems based on the analytic hierarchy process. *IEEE Access*, *8*, 145713-145737.

Baroud, H., & Barker, K. (2018). A bayesian kernel approach to modeling resilience-based network component importance. *Reliability Engineering and System Safety*, *170*, 10-19. doi: 10.1016/j.ress.2017.09.022

Bie, Z., Lin, Y., Li, G., & Li, F. (2017). Battling the extreme: A study on the power system resilience. *Proceedings of the IEEE*, *105*, 1253-1266. doi: 10.1109/JPROC.2017.2679040

Billinton, R., Wu, C., & Singh, G. (2002). Extreme adverse weather modeling in transmission and distribution system reliability evaluation. *14hth PSCC*, 1-7.

Bjarnadottir, S., Li, Y., & Stewart, M. G. (2013). Hurricane risk assessment of power distribution poles considering impacts of a changing climate. *Journal of Infrastructure Systems*, *19*(1), 12-24. doi: 10.1061/(ASCE)IS.1943-555X.0000108

Borghei, M., & Ghassemi, M. (2021, 6). Optimal planning of microgrids for resilient distribution networks. *International Journal of Electrical Power and Energy Systems*, *128*, 106682.

Brinkel, N. B., Gerritsma, M. K., AlSkaif, T. A., Lampropoulos, I. I., van Voorden, A. M., Fidder, H. A., & van Sark, W. G. (2020). Impact of rapid PV fluctuations on power quality in the low-voltage grid and mitigation strategies using electric vehicles. *International Journal of Electrical Power and Energy Systems*, *118*, 1-11. doi: 10.1016/j.ijepes.2019.105741

Bruneau, M., Chang, S. E., Eguchi, R. T., Lee, G. C., O'Rourke, T. D., Reinhorn, A. M., ... Winterfeldt, D. V. (2003). A framework to quantitatively assess and enhance the seismic resilience of communities. *Earthquake Spectra*, *19*, 733-752. doi: 10.1193/1.1623497

Cadini, F., Agliardi, G. L., & Zio, E. (2017). A modeling and simulation framework for the reliability/availability assessment of a power transmission grid subject to cascading failures under extreme weather conditions. *Applied Energy*, *185*, 267-279. doi: 10.1016/j.apenergy.2016.10.086

Celli, G., Pilo, F., Pisano, G., & Soma, G. G. (2017). Cost / benefit analysis for energy storage exploitation in distribution systems. *Cired 2017*, *2017*, 12-15. doi: 10.1049/oap-cired.2017.1004

Chathurangi, D., Jayatunga, U., & Perera, S. (2022). Recent investigations on the evaluation of solar PV hosting capacity in lv distribution networks constrained by voltage rise. *Renewable Energy*, *199*, 11-20. doi: 10.1016/j.renene.2022.08.120

Chaudry, M., Ekins, P., Ramachandran, K., Shakoor, A., Skea, J., Strbac, G., ... Whitaker, J. (2011). Building a resilient uk energy system. *UK Energy Research Centre*, 120.

Choi, J. W., Heo, S. Y., & Kim, M. K. (2016). Hybrid operation strategy of wind energy storage system for power grid frequency regulation. *IET Generation, Transmission & Distribution*, *10*, 736-749. doi: 10.1049/iet-gtd.2015.0149

Chong, W., Yunhe, H., Feng, Q., Shunbo, L., & Kai, L. (2017). Resilience enhancement with sequentially proactive operation strategies. *IEEE Transactions on Power Systems*, *32*, 2847-2857.

Clauß, J., Finck, C., Vogler-Finck, P., & Beagon, P. (2017). Control strategies for building energy systems to unlock demand side flexibility-a review. *IBPSA Building Simulation 2017*, 1-10. doi: http://hdl.handle.net/10197/9016

Cortes, C., & Garcia, Y. (2018). *Impact study of the energy injection of a photovoltaic generation system on the voltage profile and energy losses in wire conductors of the low voltage network of the electrical engineering building by simulations.* Undergraduate thesis, *Universidad Industrial de Santander*, Colombia.

Deboever, J., Grijalva, S., Reno, M. J., & Broderick, R. J. (2018). Fast quasi-static time-series (QSTS) for yearlong PV impact studies using vector quantization. *Solar Energy*, *159*, 538-547. doi: 10.1016/j.solener.2017.11.013

Dehghanian, P., Aslan, S., & Dehghanian, P. (2018). Maintaining electric system safety through an enhanced network resilience. *IEEE Transactions on Industry Applications*, *54*, 4927-4937. doi: 10.1109/TIA.2018.2828389

Dong, W., Li, Y., & Xiang, J. (2016). Sizing of a stand-alone photovoltaic/wind energy system with hydrogen and battery storage based on improved ant colony algorithm. *2016 Chinese Control and Decision Conference (CCDC)*, 4461-4466. doi: 10.1109/CCDC.2016.7531788

Dvorak, Z., Chovancikova, N., Bruk, J., & Hromada, M. (2021). Methodological framework for resilience assessment of electricity infrastructure in conditions of Slovak Republic. *International Journal of Environmental Research and Public Health*, *18*. doi: 10.3390/ijerph18168286

Emmanuel, M., & Rayudu, R. (2017). The impact of single-phase grid-connected distributed photovoltaic systems on the distribution network using p-q and p-v models. *International Journal of Electrical Power and Energy Systems, 91,* 20-33. doi: 10.1016/j.ijepes.2017.03.001

EN 50160. (2010). Voltage characteristics of electricity supplied by public electricity networks. *European Committee for Electrotechnical Standardization-ENELEC*.

Espinoza, S., Panteli, M., Mancarella, P., & Rudnick, H. (2016). Multi-phase assessment and adaptation of power systems resilience to natural hazards. *Electric Power Systems Research*, *136*, 352-361. doi: 10.1016/j.epsr.2016.03.019

Fahim, S. R., Hasanien, H. M., Turky, R. A., Aleem, S. H. E. A., & Ćalasan, M. (2022). A comprehensive review of photovoltaic modules models and algorithms used in parameter extraction. *Energies*, *15*(23). doi: 10.3390/en15238941

Ferrario, E., Poulos, A., Castro, S., de la Llera, J. C., & Lorca, A. (2022). Predictive capacity of topological measures in evaluating seismic risk and resilience of electric power networks. *Reliability Engineering and System Safety*, *217*, 1-19. doi: 10.1016/j.ress.2021.108040

Galvan, E., Mandal, P., & Sang, Y. (2020). Networked microgrids with roof-top solar PV and battery energy storage to improve distribution grids resilience to natural disasters. *International Journal of Electrical Power and Energy Systems*, *123*, 1-10. doi: 10.1016/j.ijepes.2020.106239

Ganeshan, A., & Holmes, D. G. (2017). Enhanced control of a hydrogen energy storage system in a microgrid. *2017 Australasian Universities Power Engineering Conference (AUPEC), Melbourne, VIC*, 1-6. doi: 10.1109/AUPEC.2017.8282434

Gow, J. A., & Manning, C. D. (1999). Development of a photovoltaic array model for use in power-electronics simulation studies. *IEE Proceedings: Electric Power Applications*, *146*, 193-200. doi: 10.1049/ip-epa:19990116

Gupta, R., Bruce-Konuah, A., & Howard, A. (2019). Achieving energy resilience through smart storage of solar electricity at dwelling and community level. *Energy and Buildings*, *195*, 1-15. doi: 10.1016/j.enbuild.2019.04.012

Hagemann, I. (1996). Architectural considerations for building-integrated photovoltaics. *Progress in Photovoltaics: Research and Applications*, *4*, 247-258.

Haixiang, G., Ying, C., SHengwei, M., SHaowei, H., & Yin, X. (2017). Resilience-oriented pre-hurricane resource allocation in distribution systems considering electric buses. *National Natural Science Foundation of China*, *105*. doi: 10.1109/JPROC.2017.2666548

Han, L., Zhao, X., Chen, Z., Gong, H., & Hou, B. (2021). Assessing resilience of urban lifeline networks to intentional attacks. *Reliability Engineering and System Safety*, *207*, 1-16. doi: 10.1016/j.ress.2020.107346

Hassan, A., Bass, O., & Masoum, M. A. (2023). An improved genetic algorithm based fractional open circuit voltage mppt for solar pv systems. *Energy Reports*, *9*, 1535-1548. doi: https://doi.org/10.1016/j.egyr.2022.12.088

Hellman, H.-P., Pihkala, A., Hyvärinen, M., Heine, P., Karppinen, J., Siilin, K., ... Matilainen, J. (2017). Benefits of battery energy storage system for system, market, and distribution network – case helsinki. *CIRED*, *2017*, 1588-1592. doi: 10.1049/oap-cired.2017.0810

Hernández Contreras, C., Amaya Corredor, C. A., Machado López, M. J., Pabón Toloza, G. N., & Rodriguez Perez, C. A. (2023). Environmental characterization of an urban ecosystem using the landscape interpretation methodology of the Alexander Von Humbolt Institute of Colombia. *Journal of Survey in Fisheries Sciences*, *10*, 4712-4724.

Home-Ortiz, J. M., Melgar-Dominguez, O. D., Mantovani, J. R. S., & Catalão, J. P. (2022, 12). Pv hosting capacity assessment in distribution systems considering resilience enhancement. *Sustainable Energy, Grids and Networks*, *32*, 100829. doi: 10.1016/j.segan.2022.100829

Hou, G., Muraleetharan, K. K., Panchalogaranjan, V., Moses, P., Javid, A., Al-Dakheeli, H., ... Narayanan, M. (2023). Resilience assessment and enhancement evaluation of power distribution systems subjected to ice storms. *Reliability Engineering and System Safety*, *230*, 1-12. doi: 10.1016/j.ress.2022.108964

Hussain, A., & Musilek, P. (2022). Resilience enhancement strategies for and through electric vehicles. *Sustainable Cities and Society*, *80*, 1-18. doi: 10.1016/j.scs.2022.103788

IEC 61000-3-2. (2018). Electromagnetic compatibility (EMC). Part 3-2, limits - Limits for harmonic current emissions (equipment input current ≤ 16 A per phase). *International Electrotechnical Commossion*.

IEC 61000-3-4. (1998). Electromagnetic compatibility (EMC). Part 3-4, limits - Limitation of emission of harmonic currents in low-voltage power supply systems for equipment with rated current greater than 16 A. *International Electrotechnical Commossion*.

IEC 61000-3-6. (2008). Electromagnetic compatibility (EMC). Part 3-6, limits - Assessment of emission limits for the connection of distorting installations to MV, HV and EHV power systems. *International Electrotechnical Commossion*.

IEC61000-2-2. (2018). Electromagnetic compatibility (EMC). Part 2-2, compatibility levels for low-frequency conducted disturbances and signalling in public low-voltage power supply systems. *International Electrotechnical Commossion*.

IEEE. (2018). Standard for interconnection and interoperability of distributed energy resources with associated electric power systems interfaces. *IEEE Std 1547™-2018. Standards Coordinating Committee 21*, 1-137.

IEEE Std 141. (1993). Ieee recommended practice for electric power distribution for industrial plants. *IEEE standards*, 1-768. doi: 10.1109/IEEESTD.1994.121642

IEEE Std 1547. (2018). Ieee standard for interconnection and interoperability of distributed energy resources with associated electric power systems interfaces. *IEEE standards*, 1-138.

IEEE Std 519. (2014). Ieee recommended practice and requirements for harmonic control in electric power systems sponsored by the transmission and distribution committee ieee power and energy society. *IEEE standards*, 1-29.

IRENA. (2020). Green hydrogen cost reduction: scaling up electrolysers to meet the 1.5ºc climate goal. *International Renewable Energy Agency*. Retrieved from www.irena.org/publications

Jasiūnas, J., Lund, P., & Mikkola, J. (2021). Energy system resilience – a review. *Renewable and Sustainable Energy Reviews, 150*. doi: 10.1016/j.rser.2021.111476

Javadian, S. A. M., & Massaeli, M. (2011). Impact of distributed generation on distribution system' s reliability considering recloser-fuse and miscoordination - a practical case study. *Indian Journal of Science and Technology, 4*, 1279-1284.

Kandidayeni, M., Macias, A., Boulon, L., & Trovão, J. P. F. (2020). Online modeling of a fuel cell system for an energy management strategy design. *Energies, 13*. doi: 10.3390/en13143713

Kosmadakis, I. E., Elmasides, C., Koulinas, G., & Tsagarakis, K. P. (2021). Energy unit cost assessment of six photovoltaic-battery configurations. *Renewable Energy, 173*, 24-41. doi: 10.1016/j.renene.2021.03.010

Kurdi, Y., Alkhatatbeh, B. J., & Asadi, S. (2022). The role of demand energy profile on the optimum layout of photovoltaic system in commercial buildings. *Energy and Buildings, 271*. doi: 10.1016/j.enbuild.2022.112320

Lagrange, A., de Simón-Martín, M., González-Martínez, A., Bracco, S., & Rosales-Asensio, E. (2020). Sustainable microgrids with energy storage as a means to increase power resilience in critical facilities: An application to a hospital. *International Journal of Electrical Power and Energy Systems, 119*, 1-12. doi: 10.1016/j.ijepes.2020.105865

Li, B., Chen, Y., Wei, W., Huang, S., Xiong, Y., Mei, S., & Hou, Y. (2021). Routing and scheduling of electric buses for resilient restoration of distribution system. *IEEE Transactions on Transportation Electrification, 7*(4), 2414-28. doi: 10.1109/TTE.2021.3061079

Li, B., Roche, R., & Miraoui, A. (2017). A temporal-spatial natural disaster model for power system resilience improvement using DG and lines hardening. *2017 IEEE Manchester PowerTech, Manchester, UK*, 1-6. doi: 10.1109/PTC.2017.7980851

Ma, K., Fang, L., & Kong, W. (2020). Review of distribution network phase unbalance: Scale, causes, consequences, solutions, and future research directions. *CSEE Journal of Power and Energy Systems*, *6*, 479-488. doi: 10.17775/CSEEJPES.2019.03280

Ma, L., Christou, V., & Bocchini, P. (2022). Framework for probabilistic simulation of power transmission network performance under hurricanes. *Reliability Engineering and System Safety*, *217*, 1-19. doi: 10.1016/j.ress.2021.108072

Ma, S., Chen, B., & Wang, Z. (2018). Resilience enhancement strategy for distribution systems under extreme weather events. *IEEE Transactions on Smart Grid*, *9*, 1442-1451.

Ma, S., Lin, M., Lin, T. E., Lan, T., Liao, X., Maréchal, F., ... Wang, L. (2021). Fuel cell-battery hybrid systems for mobility and off-grid applications: A review. *Renewable and Sustainable Energy Reviews*, *135*. doi: 10.1016/j.rser.2020.110119

Ma, S., Su, L., Wang, Z., Qiu, F., & Guo, G. (2018). Resilience enhancement of distribution grids against extreme weather events. *IEEE Transactions on Power Systems*, *33*, 4842-4853. doi: 10.1109/TPWRS.2018.2822295

Megdiche, M. (2020). *Dependability of distribution networks in the presence of distributed generation.* Doctoral thesis, *Institut National Polytechnique de Grenoble* - INPG, French.

Mehrjerdi, H., & Hemmati, R. (2020). Coordination of vehicle-to-home and renewable capacity resources for energy management in resilience and self-healing building. *Renewable Energy*, *146*, 568-579. doi: 10.1016/j.renene.2019.07.004

Mishra, D. K., Ghadi, M. J., Azizivahed, A., Li, L., & Zhang, J. (2021). A review on resilience studies in active distribution systems. *Renewable and Sustainable Energy Reviews*, *135*, 1-20. doi: 10.1016/j.rser.2020.110201

Mizutani, M., Monden, Y., Sato, J., Kono, T., & Nakajima, R. (2016). Energy management for hydrogen energy storage system. *CIRED Workshop -Helsinki*, *0201*, 4-7.

Montoya, O. D., González, W. G., Noreña, L. F. G., Vanegas, C. A. R., & Cabrera, A. M. (2020). Hybrid optimization strategy for optimal location and sizing of dg in distribution networks. *Tecnura*, *24*, 47-61. doi: 10.14483/22487638.16606

Moubayed, N., Kouta, J., EI-AIi, A., Dernayka, H., & Outbib, R. (2008). Parameter identification of the lead-acid battery model. *2008 33rd IEEE Photovoltaic Specialists Conference*, 1-6. doi: 10.1109/PVSC.2008.4922517

Murayama, M., Kato, S., Tsutsui, H., Tsuji-Iio, S., & Shimada, R. (2018). Combination of flywheel energy storage system and boosting modular multilevel cascade converter. *IEEE Transactions on Applied Superconductivity*, *28*, 1-4,. doi: 10.1109/TASC.2018.2806914

National Aeronautics and Space Administration-NASA, & Langley Research Center-LaRC. (2023/01/20). Prediction of Worldwide Energy Resource. *POWER Project funded through the NASA Earth Science/Applied Science Program.* Retrieved from https://power.larc.nasa.gov

Nazemi, M., Moeini-Aghtaie, M., Fotuhi-Firuzabad, M., & Dehghanian, P. (2020). Energy storage planning for enhanced resilience of power distribution networks against earthquakes. *IEEE Transactions on Sustainable Energy*, *11*(2), 795-806. doi: 10.1109/TSTE.2019.2907613

Nowbandegani, M. T., Nazar, M. S., Shafie-Khah, M., & Catalao, J. P. (2022). Demand response program integrated with electrical energy storage systems for residential consumers. *IEEE Systems Journal*, *16*(3), 4313-4324. doi: 10.1109/JSYST.2022.3148536

Osma, G., Amado, L., Villamizar, R., & Ordoñez, G. (2015). Building automation systems as tool to improve the resilience from energy behavior approach. *Procedia Engineering*, *118*, 861-868. doi: 10.1016/j.proeng.2015.08.524

Osma, G., & Ordoñez, G. (2013). Green building pilot as a living laboratory at *Universidad Industrial de Santander*. *World Engineering Education Forum 2013, Cartagena, Colombia*, 1-9. doi: 10.26507/ponencia.1325

Osma, G., & Ordoñez, G. (2019). Measuring factors influencing performance of rooftop PV panels in warm tropical climates. *Solar Energy*, *185*, 112-123. doi: 10.1016/j.solener.2019.04.053

Ouyang, M., & Dueñas-Osorio, L. (2014). Multi-dimensional hurricane resilience assessment of electric power systems. *Structural Safety*, *48*, 15-24. doi: 10.1016/j.strusafe.2014.01.001

Paliwal, P., Patidar, N. P., & Nema, R. K. (2014). Planning of grid integrated distributed generators: A review of technology, objectives and techniques. *Renewable and Sustainable Energy Reviews*, *40*, 557-570. doi: 10.1016/j.rser.2014.07.200

Panigrahi, R., Mishra, S. K., Srivastava, S. C., Srivastava, A. K., & Schulz, N. N. (2020). Grid integration of small-scale photovoltaic systems in secondary distribution network - a review. *IEEE Transactions on Industry Applications*, *56*, 3178-3195. doi: 10.1109/TIA.2020.2979789

Panteli, M., & Mancarella, P. (2015). Influence of extreme weather and climate change on the resilience of power systems: Impacts and possible mitigation strategies. *Electric Power Systems Research*, *127*, 259-270. doi: 10.1016/j.epsr.2015.06.012

Parrado, A. (2020). Proposal for an evaluation scheme of the electrical resilience of low-voltage networks with integration of photovoltaic generation - operating condition in stable state. *Master thesis, Universidad Industrial de Santander, Colombia*, 1-157.

Parrado, A., Rodriguez, R., & Osma, G. (2021). Resilience assessment in a low voltage power grid with photovoltaic generation in a university building. *International Review of Electrical Engineering*, *16*(4), 344-349. doi: 10.15866/iree.v16i4.20327

Pinzon, O., Gaviria, D., Rodriguez, A. P. R., & Osma, G. (2022). Assessment of power quality parameters and indicators at the point of common coupling in a low voltage power grid with photovoltaic generation emulated. *Electric Power Systems Research*, *203*. doi: 10.1016/j.epsr .2021.107679

Poulin, C., & Kane, M. B. (2021). Infrastructure resilience curves: Performance measures and summary metrics. *Reliability Engineering and System Safety*, *216*, 1-19. doi: 10.1016/j.ress .2021.107926

Rafi, F. H. M., Hossain, M. J., Rahman, M. S., & Taghizadeh, S. (2020). An overview of unbalance compensation techniques using power electronic converters for active distribution systems with renewable generation. *Renewable and Sustainable Energy Reviews*, *125*, 1-16. doi: 10 .1016/j.rser.2020.109812

Rahimi, K., & Davoudi, M. (2018). Electric vehicles for improving resilience of distribution systems. *Sustainable Cities and Society*, *36*, 246-256. doi: 10.1016/j.scs.2017.10.006

Rahman, M. R. U., Niknejad, P., & Barzegaran, M. R. (2021). Resilient hybrid energy system (RHES) for powering cellular base transceiver station during natural disasters. Institute of Electrical and Electronics Engineers Inc. doi: 10.1109/PECI51586.2021.9435278

Ramakumar, R., & Bigger, J. E. (1993). Photovoltaic systems. *Proceedings of the IEEE*, *81*, 365-377. doi: 10.1109/5.241491

REN21. (2023). Renewables 2022 global status report. *Renewable Energy Policy Network for the 21st Century*.

Rodriguez, A., Ocaña, R., Flores, D., Martinez, P., & Casas, A. (2021). Environment diagnosis for land-use planning based on a tectonic and multidimensional methodology. *Science of the Total Environment*, *800*, 1-22. doi: 10.1016/j.scitotenv.2021.149514

Rodriguez, R., Osma, G., Bouquain, D., Ordoñez, G., Paire, D., Solano, J., ... Hissel, D. (2024). Electrical resilience assessment of a building operating at low voltage. *Energy and Buildings*, *313*, 114217. doi: https://doi.org/10.1016/j.enbuild.2024.114217

Rodriguez, R., Osma, G., Bouquain, D., Solano, J., Ordoñez, G., Roche, R., ... Hissel, D. (2022). Sizing of a fuel cell–battery backup system for a university building based on the probability of the power outages length. *Energy Reports*, *8*, 708-722. doi: 10.1016/j.egyr.2022.07.108

Rodriguez, R., Osma, G., Solano, J., Roche, R., & Hissel, D. (2021). A framework for the resilience of LV electrical networks with photovoltaic power injection. *Tecnura*, *25*, 71-89. doi: 10.14483/22487638.18629

Rosales-Asensio, E., de Simón-Martín, M., Borge-Diez, D., Blanes-Peiró, J. J., & Colmenar-Santos, A. (2019). Microgrids with energy storage systems as a means to increase power resilience: An application to office buildings. *Energy*, *172*, 1005-1015. doi: 10.1016/j.energy.2019.02.043

Roy, T., & Matsagar, V. (2020). Probabilistic assessment of steel buildings installed with passive control devices under multi-hazard scenario of earthquake and wind. *Structural Safety*, *85*. doi: 10.1016/j.strusafe.2020.101955

Sabouhi, H., Doroudi, A., Fotuhi-Firuzabad, M., & Bashiri, M. (2020). Electrical power system resilience assessment: A comprehensive approach. *IEEE Systems Journal*, *14*, 2643-2652. doi: 10.1109/JSYST.2019.2934421

Sadeghian, H., & Wang, Z. (2020). A novel impact-assessment framework for distributed pv installations in low-voltage secondary networks. *Renewable Energy*, *147*, 2179-2194. doi: 10.1016/j.renene.2019.09.117

Salman, A. M., Li, Y., & Stewart, M. G. (2015). Evaluating system reliability and targeted hardening strategies of power distribution systems subjected to hurricanes. *Reliability Engineering and System Safety*, *144*, 319-333. doi: 10.1016/j.ress.2015.07.028

Shabbir, N., Kutt, L., Astapov, V., Husev, O., Ahmadiahangar, R., Wen, F., & Kull, K. (2022). Congestion control strategies for increased renewable penetration of photovoltaic in LV distribution networks. *Energy Reports*, *8*, 217-223. doi: 10.1016/j.egyr.2022.10.184

Shah, R., Mithulananthan, N., Bansal, R. C., & Ramachandaramurthy, V. K. (2015). A review of key power system stability challenges for large-scale PV integration. *Renewable and Sustainable Energy Reviews*, *41*, 1423-1436. doi: 10.1016/j.rser.2014.09.027

Shakeri, A., Ghanizadeh, T., & Haghifam, M.-R. (2017). The conceptual framework of resilience and its measurement approaches in electrical power systems. *IET International Conference on Resilience of Transmission and Distribution Networks (RTDN 2017)*, 1-11. doi: 10.1049/cp.2017.0335

Shang, D. (2017). Pricing of emergency dynamic microgrid power service for distribution resilience enhancement. *Energy Policy*, *111*, 321-335. doi: 10.1016/j.enpol.2017.09.043

Sharma, P., Kolhe, M., & Sharma, A. (2020). Economic performance assessment of building integrated photovoltaic system with battery energy storage under grid constraints. *Renewable Energy*, *145*, 1901-1909. doi: 10.1016/j.renene.2019.07.099

Shi, J., Huang, W., Tai, N., Qiu, P., & Lu, Y. (2017). Energy management strategy for microgrids including heat pump air-conditioning and hybrid energy storage systems. *The Journal of Engineering*, *2017*, 2412-2416. doi: 10.1049/joe.2017.0762

Shukla, A. K., Sudhakar, K., & Baredar, P. (2016). A comprehensive review on design of building integrated photovoltaic system. *Energy and Buildings*, *128*, 99-110. doi: 10.1016/j.enbuild.2016.06.077

Singh, D., Chaudhary, R., & Karthick, A. (2021). Review on the progress of building-applied/integrated photovoltaic system. *Environmental Science and Pollution Research*, *28*, 47689-47724. doi: 10.1007/s11356-021-15349-5

Siravo, G., Giuditta Fellin, M., Faccenna, C., & Maden, C. (2019). Transpression and the build-up of the cordillera: The example of the Bucaramanga fault (Eastern Cordillera, Colombia). *Journal of the Geological Society*, *177*, 14-30. doi: 10.1144/jgs2019-054

Solano, J., Jimenez, D., & Ilinca, A. (2020). A modular simulation testbed for energy management in ac/dc microgrids. *Energies*, *13*. doi: 10.3390/en13164049

Su, S., Hu, Y., He, L., Yamashita, K., & Wang, S. (2019). An assessment procedure of distribution network reliability considering photovoltaic power integration. *IEEE Access*, *7*, 60171-60185. doi: 10.1109/ACCESS.2019.2911628

Sun, Y., Zhao, Z., Yang, M., Jia, D., Pei, W., & Xu, B. (2020). Overview of energy storage in renewable energy power fluctuation mitigation. *CSEE Journal of Power and Energy Systems*, *6*, 160-173. doi: 10.17775/CSEEJPES.2019.01950

Tari, A. N., Sepasian, M. S., & Kenari, M. T. (2021). Resilience assessment and improvement of distribution networks against extreme weather events. *International Journal of Electrical Power and Energy Systems*, *125*. doi: 10.1016/j.ijepes.2020.106414

Tedoldi, S. S., Jacob, S. B., Vignerte, J., Strack, J. L., Murcia, G. J., & Garín, J. C. B. E. (2017). Impact of distributed generation with photovoltaic solar energy on electrical voltage – simulation of a case. In *CLAGTEE 2017* (p. 1-9).

Tellez, N. (2020). *Description of the electrical engineering building energy consumption from the monitoring of the low voltage boards*. Undergraduate thesis, *Universidad Industrial de Santander*, Colombia.

Tian, M.-W., & Talebizadehsardari, P. (2021). Energy cost and efficiency analysis of building resilience against power outage by shared parking station for electric vehicles and demand response program. *Energy*, *215*, 1-10. doi: 10.1016/j.energy.2020.119058

Timilsina, G. R. (2021). Are renewable energy technologies cost competitive for electricity generation? *Renewable Energy*, *180*, 658-672. doi: 10.1016/j.renene.2021.08.088

UK Cabinet Office. (2011). Keeping the country running: Natural hazards and infrastructure. *Improving the UK's ability to absorb, respond to and recover from emergencies*, 98. Retrieved from www.cabinetoffice.gov.uk/ukresilience

Ulleberg, Ø. (1997). Simulation of autonomous PV-H2 systems: analysis of the PHOEBUS plant design, operation and energy management. *In Proceedings of ISES 1997 Solar World Congress, August 24-30, Taejon, Korea*.

Ulleberg, Ø. (2003). Modeling of advanced alkaline electrolyzers: a system simulation approach. *International Journal of Hydrogen Energy*, *28*(1), 21-33. doi: 10.1016/S0360-3199(02)00033-2

Walling, R. A., Saint, R., Dugan, R. C., Burke, J., & Kojovic, L. A. (2008). Summary of distributed resources impact on power delivery systems. *IEEE Transactions on Power Delivery*, *23*, 1636-1644. doi: 10.1109/TPWRD.2007.909115

Wu, Y., Chen, Z., Dang, J., Chen, Y., Zhao, X., & Zha, L. (2022). Allocation of defensive and restorative resources in electric power system against consecutive multi-target attacks. *Reliability Engineering and System Safety*, *219*, 1-12. doi: 10.1016/j.ress.2021.108199

Yaqoob, M., Lashab, A., Vasquez, J. C., Guerrero, J. M., Orchard, M. E., & Bintoudi, A. D. (2022). A comprehensive review on small satellite microgrids. *IEEE Transactions on Power Electronics*, *37*(10), 12741-12762. doi: 10.1109/TPEL.2022.3175093